# The Enzymology of the Monooxygenase Domain of MICAL-2

By

Claudia Alejandra McDonald

A dissertation submitted in partial fulfillment
of the requirements for the degree of
Doctor of Philosophy
(Biological Chemistry)
in the University of Michigan
2013

Doctoral Committee:

Associate Professor Bruce A. Palfey, Chair
Professor Carol A. Fierke
Professor Stephen W. Ragsdale
Associate Professor Patrick J. O'Brien
Assistant Professor Ann L. Miller

# Acknowledgements

Many people have been a part of my graduate education as friends, teachers, and colleagues. I would like to thank my professor, Dr. Bruce Palfey first and foremost who has been all of these. I could not have asked for a better advisor and teacher. Thank you for your patience, kindness, support, and encouragement. I know that I am a better scientist because of you. I don't think there is enough space on this page to thank you for all that you have done for me both as a scientist and as a true friend. I have such high regard and respect for you as both. I hope that we are friends and collaborators for many years to come. Thank you professor Palfey for always being there for me, you will always be a part of my family.

I would like to express heart felt thanks to my thesis committee – Dr. Ann Miller, Dr. Carol Fierke, Dr. Pat O'Brien, and Dr. Steve Ragsdale. Thank you Ann for your advice and for providing literature papers on actin, this has been essential for moving my thesis project forward. Thank you Carol for providing the opportunity to spend time in your lab and learn about RNA methods, although I ended up changing projects, I am very grateful for the new techniques I learned in your lab. Thank you Pat for your kindness and the input you have provided on my thesis project. Thank you Steve for your advice and suggestions on my project.

I would also like to thank the biological chemistry department. I am very lucky to have been a part of such an amazing department that has provided a stimulating scientific environment filled with many kind professors. Thank you Beth Goodwin,

for being there as a friend after my preliminary exam, I needed a friend and you were above and beyond that. I thank you for your kindness all these years.

I also wish to thank all of my colleagues in the Palfey lab. Ying Yi Liu, you have been a great undergraduate to work with. Thank you for all your hard work, preparing the actin for my experiments. I have enjoyed seeing you grow in your science knowledge and taking on more challenging tasks with me in the lab. I would especially like to thank May Tsoi, you have been like a mother to me. Thank you May for making my mediums, plates, and buffers. But most of all thank you for being my friend all these years.

I would like to thank my master's thesis advisor professor Bruce Macher. Thank you Bruce for believing in me as a scientist and for encouraging me to continue my studies and apply to a doctoral program. Thank you for always listening to me and for providing good advice, for your kindness, and most of all thank you for your friendship.

To my family, thank you for your love, encouragement and laughter. To my brother and sister thank you Jesse and Jessica, you mean so much to me. Mama, thank you for loving me and encouraging me to follow my dreams.

Last but definitely not least, Anders, thank you for being you. Thank you for your patience and for always always being there for me. You are my biggest supporter and I am truly blessed to have you in my life. You brighten up all my days, thank you for always encouraging me and for always believing in me. I thank you for everything. You are my very best and dearest friend, Anders, mi amor, you will always have my heart. Jeg elsker deg.

# Table of Contents

# List of Tables

# List of Figures

# List of Appendices

# List of Abbreviations

MICAL, molecule interacting with CasL;

monoMICAL, monooxygenase domain of MICAL

KIE, Kinetic Isotope Effect

CH, calponin homology domain

PHBH, p-hydroxybenzoate hydroxylase

LIC, ligation-independent cloning

DTT, dithiothreitol

# Abstract

Molecules interacting with CasL (MICALs) are large multi-domain flavin-dependent monooxygenases that use redox chemistry to cause actin to depolymerize. Little enzymology has been reported for MICALs, and none for MICAL-2, an enzyme vital for the proliferation of prostate cancer cells. The monooxygenase domains of MICALs resemble aromatic hydroxylases, but their substrate is the sulfur of a methionine of actin. In order to determine how closely MICAL-2 conforms to the aromatic hydroxylase paradigm, the half-reactions were studied in stopped-flow experiments.

In the reaction of MICAL-2 with pyridine nucleotides, the enzyme had a strong preference for NADPH over NADH, due to very weak binding of NADH. A comparison of the reduction kinetics using *protio*-NADPH and *deutero*-NADPH showed that MICAL-2 is specific for the *proR* hydride of NADPH (like other aromatic hydroxylases), as evidenced by a 4.8-fold kinetic isotope effect. In the absence of actin, NADPH reduces the flavin relatively slowly; actin speeds that reaction significantly.

Stopped-flow experiments were also used to monitor the oxidation of the enzyme-bound reduced FAD in the absence and in the presence of f-actin, the putative substrate to be oxygenated. In the absence of actin, flavin was oxidized in two phases because there are two populations of enzyme. The comparison of increases in absorbance at 450 nm, an indicator of flavin oxidation, and 550 nm, an indicator of flavin conformation, suggests that one form reacts relatively fast with $O_2$ after the flavin moves from the “in” to the “out” conformation. The other form of the enzyme oxidizes slower, and the absorbance at 550 nm increases

even slower, suggesting that this form reacts when the flavin is “in” and subsequent movement to the “out” conformation is slow.

When f-actin was included in reaction mixtures, the flavin hydroperoxide and the flavin hydroxide were observed. The formation of the hydroperoxide was faster by an order of magnitude than the reaction of actin-free MICAL with $O_2$. At the concentrations of actin used in these experiments (tens of micromolar), about half the reactive hydroperoxide intermediate eliminated $H_2O_2$. The enzyme that successfully oxygenated actin formed the flavin hydroxide intermediate and, after eliminating $H_2O$, formed oxidized enzyme. These results show that monoMICAL-2 behaves like a typical aromatic hydroxylase in most of its reactions. The striking difference is the ability to oxygenate a non-aromatic nucleophile.

# Chapter 1
# Introduction

Flavins perform chemical reactions critical for biology. This thesis is focused on the N-terminal domain of MICAL **(M**olecule **I**nteracting with **C**as**L**), a flavin-dependent protein involved in the regulation of actin depolymerization. Depolymerization halts axon growth, vesicle fusion, apoptosis, and has other effects in biology. Uncertainty exists on whether MICAL is an oxidase or a monooxygenase. The goal of my project is to study the flavin chemistry of the N-terminal domain of MICAL-2 in order to determine whether it is an oxidase or monooxygenase. This thesis reports the catalytic cycle of monoMICAL-2 broken into half-reactions (reductive and oxidative). The reductive half-reaction and oxidative half-reaction of the N-terminal domain were examined in the presence and absence of its putative substrate, f-actin. Understanding the chemistry involved in monoMICAL-2 could lead to possible therapies for nerve regeneration or other diseases (*1*).

## 1.1 Flavins

### 1.1.1 Structure

Flavins have an isoalloxazine moiety that performs redox reactions; in almost all flavoenzymes, this is the important part (Figure 1-1). The isoalloxazine is substituted at N10 with a sugar derivative, a ribityl chain with three secondary alcohols and terminated by a primary alcohol, making riboflavin. Riboflavin is generally not involved in enzyme reactions, but, as vitamin b2, is a nutritionally important form. Once riboflavin is metabolized by cells it is either phosphorylated to make flavin mononucleotide (FMN) or else an ADP moiety is attached, making flavin adenine dinucleotide (FAD). On enzymes, FMN and FAD are prosthetic

groups. The enzyme generally binds FMN or FAD very tightly with many noncovalent interactions to the non-redox portion of the flavin. Interactions with the isoalloxazine moiety can also be important for binding, but are especially important for controlling the chemistry of the flavin.

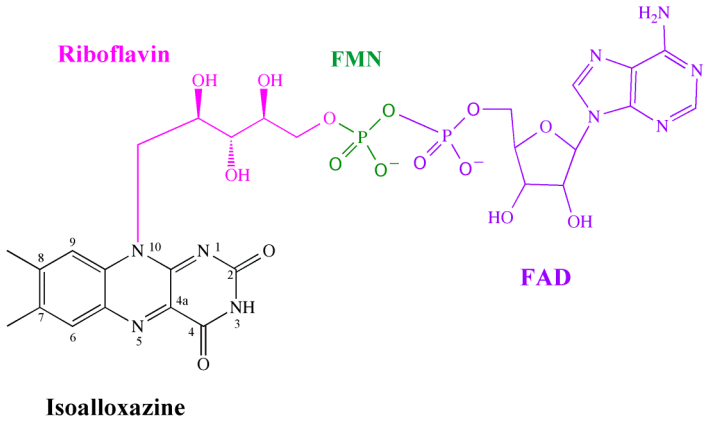


**Figure 1-1 Structures of flavins**

Structures of flavins: isoalloxazine (black), riboflavin (pink), flavin mononucleotide (FMN) shown in green, and flavin adenine dinucleotide (FAD) shown in lavender.

### 1.1.2 Chemistry

The isoalloxazine can do a variety of chemistry in solution, but proteins control which reactivities are possible on enzymes (*2*). There are three oxidation states: the oxidized isoalloxazine, the two-electron reduced isoalloxazine (also called the hydroquinone), and the one-electron reduced radical of the isoalloxazine called the semiquinone (Figure 1-2). Particularly important is the reaction of flavins with hydride donors. N5 of the isoalloxazine accepts a hydride-equivalent from a hydride-donor such as pyridine nucleotides. In the reverse reaction, N5 donates the hydride to an acceptor (Figure 1-3). The oxidized isoalloxazine can also be attacked by nucleophiles either at N5 or at C4a, while reduced isoalloxazine can be attacked by electrophiles, again either at N5 or C4a. The reduced isoalloxazine can also react with molecular oxygen to give $H_2O_2$ and oxidized isoalloxazine (Figure 1-4). However, reduced flavin is a singlet and cannot directly react with triplet $O_2$ to the singlet products – oxidized flavin and $H_2O_2$ –

because spin must be conserved. Instead reduced flavin reacts with molecular oxygen by a single-electron transfer. The formation of the caged radical pair is the rate-determining step of oxidation. It is followed by collapse of the radical-pair making the C4a-flavin hydroperoxide, which then eliminates hydrogen peroxide to give oxidized flavin. The C4a-flavin hydroperoxide is unstable, with a lifetime in aqueous solution of much less than a millisecond, but in some enzymes it can be stabilized significantly.

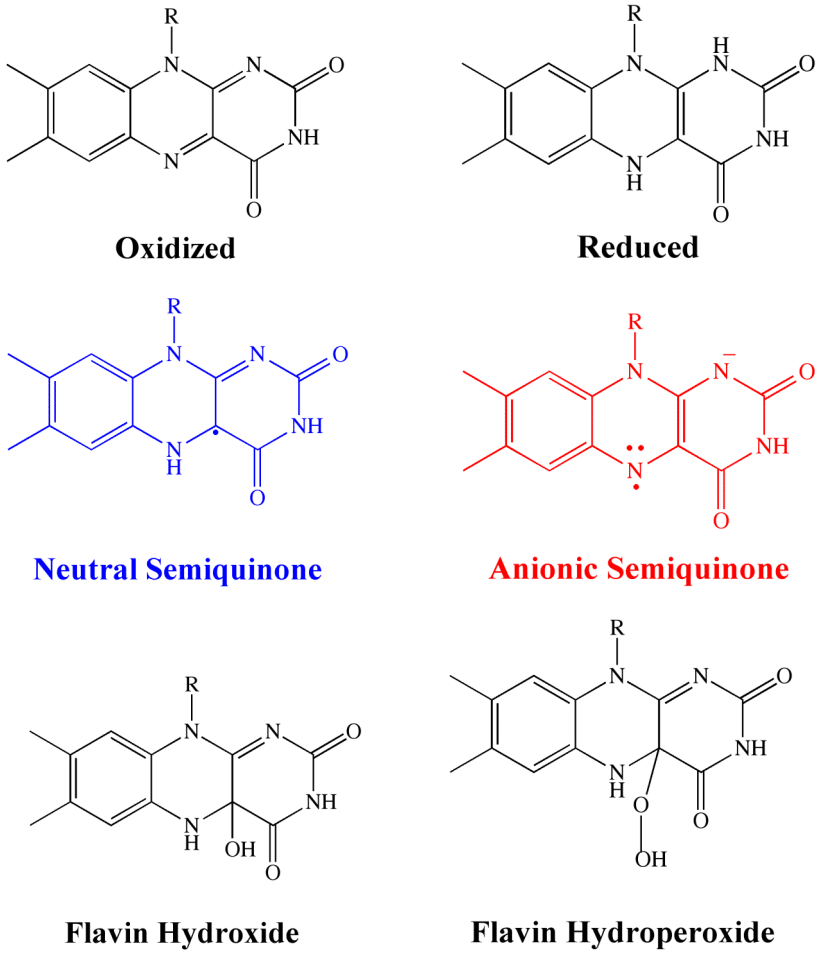


**Figure 1-2 Important isoalloxazine forms**

Important isoalloxazine forms: oxidized flavin, blue semiquinone, red semiquinone, 2-electron reduced hydroquinone, C4a-hydroxide, and C4a-hydroperoxide.

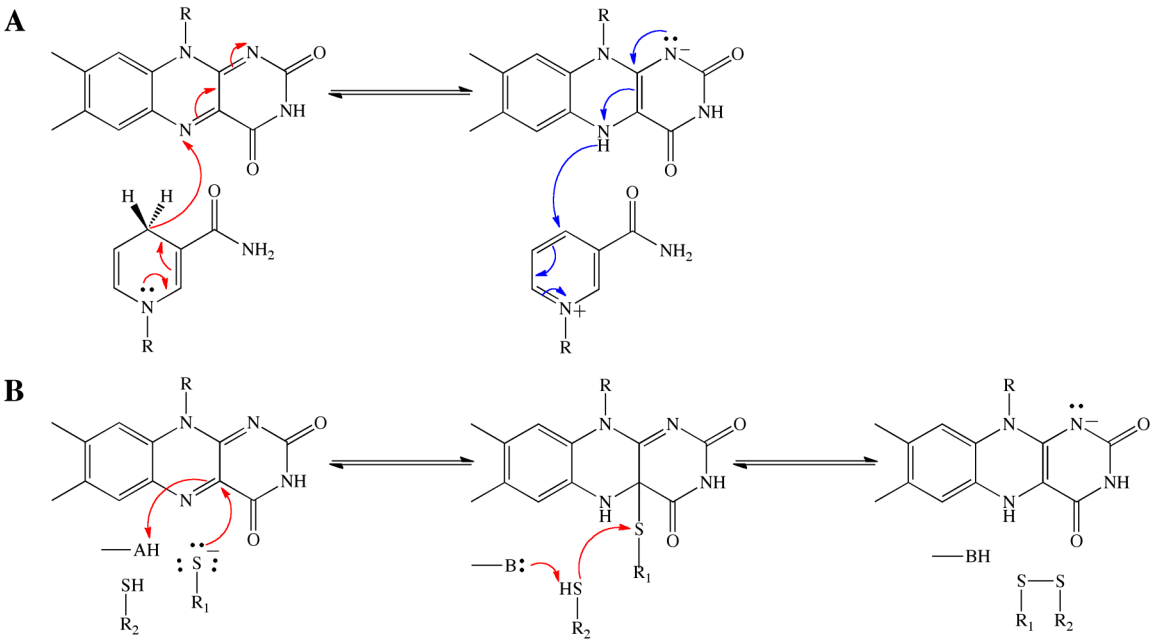


**Figure 1-3 Mechanisms for flavin reduction.**

**A.** Hydride transfers occur at N5 of the flavin. Pyridine nucleotides are frequent reactant – partners. **B.** Many flavoenzymes perform thiol/disulfide oxidation/reduction. In the direction of reduction, a nucleophilic thiolate attacks C4a, making an adduct. Attack by the second thiol on the sulfur of the first gives reduced flavin and the disulfide.

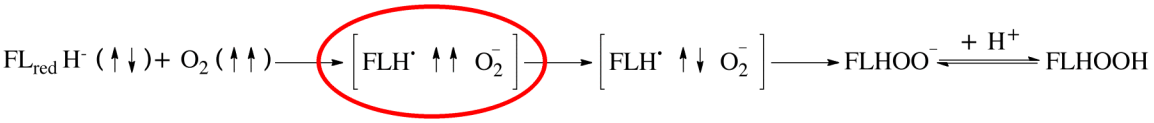

**Figure 1-4 The reaction of $O_2$ with reduced flavin.**

Reduced flavin reacts with $O_2$ to make a caged radical-pair circled in red, which is the rate-determining step of oxidation. Following spin inversion, radical coupling forms the flavin peroxide, which can be protonated to the flavin hydroperoxide.

### 1.1.3 Spectra

The isoalloxazine on flavin-containing enzymes can be used as a spectral reporter to indicate the redox state of the flavin as well as the presence of ligands. The oxidized form has a bright yellow appearance and an absorbance spectrum with peaks at ~450 nm and ~380 nm (Figure 1-5A). The semiquinone can be either neutral – it looks blue – or it can be anionic – it looks red. The blue semiquinone has a peak at 360 nm and a broad peak at 580 nm. The red semiquinone has peaks at 370 nm and 480 nm. Two-electron reduced flavin has a pale yellow appearance due to the loss of the ~450 and ~380 nm peaks. Flavins also frequently make charge-transfer complexes that have a new spectral transition. In order to make a charge-transfer complex, an electron-acceptor and electron-donor must be in van der Waals contact. The electron-acceptor needs to have a low-lying unoccupied orbital, while the electron-donor must have a high-lying occupied orbital, so that the $\Delta E$ between the two orbitals is small. Light of this energy can be absorbed, exciting one of the paired electrons from the donor into an unoccupied orbital of the acceptor. Charge-transfer complexes can be seen in organic and inorganic chemistry as well as in enzymology. An example of a charge-transfer complex from chemistry is iodine with a variety of organic compounds such as triphenylamine, triphenylarsine, triphenylphosphine and triphenylstibine (*3*). In enzymology, oxidized flavin is an electron-acceptor and makes charge-transfer complexes with electron-rich ligands, as seen in the interaction of dihydroorotate dehydrogenase with 3,4-dihydroxybenzoate (Figure 1-5B). In contrast, reduced flavins are often charge-transfer donors. For example, reduced dihydroorotate dehydrogenases make a charge-transfer interaction with orotate. Flavin adducts also have distinct absorbance spectra. Oxygen or sulfur C4a-adducts are important intermediates in many enzymes. They have absorbance peaks from 370 nm – 410 nm (Figure 1-5C).

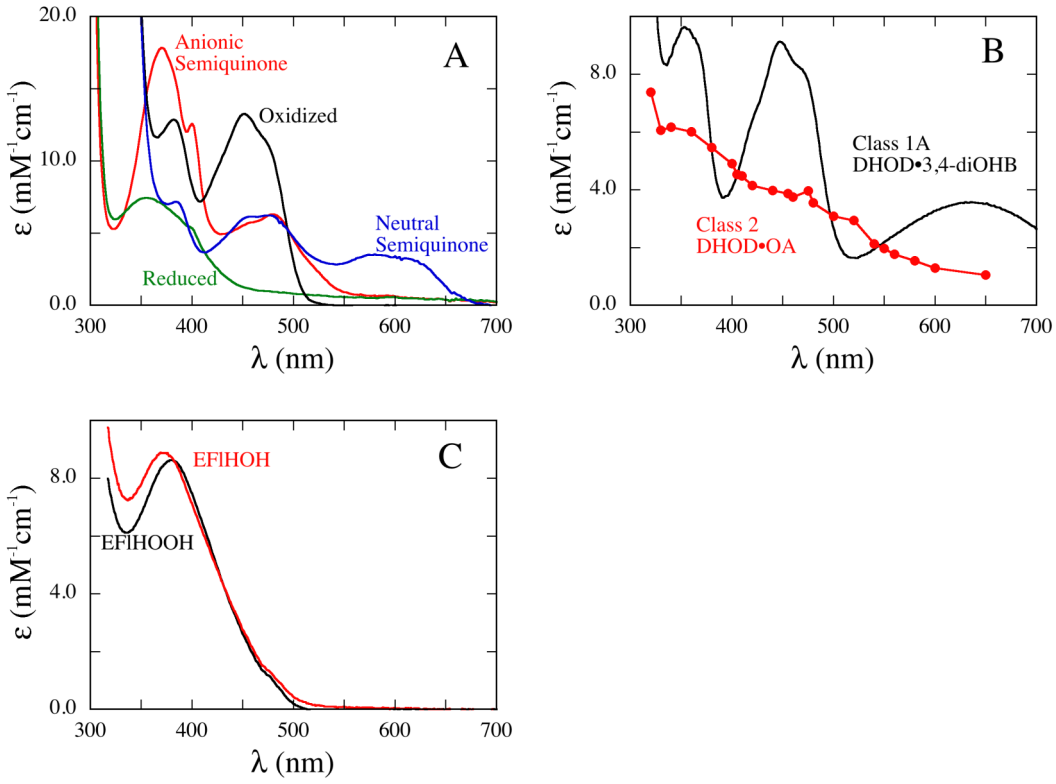


**Figure 1-5 Spectra of flavins**

Spectra of flavins **A.** Oxidized, red semiquinone, blue semiquinone, and 2-electron reduced hydroquinone. **B.** A charge-transfer complex is formed by the binding of 3,4-dihydroxybenzoate with an oxidized Class 1A dihydroorotate dehydrogenase (*4*). A new absorbance band appears at ~640 nm, caused by the excitation of an electron from 3,4-dihydroxybenzoate into an empty flavin orbital. An example of a charge-transfer complex formed by reduced flavin is also shown. In this case, a charge-transfer complex is formed when between the reduced flavin of a Class 2 dihydroorotate dehydrogenase with orotate as an intermediate complex in its reductive half-reaction (*5*). An extra absorbance band appears above ~450 nm due to the excitation of an electron from reduced flavin into the empty orbital of orotate. **C.** Absorbance spectra of the flavin hydroxide and flavin hydroperoxide formed in the oxidative half-reaction of the Pro293Ser variant of *p*-hydroxybenzoate hydroxylase (*6*). The positions of the peaks can very significantly, depending on the protein environment.

## 1.2 Flavoenzymes

### 1.2.1 General Catalytic Cycles and Half-reactions

Most flavoenzyme catalytic cycles can be divided into a reductive half-reaction and an oxidative half-reaction (Figure 1-6). In the reductive half-reaction, the oxidized flavoenzyme reacts with a reducing substrate to form reduced flavoenzyme. In the oxidative half-reaction the reduced enzyme reacts with an oxidizing substrate to form oxidized enzyme. The products of each half-reaction often dissociate before the next substrate reacts, giving true ping-pong mechanisms. This is not always the case; sometimes product does not dissociate before the next substrate reacts, and thus the mechanism can be sequential. In the reductive half-reaction, a hydride equivalent would be donated to the enzyme. Examples of some hydride donors are alcohols, amines, and NAD(P)H, an enamine. Other reductants could be thiols or iron-sulfur clusters, which are one-electron donors. In the oxidative half-reaction, the reduced flavin can react with organic hydride acceptors, disulfides, or iron-sulfur clusters. Another important oxidant is $O_2$. When it is the physiological oxidant, it can either be reduced to $H_2O_2$ (by oxidases), or an oxygen atom can added to a substrate (monooxygenase).

The variety of chemistry available to flavins is vast. Thus, they are found in all areas of biology such as classic areas like energy production, reduction, oxidation and oxygenation. Flavins are also involved in light emission, biodegradation, chromatin remodeling, apoptosis, DNA repair, and neural development.

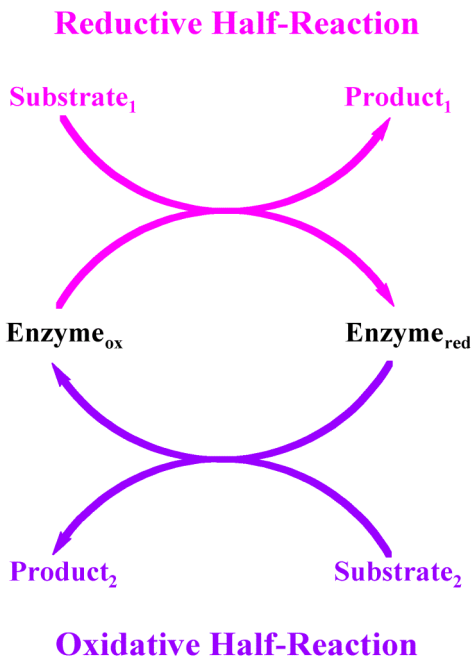


**Figure 1-6 General catalytic cycle.**

The cycle is made up of two half-reactions: a reductive half-reaction and an oxidative half-reaction.

### 1.2.2 Methods

The different chemical forms of flavins can be monitored by spectroscopic methods, especially absorbance spectroscopy. Absorbance spectroscopy requires ~10 μM or more of enzyme. Another method to monitor flavoenzymes is by fluorescence. Oxidized flavoenzymes are often fluorescent and reduced flavoenzymes are usually non-fluorescent, but there are rarely exceptions. Intermediates such as the C4a-hydroperoxide or C4a-hydroxide are often fluorescent, however semiquinones and charge-transfer complexes never are.

Absorbance or fluorescence spectroscopy on standard instruments is useful when performing ligand-titrations, determining reduction potentials, or observing slow reactions. However, if reactions of enzyme with ligands are fast, then other methods must be used. Stopped-flow methods are commonly used to study fast reactions, allowing reactions in the millisecond timescale to be monitored (Figure

1-7). These instruments are very useful for studying half-reactions as they can be maintained anaerobic, allowing mixing of enzyme with different concentrations of anaerobic substrates.

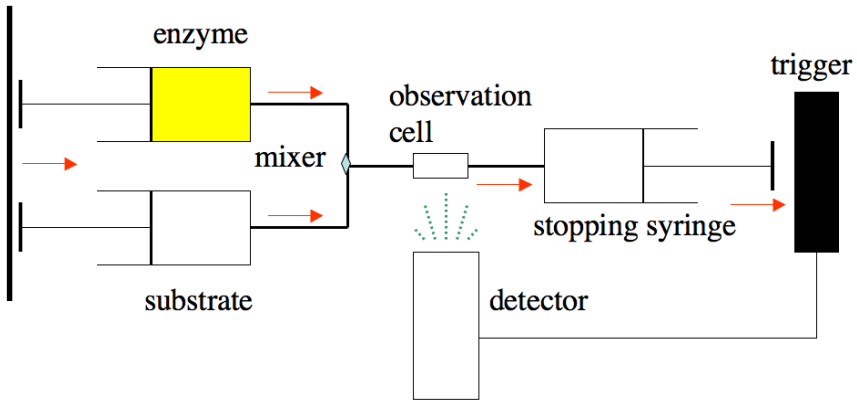


**Figure 1-7 Diagram of a stopped-flow spectrophotometer.**

Two reactants, e.g. anaerobic enzyme and substrate, are pushed from the driving syringes through a mixer and flow-cell into a stopping-syringe. The plunger of the stopping-syringe triggers data collection allowing reactions in the flow-cell to be monitored spectrally.

### 1.2.3 Oxidases

Oxidases are flavoenzymes that use $O_2$ as a physiological substrate to make $H_2O_2$ (Figure 1-8). The substrate of the reductive half-reaction is most often a hydride donor, such as amino acids or sugars. In the oxidative half-reaction of oxidases, intermediates are rarely seen. However, the flavin hydroperoxide has been reported for pyranose-2-oxidase (*7*), and the semiquinone has been reported in glycine oxidase (*8*). The generality of these intermediates is not yet established. The oxidative half-reaction of oxidases, with bimolecular rate constants ranging from $10^4$ – $10^6$ $M^{-1}$ $s^{-1}$ is fast. The factors that make oxidases fast are not understood, but sometimes a positive charge near N5 of the flavin is important (*9, 10*).

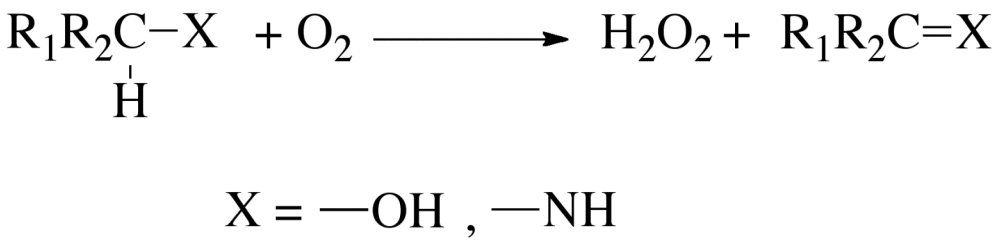

**Figure 1-8 General oxidase reaction.**

Flavoprotein oxidases usually oxidize carbon-heteroatom single-bond making double-bonds and pass the electrons to $O_2$, forming $H_2O_2$.

### 1.2.4 Monooxygenases

Monooxygenases are the other category of flavoenzymes that use oxygen as a physiological substrate (Figure 1-9). Monooxygenases add one oxygen atom derived from $O_2$ to a substrate. In the reductive half-reaction, reduced flavin is made by a hydride transfer from NAD(P)H to N5 of the flavin. Once reduced, the flavin reacts with $O_2$ to make the C4a-hydroperoxide (Figure 1-2). Using this intermediate, monooxygenases oxidize electron-rich aromatics, nucleophilic heteroatoms with lone-pairs (nitrogens or sulfurs), or electrophiles (carbonyls or boronates). Monooxygenases perform the chemistry normally accomplished by organic hydroxyperoxides used by synthetic chemists. After oxygenation of the substrate, water is eliminated from the flavin hydroxide to make oxidized enzyme.

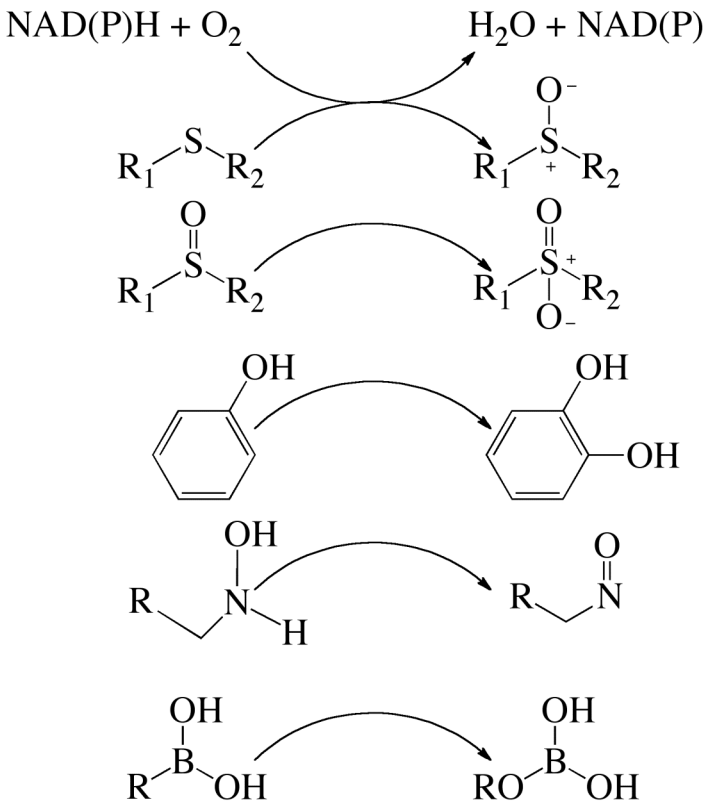


**Figure 1-9 General monooxygenase reaction.**

Monooxygenases use NAD(P)H as a reductant and transfer one oxygen atom from $O_2$ to a substrate. Nucleophilic or electrophilic substrates are possible; a few representative examples are shown.

Monooxygenases have been grouped into 6 classes (A-F) based on their structure, sequence, number of components, and substrate preference (*11*):

### 1.2.4.1 Class A

The Class A monooxygenases, also called aromatic hydroxylases, use the flavin hydroperoxide to perform electrophilic aromatic substitutions on activated aromatics. In the reductive half-reaction, they release $NAD(P)^+$ after flavin is reduced. Class A enzymes have one Rossmann fold that binds FAD tightly and no “standard” binding site for NAD(P)H. Catalysis is regulated by the rate of reduction of the flavin by NAD(P)H, which is fast only if substrate is bound (*12*).

This appears to be connected to the movement of their flavins, which can be in a mostly buried position ("in") that is inaccessible to NAD(P)H but moves to a more solvent-exposed ("out") conformation where the reaction with NAD(P)H is possible (*12, 13*). The reaction of reduced Class A monooxygenases with $O_2$ makes an unstable C4a-hydroperoxide. However the presence of substrate stabilizes this intermediate long enough for it to oxygenate the substrate and to be detected spectrally (*14*). Class A enzymes are also generally very substrate-specific and only hydroxylate aromatic rings on the *ortho* or *para* position to an electron-donating group. Oxidation of Class A enzymes is often stimulated by their aromatic substrates. Some examples of Class A monooxygenases are *p*-hydroxybenzoate hydroxylase and phenol hydroxylase, hydroxylases involved in lignin catabolism.

#### 1.2.4.2 Class B

The Class B monooxygenases use NADPH as reductant. After reduction, $NADP^+$ remains bound; bound $NADP^+$ is critical for the oxidative half-reaction (*12, 15, 16*). Unlike Class A enzymes, they have two Rossman folds, the first for FAD and the second for NADPH. Class B monooxygenases are not stimulated by their substrate in reduction or oxidation. Many Class B enzymes are not substrate-specific, in contrast to Class A monooxygenases. Class B monooxygenases can oxidize many types of nucleophilic heteroatoms or electrophiles such as carbonyls and boronates. An example of a Class B monooxygenase is the flavin-containing monooxygenases (FMO) from liver, which plays an import role in the detoxification of drugs.

#### 1.2.4.3 Class C

Unlike Class A and B, Class C monooxygenases use their flavin (FMN) as a substrate rather than a prosthetic group. Unlike Class A and B, Class C enzymes have two protein components:  a monooxygenase component and a reductase

component. The monooxygenases components are TIM-barrels. Aldehydes or sulfonates are substrates of Class C monooxygenases. Examples of Class C monooxygenases are the bacterial luciferases, which emit light and are responsible for bioluminescence in the sea.

#### 1.2.4.4 Class D

The Class D monooxygenases use FAD as a substrate. Class D monooxygenases are two-component systems, with a monooxygenase and a reductase. Similar to Class A monooxygenases, Class D monooxygenases have a preference for aromatic substrates. An example of a Class D monooxygenase is 4-hydroxyphenylacete 3-monooxygenases.

#### 1.2.4.5 Class E

Class E monooxygenases have one Rossmann fold that binds FAD, similar to Class A monooxygenases. Class E monooxygenases are two-component enzyme-systems, consisting of a monooxygenase and a reductase. Class E monooxygenases are rare; examples are styrene monooxygenases from bacteria and squalene monooxygenase in cholesterol biosynthesis.

#### 1.2.4.6 Class F

Similar to Class A, Class F monooxygenases have one Rossman fold for binding FAD. Class F enzymes are two-component enzymes similar to class C, D, and E; they have a monooxygenase and a reductase component and use FAD as a substrate. Their substrates are chlorides electron-rich aromatics or heteroaromatic. An example of this class of enzymes is tryptophan 7-halogenase.

## 1.3 MICAL

### 1.3.1 How it was found

CasL, also called HEF1, is a heavily phosphorylated protein that is involved in integrin-induced signal transduction. CasL is important for the regulation of the cytoskeleton. CasL performs its function by interacting with other molecules through its Src homology 3 (SH3) domain. Suzuki *et al.* set out in 2002 to find other molecules that interact with CasL through its SH3 domain (*17*). Using far-Western screening in hematopoietic cells, they identified a novel molecule that interacts with the CasL SH3 domain through a proline-rich (PPKPP) region. They named the novel molecule **M**olecule **I**nteracting with **Ca**s**L** (MICAL). It forms a complex with CasL in mammalian cells *in vivo*. MICAL is a large (~1000 amino acids) multi-domain flavin-containing cytoplasmic protein (*17*). The large N-terminal monooxygenase domain is followed by up to four protein-protein interacting domains. When first discovered, MICAL was found to co-localize with CasL from the perinuclear area to the peripheral part of the cell, suggesting that MICAL may play a role in the signaling pathways mediated by CasL. Interestingly, MICAL was found to not localize with f-actin or microtubules, but instead was found to interact with the intermediate filament vimentin through its C-terminal region, forming a complex (*17*). Based on this, it was suggested that MICAL might be important for maintenance of cytoskeletal integrity. MICAL, first discovered for its interaction with CasL, is now known to oxygenate f-actin (*18-20*).

### 1.3.2 Enzymology

Very little enzymology has been reported on MICAL, and the only reports have been on the isolated monooxygenase domain (monoMICAL-1) of MICAL-1. Steady-state assays on murine monoMICAL's NADPH oxidase activity gave a $k_{cat}$ of ~77 $s^{-1}$ and a $K_M$ for NADPH of 222 μM (*21*). However these results were

based on coupled assays; $H_2O_2$ was detected using horseradish peroxidase and Amplex Red. This assay was found to be artifactually fast (*20*); monitoring NADPH consumption instead of fluorescence produced by Amplex Red gave a substantially lower rate. I have shown that resorufin, the Amplex Red oxidation product, reacts with monoMICAL-2 in a complex chain reaction (unpublished). A pH dependence was determined for monoMICAL-1 using this assay, giving a bell-shaped curve, with maximum activity at pH ~7 (*21*). However it is unclear if this is a real effect or just an effect on the Amplex Red assay and subsequent artifactual reactions. In a different report (*20*), steady-state assays monitoring NADPH directly with human monoMICAL-1 gave $k_{cat}$ of 3.9 $s^{-1}$ and a $K_M$ for NADPH of 26-41 μM. NADH has a ~20-fold higher $K_M$ and a 10-fold lower $k_{cat}$. The pH dependence of the $k_{cat}$ of the oxidase activity increased with a $pK_a$ ~6.5 – not bell-shaped as seen using the Amplex Red assay. The reductive half-reaction was determined for human monoMICAL-1 at 25 °C, giving values of $k_{red}$ of 3 $s^{-1}$ and $K_d$ for NADPH of 56 μM. Consumption of NADPH in steady-state assays was stimulated by f-actin, giving a $k_{cat}$ ~12-15 $s^{-1}$. Zucchini *et al.* argued that oxygenation of actin is reversed during enzyme assays. A charge-transfer band was seen in the absorbance spectrum of oxidized monoMICAL-1. It was attributed to Trp400 interacting with the *re* face of the flavin (*20*).

*Drosophila* monoMICAL with or without a tethered CH domain was shown to use NADPH to depolymerize pyrene-labeled f-actin (*18*). Depolymerization showed a preference for NADPH versus NADH (*18*). Depolymerization of f-actin occurred even in the presence of catalase; thus monoMICAL-CH is not catalyzing depolymerization of actin by releasing $H_2O_2$ as a product (*19*). Mass spec analysis showed that a peptide with two methionines (Met44 and Met47) was modified by the addition of one oxygen to each sulfur, making sulfoxides on f-actin. F-actin with Met44 mutated to Leu was resistant to depolymerization. These findings suggest that *Drosophila* monoMICAL causes depolymerization of

actin by catalyzing the addition of one oxygen to Met44 located in the D-loop region of actin on its pointed end (*19*).

The effects of the C-terminal domains on the oxidase activity of monoMICAL were investigated. MICAL-1 truncation mutants in lysates of transfected HEK293T cells were used with the Amplex Red assay to monitor the production of $H_2O_2$ (*22*). Truncations of monoMICAL with a tethered CH domain and monoMICAL with both the CH and LIM domains had high oxidase activity while full length MICAL-1 or all the C-terminal domains tethered together (lacking the monooxygenase domain) had very little oxidase activity. They interpreted these results as indicating that the C-terminal domains are inhibitory (*22*). Also the high monoMICAL-CH-LIM oxidase activity decreased when callapsin response mediator protein (CRMP) was added. They concluded that the substrate of MICAL was either CRMP or was carried by CRMP, thus no $H_2O_2$ would be made in its presence (*22*). The use of an assay that has been shown to give artifacts and the use of crude extracts instead of pure enzyme make these conclusions uncertain.

### 1.3.3 Structure of monoMICAL-1

The crystal structure of mouse monoMICAL-1 has been solved (*21, 23*). It is most similar to the aromatic hydroxylase *p*-hydroxybenzoate hydroxylase (PHBH) that belongs to the Class A monooxygenases. There is an 11% identity between the N-terminal domain of MICAL and PHBH. However, monoMICAL-1 has two N-terminal helices which are not present in PHBH (*21*). Most aromatic hydroxylases are dimers or tetramers however monoMICAL-1 was found to be a monomer by analytical ultracentrifugation (*21*). The monomer has three domains: a large domain containing the FAD moiety, a monooxygenase domain, and a four-helix bundle domain and C-terminal linker that spans amino acid residues 445-489 (Figure 1-10). FAD is bound by a Rossmann fold, the only one in the domain.

The monooxygenase domain is missing a segment found in homologs making the active site significantly more open than typical hydroxylases. Reduction causes a 6.5° movement between the monooxygenase domain and the FAD binding domain. This is unique to monoMICAL-1 and has not been observed in other hydroxylases. There is a less rigid interface in monoMICAL-1 between the FAD binding domain and the monooxygenase domain (*23*).

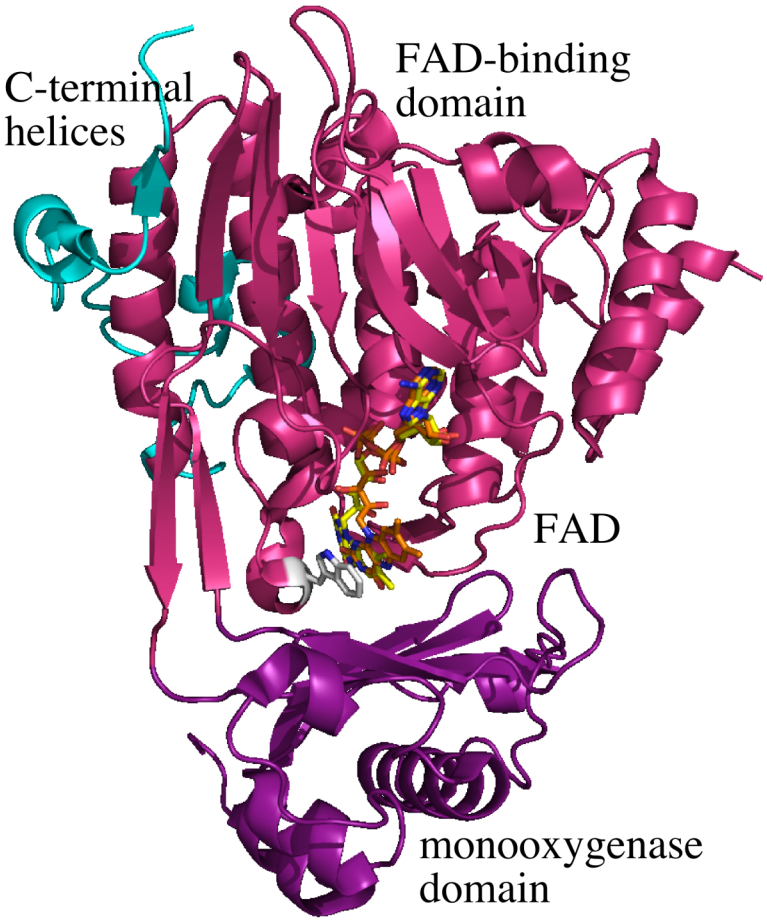


**Figure 1-10 Structure of mouse monoMICAL-1**

The FAD binding domain is shown in pink. It is connected to the monooxygenase domain (purple). The active site is at the juncture of these two domains. The C-terminal helices (cyan) are not found in most hydroxylases.

When crystals of monoMICAL-1 were soaked with NADPH, the flavin was reduced. Interestingly, while the oxidized enzyme had the flavin in the “out” conformation where it was very exposed to solvent, the reduced enzyme had a mixture of two flavin conformations, one in the “out” conformation and the other in the more buried “in” conformation (Figure 1-11). The reduced flavin in the “in” isollaxazine conformation had a “butterfly” bend along the N5-N10 axis. Large deviations from planarity like this have been observed in structures of free reduced flavins and a few flavoenzymes. Quantum calculations suggest that a “butterfly” bend occurs when N1 is protonated in reduced flavins. Flavin movement from “out” to “in” is a characteristic of aromatic hydroxylases such as PHBH. Conversely, only aromatic hydroxylases have this conformational change. The *re* face of the flavin stacks on Trp400 when it is in the “out” conformation. There is a channel lined with conserved residues leading to the flavin in the “in” conformation (*23*).

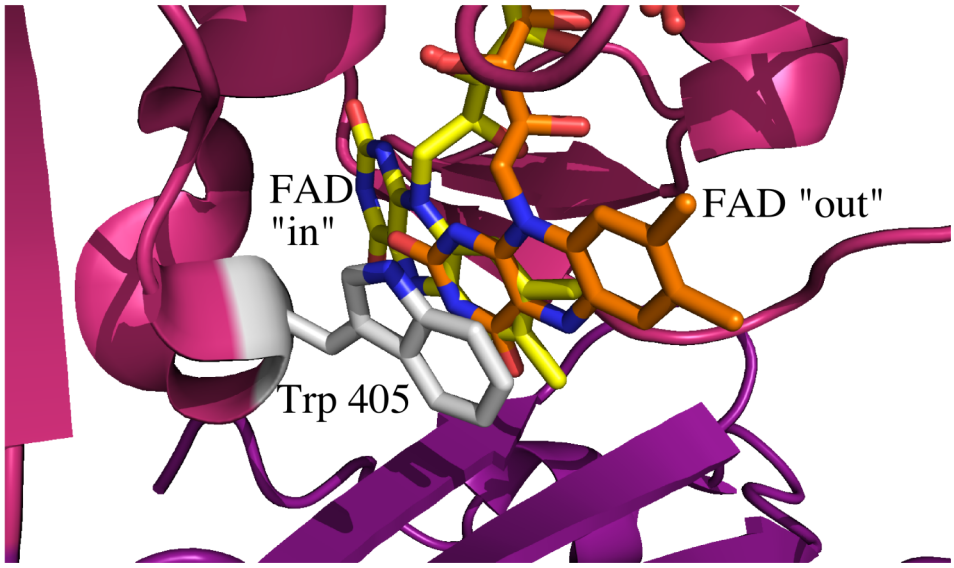


**Figure 1-11 Active site of monoMICAL-1**

The reduced flavin (yellow) is shown in the “in” conformation and the oxidized flavin is shown in the “out” conformation (orange). Trp405 (silver) is in contact with the flavin in the “out” conformation, making a charge-transfer complex.

### 1.3.4 Substrates and Interactors

Vimentin is an intermediate filament protein. It is involved in adhesion, migration and cell-signaling (*24*). Immunoprecipitation assays showed that MICAL-1 binds to vimentin with its CH domain. Immunofluorescence double-staining patterns showed that MICAL-1 colocalizes with vimentin intermediate filaments *in vivo* (*17*). Interestingly vimentin, like MICAL-2, has been found to be overexpressed in prostate cancer (*25*). Deletion of vimentin in mice causes very slow wound-healing because fibroblasts are unable to migrate to the site of injury (*26, 27*).

MICAL interacts with proteins that control cell proliferation and death. There are two nuclear kinases, NDR1 and NDR2. Both have been found to be important for controlling apoptosis (*28*). MICAL-1 interacts with both NDR1 and NDR2 kinases (*29, 30*). Pull-down assays with MICAL-1 truncations showed that NDR1 binds to MICAL C-terminal domain constructs that contained the LIM domain or the Proline rich region of MICAL-1; thus both domains are likely needed for binding. Zhou *et al.* thought that NDR-1 might be a substrate for MICAL-1 (*29*). Indeed, MICAL-1 was found to be phosphorylated, however it was not determined which residue is modified. NDR kinase activity is controlled by phosphorylation. Because of this, NDR1 or NDR2 kinase activation by MICAL-1 was investigated. MICAL-1 overexpression in cells caused phosphorylation of NDR1 and NDR2 to be inhibited. Knocking down monoMICAL-1 by siRNA increased phosphorylation of NDR1 and NDR2. MST1, a serine-threonine kinase upstream of NDR1, binds to NDR1 and NDR2 to induce its activation by phosphorylation, which leads to cellular apoptosis. MICAL-1 was found to compete with MST1 for binding NDR1, thus leading to a loss in apoptosis (*29*).

Collapsin-response-mediator proteins (CRMPs) are expressed in the nervous system (*31, 32*). During the development of the brain CRMPs are one of the first proteins expressed (*33*). Their expression is especially high during axon growth

(*32*). CRMPs are a family of proteins that are involved in Semaphorin 3A signaling that mediates the development of the nervous system (*34*). It was thought by Schmidt *et al.* that CRMPs could bind to MICALs because the structure of the CRMP tetramer resembles dihydropyrimidinase. MICAL-1 coimmunoprecipitated with CRMPs, and the amount increased if cultures were treated with Semaphorin 3A. Truncations of MICAL-1 and the full-length enzyme were immunoprecipitated; it was found that truncated enzymes did not interact as well with CRMPs as full-length MICAL-1. Amplex red assays were used to measure the amount of $H_2O_2$ produced from cell lysates expressing full-length MICAL. Cell lysates expressing full-length MICAL did not change their $H_2O_2$ production in the presence or absence of CRMP. However truncations of MICAL-1 – monoMICAL-1 tethered to a CH domain and a LIM domain – had high $H_2O_2$ production compared to production (below zero) of $H_2O_2$ in the presence of CRMP. Schmidt *et al.* attributed this observation to the idea that CRMP was the substrate for MICAL (*22*). However, the Amplex red assay has been shown to give artifactual results with pure monoMICAL-1, (*20*) making it difficult to know if the results reported by Schmidt *et al.*, obtained from crude extracts are reliable.

Actin is a substrate for MICAL (*18*-*20*). Actin has a molecular weight of ~43,000 daltons. It is one of the most highly conserved proteins and is very abundant in all cells. It is found in eukaryotes but in prokaryotes there is a homolog, MreB. Eukaryotes have three different isoforms of actin: alpha, beta, and gamma. Skeletal and cardiac muscle cells have the $\alpha$-isoform. Smooth muscle cells have both the $\alpha$-isoform and $\gamma$-isoform and non-muscle cells have the $\beta$-isoform and the $\gamma$-isoform. Actin has many roles in the cell. It is involved in muscle contraction actinomyosin, collapse of the axon growth cone, endocytosis, cytokinesis, cell migration, cell shape for the cytoskeleton, and signal-transduction pathways (*35*). Actin is very dynamic because it can polymerize and depolymerize. In its monomer form it is globular actin (g-actin) and when it polymerizes, it becomes

filamentous actin (f-actin also called microfilaments or thin filaments). ATP is required for actin polymerization. Actin binds ATP, hydrolyzes its phosphate and then begins assembling a filament. This filament has a structural polarity of a pointed end (minus) and a barbed end (plus) when polymerized. During depolymerization after the addition of salt, monomers are lost from the pointed end and the barbed end gains monomers. This process is dependent on the concentrations of monomers; the actin filament grows until it reaches the steady state known as the critical concentration (Cc). Actin polymers will continue to grow until their concentration is equal to the critical concentration ($C = C_c$) (*36*).

When actin is purified it binds to profilin. The profilin site where actin binds is homologous to the SH3 domain. This is interesting because it suggests that actin might bind to MICAL on its proline rich region where it has a SH3 domain. Profilin binds monomers and speeds elongation (polymerization). It does this by binding to g-actin and attracting more monomers to be added to the barbed-end (*37*). Oxidants such as $H_2O_2$ cause actin to depolymerize. Drugs and small molecules such as Cytochalasin D and Phalloidin alter polymerization. Cytochalasin D is an inhibitor, binding to the pointed end of f-actin and preventing any monomers to be added to that end. Phalloidin a drug found in poisonous mushrooms that also binds actin stabilizes filaments (*38*).

Many proteins associate with actin, such as cofilin, which severs actin monomers and causes depolymerization. DNase I binds very tightly to actin and removes actin monomers causing actin depolymerization. Myosin interacts with actin to allow cellular movements such as muscle contractions. Vimentin, a protein that interacts with MICAL, also interacts with actin (*17*).

Rab1 GTPases interact with MICAL. Rab1 GTPases are involved in vesicular trafficking between membranes of the endoplasmic reticulum and the Golgi (*39-41*). To determine the function of Rab1 GTPases, yeast two-hybrid screening was performed to find interactors of Rab1. Rab1 was found to interact with the C-terminal part of MICAL-1. Mammalian MICAL-1 interacted with both yeast and mammalian Rab1, suggesting that this relationship is evolutionarily conserved (*42*). MICAL-2 and MICAL-3 also were found to interact by their C-termini with Rab1 in the same way as MICAL-1. HeLa cells were stained before and after treatment with nocodazole (a drug that prevents polymerization of microtubules). The microtubules dissociated and MICAL-1 and MICAL-3 appeared to be disbursed throughout the cell. These data suggest that MICAL-1 and MICAL-3 associate with the cytoskeleton in the cell (*43*).

Similar to Rab1, Rab6 and Rab8 GTPases are also involved in vesicular trafficking between membranes of the endoplasmic reticulum and the Golgi (*44-48*). MICAL-3 was shown to interact with Rab8A through its C-terminus. Another protein, ELKS, a transcription activator implicated in neurodegenerative diseases such as Alzhiemer's disease, Huntington's disease (*49*), Down syndrome, depression, Parkinson's, drug addiction, and long-term memory loss (*50*), interacts with MICAL-3, but no interaction with ELKS was observed with MICAL-1. ELKS was found to interact with the C-terminal part of MICAL-3 (residues 1819-2002); this region includes the coiled-coils. This interaction was different than that observed for Rab8 (residues 1174-1819) which interacts on the C-terminus of MICAL-3; the area in which they interact does not include the last coiled-coil. Rab6 interacts with MICAL on the C-terminus between residues 950-1015. Coprecipitation experiments showed that Rab8A coprecipitated better with ELKS when MICAL-3 was present. Site-directed mutagenesis was used on the FAD binding motif of MICAL-3. Cells with this mutation made large quantities of secretory vesicles but these vesicles were immobile and unable to fuse with the

plasma membrane. Overexpression of the monooxygenase domain of MICAL-3 in cells decreased the amount of f-actin; overexpression of full-length MICAL-3 showed no effects on f-actin. It was suggested that MICAL-3 promotes the disassembly of cortical actin during vesicle fusion. Thus, MICAL-3, Rab6, and Rab8 are working together to control docking and fusion of exocytic carriers (*51*).

### 1.3.5 Inhibitors

The activity of MICAL is inhibited by the hydroxylase inhibitor (Figure 1-12) epigallocatechin-3-gallate (EGCG), both *in vitro* and *in vivo* (*21, 52*). Nadella *et al.* found EGCG to be a non-competitive inhibitor versus NADPH with a $K_i$ of 2 μM in the NADPH oxidase reaction of monoMICAL-1 (*21*). When monoMICAL-1 was titrated with increasing amounts of EGCG to determine inhibition velocity, the protein precipitated (*20*). Although EGCG is often claimed to be a specific hydroxylase inhibitor and used for that purpose in cell biology studies on MICAL, many other enzymes have been reported to be inhibited (*53-57*). Therefore, a need still remains for inhibitors specific for MICAL.

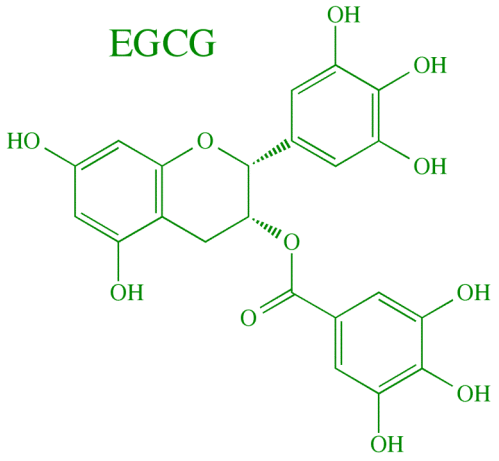


**Figure 1-12 Structure of EGCG**

Epigallocatechin-3-gallate (EGCG) a natural product found in green tea has been claimed to be an inhibitor specific for flavoprotein hydroxylases.

### 1.3.6 Different MICALs

Three MICALs (Figure 1-13) have been identified in mammals (MICAL-1, MICAL-2, and MICAL-3). While only one MICAL exists in *Drosophila*. In the cell MICAL-1 and MICAL-3 have been found to localize in the cytoplasm (*17, 22, 42*). Interestingly, it has not yet been determined where MICAL-2 resides in the cell. Various tissues express MICALs such as lung, thymus, spleen, testis, and brain (*17, 42*).

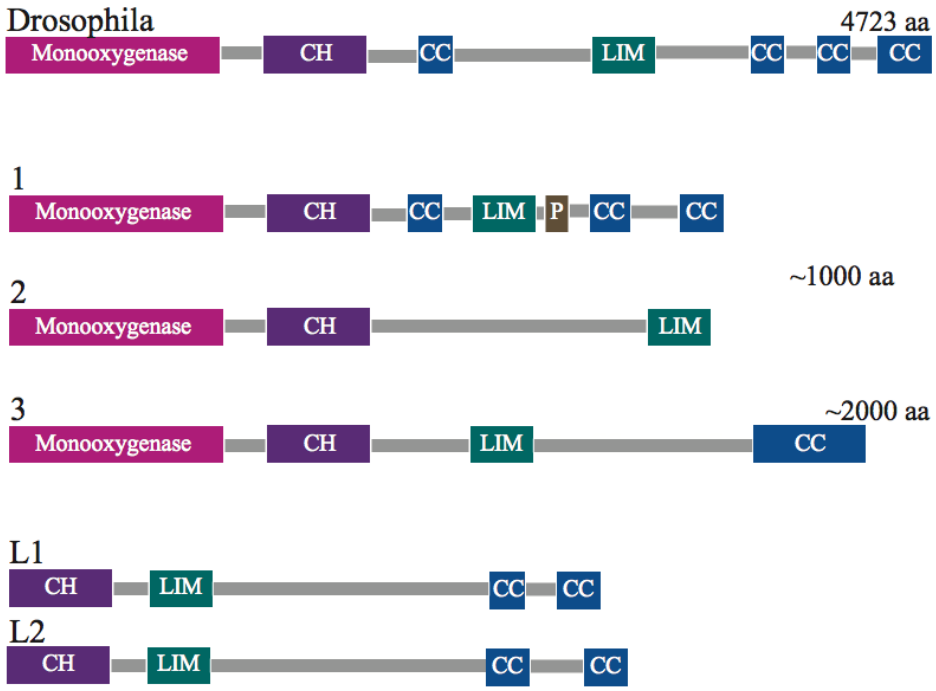


**Figure 1-13 Domains of various MICALs.**

The domain composition of the single MICAL from *Drosophila* and the three MICALs from mammals are shown. All have an N-terminal monooxygenase domain (pink) and CH and LIM domains (purple and blue, respectively). Several have additional domains. The MICAL-like proteins, L1 and L2, lack the N-terminal monooxygenase domain and are therefore, much less interesting; they participate in functions different from those that involve MICALs. Note figure is not to scale.

All MICALs have an N-terminal monooxygenase domain that binds FAD followed by C-terminal protein-protein interacting domains. The C-terminal domains of all MICALs have a CH and LIM domain. *Drosophila* MICAL is much larger than any of the MICALs identified in mammals; it has 4723 amino acids. MICALs from mammals are ~1000 amino acids in length except for MICAL-3, which is much larger with almost 2000 amino acids. MICAL-1 has the most domains with three coiled-coil regions and a proline-rich region. MICAL-3 has one coiled-coil region and *Drosophila* MICAL has four coiled-coil regions. MICALs are phosphorylated (Table 1-1). MICAL-1 is phosphorylated both *in vitro* (HEK293 cells) and *in vivo* (neuronal cells and brain lysates) (*58*). MICAL-2 was shown in human lung carcinoma to be phosphorylated on Tyr653 (*59*). MICAL-3 is phosphorylated on Ser649 and Thr684 (*60*). Human MICAL-1 is modified by ubiquination on lysine residues Lys488, Lys637, Lys1036. Human MICAL-2 is ubiquinated on Lys458, Lys634, and Lys646 and mouse MICAL-3 is ubiquinated on Lys1946. MICAL-2 and MICAL-3 are acetylated on lysine residues. Human MICAL-2 is ubiquinated on Lys597 and mouse MICAL-2 Lys705, Lys712, Lys714. Human MICAL-3 is acetylated on Lys117 and mouse MICAL-3 Lys1700, Lys1703, and Lys1704 (www.phosphosite.org).

| Mouse Enzyme | Phosphorylation | Acetylation | Ubiquination |
|---|---|---|---|
| MICAL-1 | S777 | | |
| MICAL-1 | S781 | | |
| MICAL-1 | S783 | | |
| MICAL-1 | S793 | | |
| MICAL-1 | S794 | | |
| MICAL-2 | T282 | | K705 |
| MICAL-2 | Y292 | | K712 |
| MICAL-2 | S507 | | K714 |
| MICAL-2 | S511 | | |
| MICAL-2 | S515 | | |
| MICAL-2 | S860 | | |
| MICAL-2 | S865 | | |
| MICAL-2 | S867 | | |
| MICAL-3 | T684 | K1946 | K1700 |
| MICAL-3 | S685 | | K1703 |
| MICAL-3 | S687 | | K1704 |
| MICAL-3 | S977 | | |
| MICAL-3 | S1131 | | |
| MICAL-3 | S1150 | | |
| MICAL-3 | S1153 | | |
| MICAL-3 | S1154 | | |
| MICAL-3 | S1167 | | |
| MICAL-3 | S1171 | | |
| MICAL-3 | S1179 | | |
| MICAL-3 | S1187 | | |
| MICAL-3 | T1195 | | |
| MICAL-3 | S1216 | | |
| MICAL-3 | T1289 | | |
| MICAL-3 | S1276 | | |
| MICAL-3 | T1292 | | |
| MICAL-3 | S1307 | | |
| MICAL-3 | S1356 | | |
| MICAL-3 | S1365 | | |
| MICAL-3 | S1369 | | |

**Table 1-1 Modifications of mouse MICALs**

(www.phosphosite.org).

*Drosophila* MICAL is believed to interact with plexin A during axon guidance. When axons develop in *Drosophila*, they exit the central nervous system by either entering the intersegmental nerve or the segmental nerve. Next, they move into five major nerve branches, which lead to individual muscles. Mutating residues that bind FAD in the monooxygenase domain of MICAL in *Drosophila* prevented axons from entering the intersegmental nerve or the segmental nerve. The few axons that did exit the nervous system either did not move past the major nerve branches or completely missed their target muscles. Similar effects

on axon motor deficiencies were seen when *Drosophila* MICAL was completely deleted (*52*). Thus the flavin chemistry controls the biology of MICAL. MICAL-1 from mouse is also important for axon guidance by interacting with the plexins A1 and A3 (*22*) as well as CRMP-1 and CRMP-2 (*22, 61*) and RanBPM (*62*). MICAL-1 from mouse interacts with NDR1 and NDR2 and regulate apoptosis (*58*). MICAL-1 was first discovered to interact with CasL and Vimentin (*17*) and be important for the cytoskeleton and in *Drosophila* f-actin is the putative substrate for MICAL (*19*). Another function for MICAL-1 has been suggested to be vesicle trafficking using Rab1, 8a, 10, 13, 15, 35, 36 (*42, 43, 51, 63, 64*) and in MICAL-2 Rab1 (*43*) and MICAL-3 by using Rab1, 8a, 35 and ELKS docking and fusion are other functions (*43, 51, 63, 64*).

There is only one MICAL in *Drosophila* while zebrafish have eight. In rodents and humans there are three MICALs. The monooxygenase domain of MICAL-2 from mouse was blasted against other published genomes. There was a wide range of monoMICALs identified from pigs, chicken, fish, and insects. Interestingly, MICAL is even hypothesized to have existed in monotremes such as the primitive platypus. All these species have a residues homologous to Trp405 (MICAL-2 numbering), which interacts with the *re* face of the flavin to create a charge-transfer interaction. Thus all these species are likely to have a charge-transfer interaction, suggesting that it may play some important role because of its conservation across a variety of species. The sequence of mouse monoMICAL-2 was 74% homologous to chicken, 77% homologous to fish, and 75% homologous to ticks.

Using blast to compare the monooxygenase of MICAL-1, the results were similar, but interestingly, monoMICAL-1 from mouse was also found in reptiles and Tasmanian devils. The sequence of Tasmanian devil monoMICAL-1 is 83% similar to mouse monoMICAL-1 while reptile is 64%. They also had a conserved

Trp400 (MICAL-1 numbering). The monooxygenase domain of MICAL-3 was also searched against different organisms and it was found to be similar to MICAL-1 and MICAL-2 except that it was also found in frogs and bats with a sequence homology to MICAL-3 of 86% and 78%, respectively. All monooxygenase domains of MICAL-3 had a conserved Trp405.

There are other proteins called MICAL-like. These are very similar to MICALs except they lack the N-terminal monooxygenase domain and instead have only the C-terminal domains; CH, LIM, and coil-coil. There are two MICAL-like proteins; MICAL-L1 and MICAL-L2 and both have two coiled-coil regions. The MICAL-L1 protein has been implicated in endocytic recycling (*65*) and functional tight junction formation (*66*). It is possible that MICALs evolved from a fusion of monooxygenase domains and the MICAL-like proteins.

### 1.3.7 Domains

The functions of the four protein-protein interaction domains in MICAL-1 remain unknown. However, studies of homologs in other systems show that, in general, these domains are important for signal transduction, protein-protein interactions and cytoskeletal organization.

#### 1.3.7.1 Calponin Homology (CH) Domain

MICALs have a calponin homology (CH) domain (~100 residues). CH domains (Figure 1-14) are homologous to calponin, an actin binding protein. However, the presence of a CH domain is not always an indicator of actin binding. There are three types of CH domains: single CH, CH1, and CH2 domains. Their classification is based on their sequence. Proteins can have one CH domain, two CH domains (made up of CH1 and CH2), or four CH domains comprised of a repeat of CH1 and CH2. The function of CH domains is not well-understood, but two CH domains, a CH1 domain followed by a CH2 domain, are required to bind

actin. CH2 domains are thought to assist CH1 domains to bind f-actin. CH2 domains contain a phosphatidylinositol 4,5-bisphosphate (PIP2) binding site. CH2 domains may be involved in the regulation of the activity of f-actin (*67*).

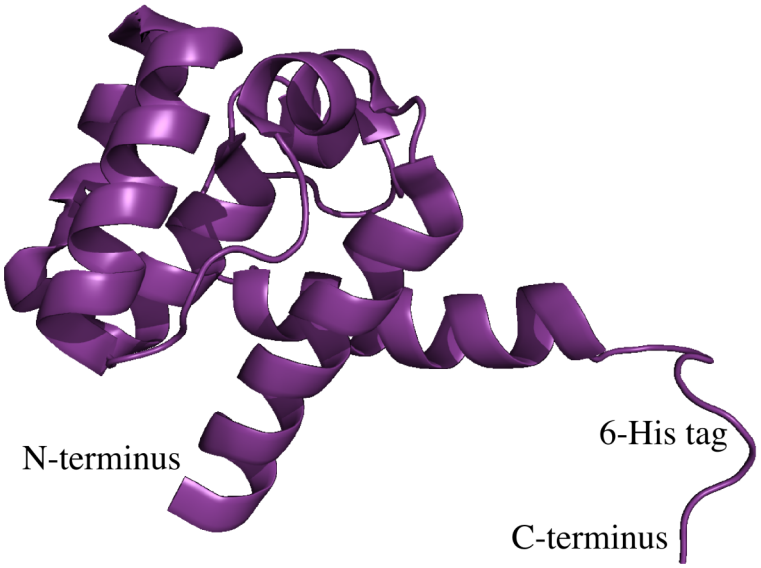


**Figure 1-14 Structure of the CH domain of human MICAL-1**

The structure of the heterologously expressed CH domain was determined by NMR. No evidence for binding to actin was found.

In MICAL-1 there is one CH2 domain. The structure of the CH domain of human MICAL-1 was solved by NMR. The structure of this 23 kDa domain is similar to other CH domains (*68*). $^{15}$N-HSQC titrations using the MICAL-1 CH domain and f-actin showed no spectral changes, demonstrating that they do not bind (*68*). The function of the CH domain of MICALs remains unknown.

### 1.3.7.2 LIM (LIN-11, Isl 1, MEC-3) Domain

A novel protein motif with many cysteine residues was found in three homeodomain proteins: **L**IN-11, **I**sl1, and **M**EC-3 (*69-71*). LIM domains have 8 highly conserved residues (mostly cysteines and histidines), which are zinc-binding residues. The LIM consensus sequence is $CX_2CX_{16-23}HX_2CX_2CX_2CX_{16-21}CX_2$(C/H/D); the X can be any amino acid. LIM domains can be classified into

four groups based on their arrangement and positioning of the LIM domain in the protein sequence. The first group has N-terminal LIM domains; these proteins typically function as transcription factors and are located in the nucleus of the cell. The second group of proteins has two or three LIM domains on their N-terminus or C-terminus and these proteins are located both in the cytoplasm and nucleus. The third group has LIM domains and other protein-protein interacting domains such as actin-targeting domains. The fourth group has a monooxygenase domain or kinase catalytic motif. The LIM domain of MICALs belongs to the fourth group and are thought to be involved in intermediate filament interactions.

Many proteins that associate with the actin cytoskeleton have LIM domains. Some proteins with LIM domains are also known to shuttle between the cytoplasm and nucleus and are involved with gene expression. LIM domains are believed to contribute to protein function by binding to other proteins, hence the term protein-protein interactors. Many of the LIM domains contained in proteins that residue in the cytoplasm have been identified to interact with f-actin. An example of this is actin-binding LIM protein (ABLIM) that binds f-actin and is involved in changing the morphology of the cell (*72, 73*). The exact role of LIM domains has not been identified but it is feasible to speculate that they may play a role in the binding and regulation of actin. The LIM domain of MICAL-1 is required for interaction with a nuclear kinase protein important for apoptosis (NDR1) (*58*). The LIM domain in MICAL-1 has been suggested to regulate the interaction of the C-terminal part of the protein with the monooxygenase domain (*22*).

#### 1.3.7.3 SH3 Domains

Src homology (SH3) domains interact with a conserved binding motif of PXXP (*74*). X can be any amino acid. The Proline-rich regions (Pro-rich) are often involved in signal transduction and are also important for interacting with other proteins to promote proper folding (*75, 76*). Many cytoskeletal proteins with Pro-rich regions are involved in protein-protein interactions (*77*) or facilitating cell compartmentalization (*78*). The Pro-rich regions of MICAL interact with the SH3 domains of CasL and Cas (*17*). The Pro-rich region motif in MICAL-1 is Pro-Pro-Lys-Pro-Pro. The Pro-rich region is found in MICAL-1 but not MICAL-2 or MICAL-3.

#### 1.3.7.4 Coiled-coil regions

Astbury discovered using x-ray photography the pattern of coiled-coil called the $\alpha$-pattern using Mozart's hair (*79*). Crick, Pauling, and Corey in the 1950s were the first to describe the structure of $\alpha$-keratin, which contained coiled-coils (*80, 81*). Coiled-coils can be right or left-handed turns. Right-handed turns have an eleven-residue repeat, and left-handed turns have a seven-residue repeat (heptad). The first and fourth residues are non-polar, and residues 5 and 7 are polar/charged. These heptads are also called leucine zippers. Coiled-coils all have a "knobs-into-holes" core which is composed of two ribbons (alpha-helices) coming together and twisting around each other (*82*). Proteins can have two or up to 200 coiled-coils (*83*). Intermediate-filaments have coiled-coil domains. Motor proteins such as myosin and kinesin also have coiled-coil regions. The most C-terminal domain found on MICAL-1 and MICAL-3 are coiled-coils. MICAL-2 is missing this domain. The coiled-coils of MICAL are similar by sequence identity to the proteins Ezrin, Radixin, and Moesin (ERM) proteins (*52, 84*). Interestingly, ERM proteins are proteins that link f-actin to other proteins and cell structures (*84*).

### 1.3.8 Diseases

For proper development of the nervous system, axons and dendrites use a mechanism called pruning in which they remove excess or incorrect projections. The method of pruning is very similar to the process of degeneration which occurs after an injury to an axon called Wallerian degeneration (*85*). This pathology has been observed after spinal cord injuries and in motor neuron diseases (*86*) such as Alzheimer's and Parkinson's disease (*87*). MICAL from *Drosophila* was found to be critical for severing of dendrites during pruning. Mutations were created using ethyl-methyl-sulfonate of *Drosophila* MICAL creating a truncated protein (1-534 amino acids). Flies with this truncated protein or mutations of full-length MICAL had severe defects in dendrites as pruning was inhibited. *Drosophila* were fully rescued when full-length MICAL was overexpressed in these mutants (*88*). Interestingly, when another protein, Sox14, was deleted MICAL mRNA and protein levels were dramatically reduced to almost undetectable levels. Overexpression of Sox14 resulted in induction of MICAL expression. MICAL was also able to rescue dendrite-pruning defects caused by Sox14 mutants. These results suggest that MICAL is a Sox14 downstream target (*88*).

The spinal cord and dorsal root ganglia express MICAL-1, 2, and 3 during development. Interestingly, in the adult rat nervous system in the white matter, MICAL-2 is not expressed. To determine if the levels of MICALs changed during spinal cord injury, rats were injured on their spine and their MICAL expression levels were measured (*89*). At the location of injury in the white matter, small cells (oligodendrocytes and meningeal fibroblasts) increased their expression of MICAL-1 and 3. The scar tissue of the injured rats had MICAL-2 expression in meningeal fibroblasts. There was also an increase in the surrounding white matter but highest levels were found at the location of injury. The high MICAL1 and 3 levels were observed for as long as 56 days. This finding suggests that

MICAL1 and 3 may be preventing neuronal regeneration after spinal cord injuries (*89*). MICAL-2 and MICAL-3 genes are possible therapeutic targets for muscle necrosis in Duchenne patents who suffer from skeletal muscle dystrophy (*90*).

MICAL-1 has been implicated in epilepsy. Epileptic seizures have been shown in studies to cause functional and morphological changes in neuronal dendritic spines. Damage to dendritic spines may cause damage to the cognitive part of the brain. F-actin is highly concentrated in dendritic spines (*91, 92*) and dendritic spines are directly affected by seizures (*92*). Mice were given 4-aminopyridine to induce seizures in the hippocampus. It was found that f-actin depolymerization was increased *in vitro* and *in vivo* (*93*). Seizures were found to cause the depolymerization of f-actin in dendrites (*93*). This finding led another group to investigate MICAL levels. Reports suggest that after seizures, remodeling of the hippocampus happens lasting until 15 days post seizures and then more seizures start happening afterward (*94*). It was found that MICAL-1 levels in the hippocampus increased in rats after pilocarpine-induced seizures, and decreased over time to levels below normal by day 7-14 (*95*). This suggests that MICAL-1 increases after injury to the brain from epileptic seizures, also causing actin depolymerization to increase, and that the low-levels of MICAL-1 allow networks to reform, causing seizure relapse. Temporal lobe cortex MICAL-1 levels in rat and human samples also decreased after seizures (*95*).

Five MICAL homologs have been detected in the heart of embryonic zebrafish (MICAL-1, 2a, 2b, 3a, 3b). Expression of MICAL-2a was detected as early as 24 hours post-fertilization in zebrafish. MICAL expression in the heart during development of the zebrafish shows that MICALs may play a key role in the development of the cardiovascular system (*96*).

MICAL-2 is implicated in controlling the aggressiveness of prostate and breast cancer. MICAL-2 variants were found to have high expression in prostate cancer cells *in vivo* and *in vitro*. Gleason scores are used as a pathology grade-scale to differentiate less from more aggressive tumors. Prostate cancer cells with high levels of MICAL-2 variants also had high Gleason scores, making a worse prognosis likely. Knocking down MICAL-2 variants in human prostate cancer cell lines by siRNA resulted in cell viability decreasing substantially. These findings suggest that MICAL-2 could be a target for prostate cancer therapies (*97*). Human breast cancer cells were found to have increases in semaphorin3b and MICAL-2. These increases were regulated by estrogen and the estrogen receptor ERβ (*98*). Estrogen receptors have two subtypes, ERα and ERβ. However, higher levels of ERs correlate with more aggressive breast cancers.

### 1.4 Purpose of this thesis

It is clear that MICALs are very important in many biological processes. It is also clear that the monooxygenase domain is critical for MICAL's activity. The other C-terminal domains of MICAL control the target that the monooxygenase acts on. MICAL's putative substrate, actin has also been identified. Therefore, I have set out to study the catalytic cycle of monoMICAL-2 in detail in the presence and absence of actin in order to set the stage for learning how the other domains and its substrate alter its activity.

## 1.5 References


1. Bhaskar, K. R., Bhat, S. N., Singh, S., and Rao, C. N. R. (1966) Spectroscopic studies of the donor properties of triphenyl-amine, -phosphine, -arsine and -stibine interaction with iodine and phenol, J. Inorg. Nucl. Chem. 28, 1915-1925.
2. Sucharitakul, J., Prongjit, M., Haltrich, D., and Chaiyen, P. (2008) Detection of a C4a-hydroperoxyflavin intermediate in the reaction of a flavoprotein oxidase, Biochemistry 47, 8485-8490.
3. Pennati, A., and Gadda, G. (2011) Stabilization of an intermediate in the oxidative half-reaction of human liver glycolate oxidase, Biochemistry 50, 1-3.
4. Zhao, G., Bruckner, R. C., and Jorns, M. S. (2008) Identification of the oxygen activation site in monomeric sarcosine oxidase: role of Lys265 in catalysis, Biochemistry 47, 9124-9135.
5. McDonald, C. A., Fagan, R. L., Collard, F., Monnier, V. M., and Palfey, B. A. (2011) Oxygen reactivity in flavoenzymes: context matters, J. Am. Chem. Soc. 133, 16809-16811.
6. van Berkel, W. J., Kamerbeek, N. M., and Fraaije, M. W. (2006) Flavoprotein monooxygenases, a diverse class of oxidative biocatalysts, J. Biotechnol. 124, 670-689.
7. Palfey, B. A., and McDonald, C. A. (2010) Control of catalysis in flavin-dependent monooxygenases, Arch. Biochem. Biophys. 493, 26-36.
8. Gatti, D. L., Palfey, B. A., Lah, M. S., Entsch, B., Massey, V., Ballou, D. P., and Ludwig, M. L. (1994) The mobile flavin of 4-OH benzoate hydroxylase, Science 266, 110-114.
9. Entsch, B., Ballou, D. P., and Massey, V. (1976) Flavin-oxygen derivatives involved in hydroxylation by p-hydroxybenzoate hydroxylase, J. Biol. Chem. 251, 2550-2563.

10. Alfieri, A., Malito, E., Orru, R., Fraaije, M. W., and Mattevi, A. (2008) Revealing the moonlighting role of NADP in the structure of a flavin-containing monooxygenase, Proc. Natl. Acad. Sci. U. S. A. 105, 6572-6577.
11. Jones, K. C., and Ballou, D. P. (1986) Reactions of the 4a-hydroperoxide of liver microsomal flavin-containing monooxygenase with nucleophilic and electrophilic substrates, J. Biol. Chem. 261, 2553-2559.
12. Suzuki, T., Nakamoto, T., Ogawa, S., Seo, S., Matsumura, T., Tachibana, K., Morimoto, C., and Hirai, H. (2002) MICAL, a novel CasL interacting molecule, associates with vimentin, J. Biol. Chem. 277, 14933-14941.
13. Zucchini, D., Caprini, G., Pasterkamp, R. J., Tedeschi, G., and Vanoni, M. A. (2011) Kinetic and spectroscopic characterization of the putative monooxygenase domain of human MICAL-1, Arch. Biochem. Biophys. 515, 1-13.
14. Hung, R. J., Yazdani, U., Yoon, J., Wu, H., Yang, T., Gupta, N., Huang, Z., van Berkel, W. J., and Terman, J. R. (2010) Mical links semaphorins to F-actin disassembly, Nature 463, 823-827.
15. Hung, R. J., Pak, C. W., and Terman, J. R. (2011) Direct redox regulation of F-actin assembly and disassembly by Mical, Science 334, 1710-1713.
16. Nadella, M., Bianchet, M. A., Gabelli, S. B., Barrila, J., and Amzel, L. M. (2005) Structure and activity of the axon guidance protein MICAL, Proc. Natl. Acad. Sci. U.S.A. 102, 16830-16835.
17. Schmidt, E. F., Shim, S. O., and Strittmatter, S. M. (2008) Release of MICAL autoinhibition by semaphorin-plexin signaling promotes interaction with collapsin response mediator protein, J. Neurosci. 28, 2287-2297.
18. Siebold, C., Berrow, N., Walter, T. S., Harlos, K., Owens, R. J., Stuart, D. I., Terman, J. R., Kolodkin, A. L., Pasterkamp, R. J., and Jones, E. Y. (2005) High-resolution structure of the catalytic region of MICAL (molecule

interacting with CasL), a multidomain flavoenzyme-signaling molecule, Proc. Natl. Acad. Sci. U.S.A. 102, 16836-16841.

19. Ivaska, J., Pallari, H. M., Nevo, J., and Eriksson, J. E. (2007) Novel functions of vimentin in cell adhesion, migration, and signaling, Exp. Cell Res. 313, 2050-2062.
20. Satelli, A., and Li, S. (2011) Vimentin in cancer and its potential as a molecular target for cancer therapy, Cell Mol. Life Sci. 68, 3033-3046.
21. Eckes, B., Dogic, D., Colucci-Guyon, E., Wang, N., Maniotis, A., Ingber, D., Merckling, A., Langa, F., Aumailley, M., Delouvee, A., Koteliansky, V., Babinet, C., and Krieg, T. (1998) Impaired mechanical stability, migration and contractile capacity in vimentin-deficient fibroblasts, J. Cell Sci. 111 ( Pt 13), 1897-1907.
22. Eckes, B., Colucci-Guyon, E., Smola, H., Nodder, S., Babinet, C., Krieg, T., and Martin, P. (2000) Impaired wound healing in embryonic and adult mice lacking vimentin, J. Cell Sci. 113 ( Pt 13), 2455-2462.
23. Hergovich, A., Stegert, M. R., Schmitz, D., and Hemmings, B. A. (2006) NDR kinases regulate essential cell processes from yeast to humans, Nat. Rev. Mol. Cell Biol. 7, 253-264.
24. Zhou, Y., Adolfs, Y., Pijnappel, W. W., Fuller, S. J., Van der Schors, R. C., Li, K. W., Sugden, P. H., Smit, A. B., Hergovich, A., and Pasterkamp, R. J. (2011) MICAL-1 is a negative regulator of MST-NDR kinase signaling and apoptosis, Mol. Cell Biol. 31, 3603-3615.
25. Zhao B Fau - Li, L., Li L Fau - Lei, Q., Lei Q Fau - Guan, K.-L., and KL, G. (2010) - The Hippo-YAP pathway in organ size control and tumorigenesis: an updated version, Genes Dev. 24, 862-874.
26. Wang, L. H., and Strittmatter, S. M. (1996) A family of rat CRMP genes is differentially expressed in the nervous system, J. Neurosci. 16, 6197-6207.

27. Fukada, M., Watakabe, I., Yuasa-Kawada, J., Kawachi, H., Kuroiwa, A., Matsuda, Y., and Noda, M. (2000) Molecular characterization of CRMP5, a novel member of the collapsin response mediator protein family, J. Biol. Chem. 275, 37957-37965.
28. Minturn, J. E., Fryer, H. J., Geschwind, D. H., and Hockfield, S. (1995) TOAD-64, a gene expressed early in neuronal differentiation in the rat, is related to unc-33, a C. elegans gene involved in axon outgrowth, J. Neurosci. 15, 6757-6766.
29. Goshima, Y., Nakamura, F., Strittmatter, P., and Strittmatter, S. M. (1995) Collapsin-induced growth cone collapse mediated by an intracellular protein related to UNC-33, Nature 376, 509-514.
30. Neuhaus, J. M., Wanger, M., Keiser, T., and Wegner, A. (1983) Treadmilling of actin, J. Muscle Res. Cell Motil. 4, 507-527.
31. Wegner, A., and Isenberg, G. (1983) 12-fold difference between the critical monomer concentrations of the two ends of actin filaments in physiological salt conditions, Proc. Natl. Acad. Sci. U. S. A. 80, 4922-4925.
32. Dominguez, R., and Holmes, K. C. (2011) Actin structure and function, Annu. Rev. Biophys. 40, 169-186.
33. Cooper, J. A. (1987) Effects of cytochalasin and phalloidin on actin, J. Cell Biol. 105, 1473-1478.
34. Sutherland, J. D., and Witke, W. (1999) Molecular genetic approaches to understanding the actin cytoskeleton, Curr. Opin. Cell Biol. 11, 142-151.
35. Tisdale, E. J., Bourne, J. R., Khosravi-Far, R., Der, C. J., and Balch, W. E. (1992) GTP-binding mutants of rab1 and rab2 are potent inhibitors of vesicular transport from the endoplasmic reticulum to the Golgi complex, J. Cell Biol. 119, 749-761.

36. Saraste, J., Lahtinen, U., and Goud, B. (1995) Localization of the small GTP-binding protein rab1p to early compartments of the secretory pathway, J. Cell Sci. 108 ( Pt 4), 1541-1552.
37. Nuoffer, C., Davidson, H. W., Matteson, J., Meinkoth, J., and Balch, W. E. (1994) A GDP-bound of rab1 inhibits protein export from the endoplasmic reticulum and transport between Golgi compartments, J. Cell Biol. 125, 225-237.
38. Weide, T., Teuber, J., Bayer, M., and Barnekow, A. (2003) MICAL-1 isoforms, novel rab1 interacting proteins, Biochem. Biophys. Res. Commun. 306, 79-86.
39. Fischer, J., Weide, T., and Barnekow, A. (2005) The MICAL proteins and rab1: a possible link to the cytoskeleton?, Biochem. Biophys. Res. Commun. 328, 415-423.
40. Huber, L. A., Pimplikar, S., Parton, R. G., Virta, H., Zerial, M., and Simons, K. (1993) Rab8, a small GTPase involved in vesicular traffic between the TGN and the basolateral plasma membrane, J. Cell Biol. 123, 35-45.
41. Ang, A. L., Folsch, H., Koivisto, U. M., Pypaert, M., and Mellman, I. (2003) The Rab8 GTPase selectively regulates AP-1B-dependent basolateral transport in polarized Madin-Darby canine kidney cells, J. Cell Biol. 163, 339-350.
42. Grigoriev, I., Splinter, D., Keijzer, N., Wulf, P. S., Demmers, J., Ohtsuka, T., Modesti, M., Maly, I. V., Grosveld, F., Hoogenraad, C. C., and Akhmanova, A. (2007) Rab6 regulates transport and targeting of exocytotic carriers, Dev. Cell 13, 305-314.
43. Sato, T., Mushiake, S., Kato, Y., Sato, K., Sato, M., Takeda, N., Ozono, K., Miki, K., Kubo, Y., Tsuji, A., Harada, R., and Harada, A. (2007) The Rab8 GTPase regulates apical protein localization in intestinal cells, Nature 448, 366-369.

44. Hattula, K., Furuhjelm, J., Tikkanen, J., Tanhuanpaa, K., Laakkonen, P., and Peranen, J. (2006) Characterization of the Rab8-specific membrane traffic route linked to protrusion formation, J. Cell Sci. 119, 4866-4877.
45. Sharma, A., Callahan, L. M., Sul, J. Y., Kim, T. K., Barrett, L., Kim, M., Powers, J. M., Federoff, H., and Eberwine, J. (2010) A neurotoxic phosphoform of Elk-1 associates with inclusions from multiple neurodegenerative diseases, PLoS One 5, e9002.
46. Besnard, A., Galan-Rodriguez, B., Vanhoutte, P., and Caboche, J. (2011) Elk-1 a transcription factor with multiple facets in the brain, Front. Neurosci. 5, 35.
47. Grigoriev, I., Yu, K. L., Martinez-Sanchez, E., Serra-Marques, A., Smal, I., Meijering, E., Demmers, J., Peranen, J., Pasterkamp, R. J., van der Sluijs, P., Hoogenraad, C. C., and Akhmanova, A. (2011) Rab6, Rab8, and MICAL3 cooperate in controlling docking and fusion of exocytotic carriers, Curr. Biol. 21, 967-974.
48. Nadella, M., Bianchet, M. A., Gabelli, S. B., Barrila, J., and Amzel, L. M. (2005) Structure and activity of the axon guidance protein MICAL, Proc. Natl. Acad. Sci. U. S. A. 102, 16830-16835.
49. Terman, J. R., Mao, T., Pasterkamp, R. J., Yu, H. H., and Kolodkin, A. L. (2002) MICALs, a family of conserved flavoprotein oxidoreductases, function in plexin-mediated axonal repulsion, Cell 109, 887-900.
50. Noberini, R., Koolpe, M., Lamberto, I., and Pasquale, E. B. (2012) Inhibition of Eph receptor-ephrin ligand interaction by tea polyphenols, Pharmacol. Res. 66, 363-373.
51. Soler, F., Asensio, M. C., and Fernandez-Belda, F. (2012) Inhibition of the intracellular Ca(2+) transporter SERCA (Sarco-Endoplasmic Reticulum Ca(2+)-ATPase) by the natural polyphenol epigallocatechin-3-gallate, J. Bioenerg. Biomembr. 44, 597-605.

52. Weng, Z., Greenhaw, J., Salminen, W. F., and Shi, Q. (2012) Mechanisms for epigallocatechin gallate induced inhibition of drug metabolizing enzymes in rat liver microsomes, Toxicol. Lett. 214, 328-338.

53. Nguyen, T. T., Moon, Y. H., Ryu, Y. B., Kim, Y. M., Nam, S. H., Kim, M. S., Kimura, A., and Kim, D. (2013) The influence of flavonoid compounds on the in vitro inhibition study of a human fibroblast collagenase catalytic domain expressed in E. coli, Enzyme Microb. Technol. 52, 26-31.

54. Misaka, S., Kawabe, K., Onoue, S., Werba, J. P., Giroli, M., Tamaki, S., Kan, T., Kimura, J., Watanabe, H., and Yamada, S. (2012) Effects of Green Tea Catechins on Cytochrome P450 2B6, 2C8, 2C19, 2D6 and 3A Activities in Human Liver and Intestinal Microsomes, Drug Metab. Pharmacokinet.

55. Zhou, Y., Gunput, R. A., Adolfs, Y., and Pasterkamp, R. J. (2011) MICALs in control of the cytoskeleton, exocytosis, and cell death, Cell Mol. Life Sci. 68, 4033-4044.

56. Rikova, K., Guo, A., Zeng, Q., Possemato, A., Yu, J., Haack, H., Nardone, J., Lee, K., Reeves, C., Li, Y., Hu, Y., Tan, Z., Stokes, M., Sullivan, L., Mitchell, J., Wetzel, R., Macneill, J., Ren, J. M., Yuan, J., Bakalarski, C. E., Villen, J., Kornhauser, J. M., Smith, B., Li, D., Zhou, X., Gygi, S. P., Gu, T. L., Polakiewicz, R. D., Rush, J., and Comb, M. J. (2007) Global survey of phosphotyrosine signaling identifies oncogenic kinases in lung cancer, Cell 131, 1190-1203.

57. Dephoure, N., Zhou, C., Villen, J., Beausoleil, S. A., Bakalarski, C. E., Elledge, S. J., and Gygi, S. P. (2008) A quantitative atlas of mitotic phosphorylation, Proc. Natl. Acad. Sci. U. S. A. 105, 10762-10767.

58. Morinaka, A., Yamada, M., Itofusa, R., Funato, Y., Yoshimura, Y., Nakamura, F., Yoshimura, T., Kaibuchi, K., Goshima, Y., Hoshino, M., Kamiguchi, H., and Miki, H. (2011) Thioredoxin mediates oxidation-

dependent phosphorylation of CRMP2 and growth cone collapse, Sci. Signal. 4, ra26.

59. Togashi, H., Schmidt, E. F., and Strittmatter, S. M. (2006) RanBPM contributes to Semaphorin3A signaling through plexin-A receptors, J. Neurosci. 26, 4961-4969.

60. Yamamura, R., Nishimura, N., Nakatsuji, H., Arase, S., and Sasaki, T. (2008) The interaction of JRAB/MICAL-L2 with Rab8 and Rab13 coordinates the assembly of tight junctions and adherens junctions, Mol. Biol. Cell 19, 971-983.

61. Fukuda, M., Kanno, E., Ishibashi, K., and Itoh, T. (2008) Large scale screening for novel rab effectors reveals unexpected broad Rab binding specificity, Mol. Cell. Proteomics 7, 1031-1042.

62. Rahajeng, J., Giridharan, S. S., Cai, B., Naslavsky, N., and Caplan, S. (2010) Important relationships between Rab and MICAL proteins in endocytic trafficking, World J. Biol. Chem. 1, 254-264.

63. Nakatsuji, H., Nishimura, N., Yamamura, R., Kanayama, H. O., and Sasaki, T. (2008) Involvement of actinin-4 in the recruitment of JRAB/MICAL-L2 to cell-cell junctions and the formation of functional tight junctions, Mol. Cell. Biol. 28, 3324-3335.

64. Fukami, K., Furuhashi, K., Inagaki, M., Endo, T., Hatano, S., and Takenawa, T. (1992) Requirement of phosphatidylinositol 4,5-bisphosphate for alpha-actinin function, Nature 359, 150-152.

65. Sun, H., Dai, H., Zhang, J., Jin, X., Xiong, S., Xu, J., Wu, J., and Shi, Y. (2006) Solution structure of calponin homology domain of Human MICAL-1, J. Biomol. NMR 36, 295-300.

66. Way, J. C., and Chalfie, M. (1988) mec-3, a homeobox-containing gene that specifies differentiation of the touch receptor neurons in C. elegans, Cell 54, 5-16.

67. Freyd, G., Kim, S. K., and Horvitz, H. R. (1990) Novel cysteine-rich motif and homeodomain in the product of the Caenorhabditis elegans cell lineage gene lin-11, Nature 344, 876-879.
68. Roof, D. J., Hayes, A., Adamian, M., Chishti, A. H., and Li, T. (1997) Molecular characterization of abLIM, a novel actin-binding and double zinc finger protein, J. Cell. Biol. 138, 575-588.
69. Barrientos, T., Frank, D., Kuwahara, K., Bezprozvannaya, S., Pipes, G. C., Bassel-Duby, R., Richardson, J. A., Katus, H. A., Olson, E. N., and Frey, N. (2007) Two novel members of the ABLIM protein family, ABLIM-2 and -3, associate with STARS and directly bind F-actin, J. Biol. Chem. 282, 8393-8403.
70. Ren, R., Mayer, B. J., Cicchetti, P., and Baltimore, D. (1993) Identification of a ten-amino acid proline-rich SH3 binding site, Science 259, 1157-1161.
71. Williamson, M. P. (1994) The structure and function of proline-rich regions in proteins, Biochem. J. 297 ( Pt 2), 249-260.
72. Kay, B. K., Williamson, M. P., and Sudol, M. (2000) The importance of being proline: the interaction of proline-rich motifs in signaling proteins with their cognate domains, FASEB J. 14, 231-241.
73. Koch, C. A., Anderson, D., Moran, M. F., Ellis, C., and Pawson, T. (1991) SH2 and SH3 domains: elements that control interactions of cytoplasmic signaling proteins, Science 252, 668-674.
74. Bar-Sagi, D., Rotin, D., Batzer, A., Mandiyan, V., and Schlessinger, J. (1993) SH3 domains direct cellular localization of signaling molecules, Cell 74, 83-91.
75. Parry, D. A., Fraser, R. D., and Squire, J. M. (2008) Fifty years of coiled-coils and alpha-helical bundles: a close relationship between sequence and structure, J. Struct. Biol. 163, 258-269.

76. Pauling, L., and Corey, R. B. (1953) Compound helical configurations of polypeptide chains: structure of proteins of the alpha-keratin type, Nature 171, 59-61.
77. Crick, F. (1953) The packing of [alpha]-helices: simple coiled-coils, Acta. Crystallographica 6, 689-697.
78. Mason, J. M., and Arndt, K. M. (2004) Coiled coil domains: stability, specificity, and biological implications, Chembiochem. 5, 170-176.
79. Kohn, W. D., Mant, C. T., and Hodges, R. S. (1997) Alpha-helical protein assembly motifs, J. Biol. Chem. 272, 2583-2586.
80. Bretscher, A., Chambers, D., Nguyen, R., and Reczek, D. (2000) ERM-Merlin and EBP50 protein families in plasma membrane organization and function, Annu. Rev. Cell. Dev. Biol. 16, 113-143.
81. Luo, L., and O'Leary, D. D. (2005) Axon retraction and degeneration in development and disease, Annu. Rev. Neurosci. 28, 127-156.
82. Azzouz, M., Leclerc, N., Gurney, M., Warter, J. M., Poindron, P., and Borg, J. (1997) Progressive motor neuron impairment in an animal model of familial amyotrophic lateral sclerosis, Muscle Nerve. 20, 45-51.
83. Iseki, E., Kato, M., Marui, W., Ueda, K., and Kosaka, K. (2001) A neuropathological study of the disturbance of the nigro-amygdaloid connections in brains from patients with dementia with Lewy bodies, J. Neurol. Sci. 185, 129-134.
84. Kirilly, D., Gu, Y., Huang, Y., Wu, Z., Bashirullah, A., Low, B. C., Kolodkin, A. L., Wang, H., and Yu, F. (2009) A genetic pathway composed of Sox14 and Mical governs severing of dendrites during pruning, Nat. Neurosci. 12, 1497-1505.
85. Pasterkamp, R. J., Dai, H. N., Terman, J. R., Wahlin, K. J., Kim, B., Bregman, B. S., Popovich, P. G., and Kolodkin, A. L. (2006) MICAL flavoprotein monooxygenases: expression during neural development and following spinal cord injuries in the rat, Mol. Cell. Neurosci. 31, 52-69.

86. Marotta, M., Ruiz-Roig, C., Sarria, Y., Peiro, J. L., Nu√±ez, F., Ceron, J., Munell, F., and Roig-Quilis, M. (2009) Muscle genome-wide expression profiling during disease evolution in mdx mice, Physiol. genom. 37, 119-132.
87. Xue, Y., Kuok, C., Xiao, A., Zhu, Z., Lin, S., and Zhang, B. (2010) Identification and expression analysis of< i> mical</i> family genes in zebrafish, J. of Genet. Genomics 37, 685-693.
88. Ashida, S., Furihata, M., Katagiri, T., Tamura, K., Anazawa, Y., Yoshioka, H., Miki, T., Fujioka, T., Shuin, T., Nakamura, Y., and Nakagawa, H. (2006) Expression of novel molecules, MICAL2-PV (MICAL2 prostate cancer variants), increases with high Gleason score and prostate cancer progression, Clin. Cancer Res. 12, 2767-2773.
89. Chang, E. C., Frasor, J., Komm, B., and Katzenellenbogen, B. S. (2006) Impact of estrogen receptor Œ≤ on gene networks regulated by estrogen receptor Œ± in breast cancer cells, Endocrinology 147, 4831-4842.
90. Capani, F., Martone, M. E., Deerinck, T. J., and Ellisman, M. H. (2001) Selective localization of high concentrations of F,Äêactin in subpopulations of dendritic spines in rat central nervous system: A three,Äêdimensional electron microscopic study, J. compar. neurol. 435, 156-170.
91. Swann, J. W., Al,ÄêNoori, S., Jiang, M., and Lee, C. L. (2000) Spine loss and other dendritic abnormalities in epilepsy, Hippocampus 10, 617-625.
92. Ouyang, Y., Yang, X. F., Hu, X. Y., Erbayat-Altay, E., Zeng, L. H., Lee, J. M., and Wong, M. (2007) Hippocampal seizures cause depolymerization of filamentous actin in neurons independent of acute morphological changes, Brain Res. 1143, 238-246.
93. Becker, A. J., Chen, J., Zien, A., Sochivko, D., Normann, S., Schramm, J., Elger, C. E., Wiestler, O. D., and Blumcke, I. (2003) Correlated stage- and subfield-associated hippocampal gene expression patterns in

experimental and human temporal lobe epilepsy, Eur. J. Neurosci. 18, 2792-2802.

94. Luo, J., Xu, Y., Zhu, Q., Zhao, F., Zhang, Y., Peng, X., Wang, W., and Wang, X. (2011) Expression pattern of Mical-1 in the temporal neocortex of patients with intractable temporal epilepsy and pilocarpine-induced rat model, Synapse 65, 1213-1221.

95. Palfey, B. A., Bjornberg, O., and Jensen, K. F. (2001) Specific inhibition of a family 1A dihydroorotate dehydrogenase by benzoate pyrimidine analogues, J Med Chem 44, 2861-2864.

96. Palfey, B. A., Bjornberg, O., and Jensen, K. F. (2001) Insight into the chemistry of flavin reduction and oxidation in Escherichia coli dihydroorotate dehydrogenase obtained by rapid reaction studies, Biochemistry 40, 4381-4390.

97. Palfey, B. A., Basu, R., Frederick, K. K., Entsch, B., and Ballou, D. P. (2002) Role of protein flexibility in the catalytic cycle of p-hydroxybenzoate hydroxylase elucidated by the Pro293Ser mutant, Biochemistry 41, 8438-8446.

# Chapter 2
# Actin Stimulates the Reduction of the MICAL-2 Monooxygenase Domain

## 2.1 Introduction

MICALs are large multi-domain flavin-dependent monooxygenases that use redox chemistry to cause actin to depolymerize (*1, 2*). The actin cytoskeleton is fundamentally important for most cellular developmental processes. MICAL is vital in the development of axons (*3*) and the viability of prostate cancer cells (*4*). There are three MICAL isozymes found in vertebrates: MICAL-1, MICAL-2, and MICAL-3. All MICALs have an N-terminal flavin-dependent monooxygenase domain (monoMICAL) (Figure 2-1) followed by a calponin homology region (CH domain) and a LIM domain. MICAL-1 has two more domains after the LIM domain: a proline-rich region and coiled-coils. MICAL-3 is missing the proline-rich region but has four domains including the coiled-coils. MICAL-2 only has three domains (Figure 2-1). Studies on *Drosophila* have demonstrated that the flavin of the monooxygenase domain of MICAL is vital for its signal-transduction function (*3*). Some enzymology has been reported for MICALs (*5*), but none for MICAL-2. Detailed mechanistic enzymological studies are needed to understand how this monooxygenase causes actin depolymerization.

The key intermediate in flavin monooxygenase chemistry is the flavin-hydroperoxide. The hydroperoxide is a versatile reagent, able to oxygenate nucleophiles or electrophiles (*6*). The hydroperoxide is produced on the enzyme by the reaction of reduced flavin with dioxygen. Reduced flavin is produced by the reaction of oxidized flavin with reduced pyridine nucleotide. Monooxygenases regulate catalysis in different ways (*6*). Regulation is important because the flavin

hydroperoxide is unstable and if no substrate is present, it will eventually decay to oxidized flavin and hydrogen peroxide, producing a toxin and wasting valuable reducing equivalents. Different classes of monooxygenases have different regulatory strategies. The aromatic hydroxylases (Class A) (*7*) do not allow rapid flavin reduction unless substrate is present. In contrast the Class B monooxygenases rapidly react with NAD(P)H and $O_2$ but stabilize the hydroperoxide.

monoMICAL has properties of both the aromatic hydroxylases and the Class B monooxygenases. The structure of the monooxygenase domain of MICAL is very similar to aromatic hydroxylases such as *p*-hydroxybenzoate hydroxylase (PHBH) (*8, 9*). Aromatic hydroxylases like PHBH have a unique flavin conformational change; the flavin moves from a buried “in” conformation to an exposed “out” conformation (*6*). These conformational changes were also observed in the crystal structures of monoMICAL-1 (*8, 9*). In the structure of the oxidized monooxygenase domain, the flavin is in the “out” conformation (Figure 2-1). In the structure of the reduced monooxygenase domain, the flavin adopts both conformations. Contrasting its structural similarities to aromatic hydroxylases, monoMICAL-1 has been found to oxygenate Met44 on f-actin, making methionine sulfoxide (*10*). The oxygenation of thioethers by Class B monooxygenases is well known but that reaction has never been reported for aromatic hydroxylases. Therefore, monoMICAL is uniquely exhibiting characteristics of both groups.

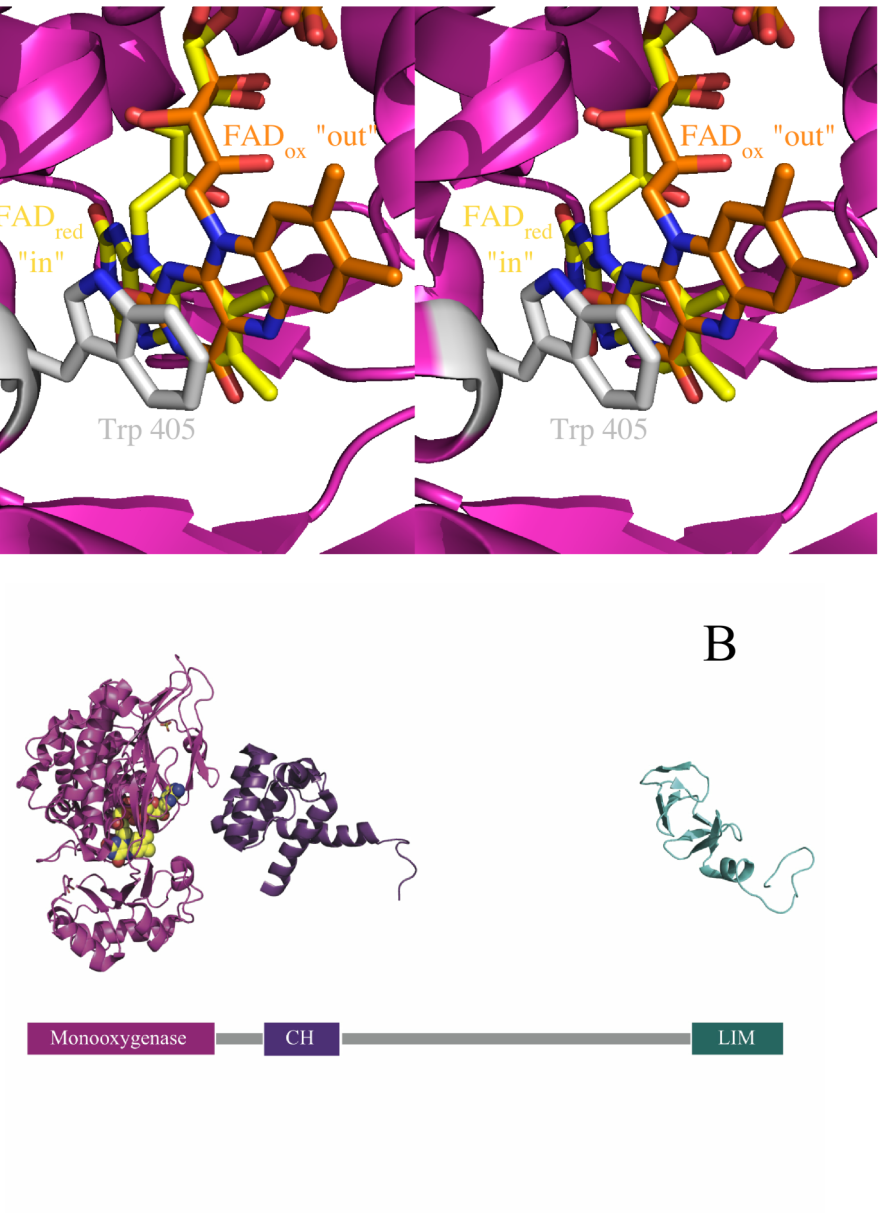


**Figure 2-1 Structures of oxidized and reduced human monoMICAL-1**

**A.** Structures of oxidized and reduced human monoMICAL-1. The “in” conformation of the flavin, from the reduced structure (2C4C), is shown in yellow. The “out” conformation is shown in orange (2BRY). Note Trp 405 (platinum), which stacks on the isoalloxazine in the “out” conformation. **B.** Domains of MICAL-2. The N-terminal monooxygenase domain of MICAL-2, shown in pink, is followed by the CH domain in purple and the C-terminal LIM domain in blue. Cartoons of structures of each domain (2BRY, 2DK9, and 1IML) are placed above their position in the domain diagram, after the fashion of Siebold *et. al.* (*8*).

A detailed examination of the steps in the catalytic cycle is needed to further learn which group monoMICAL most resembles – an important first step in uncovering the regulation of the chemistry by cellular signals. The reductive half-reaction is a key difference between the two groups of monooxygenases. Here we examine the reductive half-reaction kinetically to find out which model of regulation applies to monoMICAL. We find that monoMICAL-2 reacts with NADPH slowly, but in the presence of f-actin, reduction is stimulated. monoMICAL-2 has a preference for NADPH over NADH. Similar to aromatic hydroxylases, monoMICAL-2 transfers the *pro-R* hydride of NADPH.

## 2.2 Experimental Procedures

### 2.2.1 Expression construct.

To construct the pMICAL-2 plasmid, the segment of the MICAL-2 gene encoding the monooxygenase domain of MICAL-2 (residues 1-494) from *Mus musculus* was cloned from Mammalian Gene Collection MICAL-2 cDNA Clone ID 40061128 (Thermo Scientific). The MICAL-2 monooxygenase gene was amplified using primers 5'-TACTTCCAATCCAATGCCATGGGAGAGAATGAAGATGAGAAG and 5'-TTATCCACTTCCAATGCTAGTCCATCTCCTTAGTGATGTACAAAT (Invitrogen). To generate an overhang for ligation-independent cloning (LIC), the PCR product was processed with DTT, dGTP (Roche) and T4 DNA polymerase (Novagen, LIC qualified) for 30 minutes at 22 °C and then 75 °C for 20 minutes. The pMCSG7 vector (*11*), which encodes a 6-His tag on its N-terminus, was digested with restriction enzyme SspI (New England Biolabs), processed with dCTP (Roche) and T4 DNA polymerase (Novagen, LIC qualified) for 30 minutes at 22 °C and then 75 °C for 20 minutes. To anneal the vector with the insert, they were mixed and incubated at 22 °C for 10 minutes, EDTA was added, and the reaction was incubated for an additional 5 minutes. The mixture was used to transform *E. coli*

XL-1 Blue cells (Agilent Technologies). The construct was verified by sequencing.

### 2.2.2 Enzyme expression

Rosetta2 DE3 pLysS (EMD Millipore) cells were transformed with pMICAL-2 and grown with shaking at 25 °C in Luria Bertani Broth with 100 µg/mL of ampicillin. Bacterial cultures were induced when $A_{600}$ = 1 with 1 mM IPTG and then harvested by centrifugation after 19-24 hours at 15 °C. Bacterial pellets were resuspended with MICAL Buffer (50 mM $NaH_2PO_4$, 100 mM NaCl, 10% glycerol, pH 7.5) and stored at -20 °C until ready to purify.

### 2.2.3 Enzyme purification

After bacterial pellets were thawed, 1 mM PMSF and 5 mM 2-mercaptoethanol were added and sonicated for 10 minutes (30-second bursts followed by 1 min cooling) in an ice-salt bath. The lysate was centrifuged for 1 hour at 40,000 rpm (Beckman Ti45) at 4 °C. The supernatant was then loaded onto a nickel column (Clontec) pre-equilibrated in MICAL Buffer with 5 mM 2-mercaptoethanol. To remove nonspecific binding proteins, the column was washed with MICAL Buffer, 5 mM 2-mercaptoethanol, followed by MICAL Buffer, 10 mM imidazole, 5 mM 2-mercaptoethanol. To elute the enzyme, a gradient was applied starting with MICAL Buffer, 10 mM imidazole, 5 mM 2-mercaptoethanol, and running to MICAL Buffer, 300 mM imidazole, 5 mM 2-mercaptoethanol. Brownish-colored fractions were collected and pooled based on their absorbance spectra, which were recorded on a Shimadzu UV-2501PC scanning spectrophotometer. Purified enzyme was concentrated (~60 µM) and exchanged into 20 mM HEPES, pH 8.0, 1 M NaCl, using Econo-Pac 10DG columns (Bio-Rad) and stored at 4 °C.

### 2.2.4 Actin Extraction and Purification.

Actin was extracted from rabbit hind-leg skeletal muscle using a published method (*12*) to make an acetone powder. To isolate actin from the acetone powder, every one gram of powder was dissolved into 15 mL of Buffer G (2 mM Tris-HCl, 0.1 mM $CaCl_2$, 0.2 mM ATP, 1 mM sodium azide, 0.5 mM 2-mercaptoethanol, pH 8.0) and stirred at 4 °C for 30 minutes. Sample was added to a new pair of woman's pantyhose (Leggs Everyday knee-highs, nude color) to strain the filtrate from the solid; this process was repeated twice. The filtrate was centrifuged at 10,000 rpm (Sorval SS34) for 20 minutes at 4 °C. The supernatant was polymerized by adding 50 mM KCl, 2 mM $MgCl_2$, and 1 mM $Na_2ATP$ or $K_2ATP$ (Fisher, MP Biomedicals) and stirred overnight at 4 °C. The next day more KCl was added to a final concentration of 0.8 M and stirred for 30 minutes at 4 °C. The sample was centrifuged for 45 minutes at 49,000 rpm (Beckman Ti70). Pellets were resuspended into 2 mM Tris-HCl, 0.1 mM $CaCl_2$, 0.6 M KCl, 2 mM $MgCl_2$, 1 mM ATP, 0.5 mM 2-mercaptoethanol, pH 8.0, homogenized using a pre-chilled dounce homogenizer, and centrifuged for 60 minutes at 49,000 rpm (Beckman Ti70) at 4 °C. The supernatant was dialyzed overnight in 4-6 L of 20 mM HEPES, 0.2 mM ATP, 0.1 mM $CaSO_4$, 0.5 mM 2-mercaptoethanol, pH 8.0 at 4 °C. The purity of actin was checked by SDS-PAGE (Lonza). If actin was not used immediately, it was centrifuged at 50,000 rpm (Beckman Ti70) for 90 minutes at 4 °C. Sucrose was added (10% (w/v)) to the supernatant (g-actin), and the solution was frozen, then lyophilized, and stored in a desiccator for no more than 6 months.

### 2.2.5 Preparation of actin for stopped-flow experiments.

Lyophilized g-actin was resuspended in water and dialyzed overnight in 6 L of 20 mM HEPES, pH 8.0 at 4 °C. Actin was centrifuged at 50,000 rpm (Beckman Ti70) for 90 minutes at 4 °C. The concentration of g-actin in the supernatant was determined by diluting into 8 M guanidinium and recording the absorbance

spectrum (Shimadzu UV-2501PC scanning spectrophotometer). The extinction coefficient of unfolded actin (45,840 $M^{-1}cm^{-1}$) at 280 nm was calculated from the sequence using UniProtKB/Swiss-Prot database. Actin was polymerized by adding 10 mM $K_2SO_4$, 2 mM $MgSO_4$, and 0.5 mM 2-mercaptoethanol and incubating at room temperature for ~20 minutes. To remove aggregates, actin, was centrifuged for 10 minutes at room temperature at 14,500 rpm. To make polymers smaller, polymerized actin was passed through a 22½-gauge needle twice.

### 2.2.6 Synthesis of [4R-2H]NADPH and [4S-2H]NADPH

[4R-$^2$H]NADPH was synthesized by published methods (*13, 14*) with the following modifications. Reaction mixtures had 13 mM NADP (Research Products International), 0.5 M $d_8$-isopropanol (Acros Organics), 20 units of alcohol dehydrogenase from *Thermoanaerobacter brockii* (Sigma) into a final volume of 10 mL. The buffer was 50 mM $NH_4HCO_3$ adjusted to pH 7.8 with NaOH. The reaction mixture was incubated at room temperature for 2 hours and monitored spectrophotometrically. Upon completion of the reaction, the mixture was added to a DEAE Sepharose Fast-flow column which had been pre-equilibrated with 50 mM $NH_4HCO_3$ pH 7.8. Deuterated NADPH was removed from the column by running a gradient of 50 - 500 mM $NH_4HCO_3$, pH 8.5. Fractions were pooled that had a ratio of $A_{260}/A_{350}$ = 2.5 or less (*15*). The pH of the pooled fractions was adjusted to 9.8 with $NH_4OH$. The pooled fractions were concentrated by lyophilization and stored at -20 °C.

To synthesize [4S-$^2$H]NADPH, a reaction mixture was made consisting of 15 mM 1-D-glucose (Cambridge Isotope Laboratories Inc.), 15 mM ATP, 15 mM NADP, 100 units of glucose-6-phosphate dehydrogenase, 100 units of hexokinase, 15 mM $MgCl_2$ in 6 mL of 50 mM HEPES, pH 7.5. The reaction mixture was

incubated for 2 hours and monitored spectrophotometrically. The [4S-$^2$H]NADPH was purified and stored as described for [4R-$^2$H]NADPH.

### 2.2.7 Reductive Half-Reaction

Enzyme was exchanged into 20 mM HEPES with ~0.5 mM 2-mercaptoethanol, pH 8.0, using Econo-Pac 10DG columns (Bio-Rad). The reaction of the monoMICAL-2 (with or without actin) was studied in a Hi-Tech Scientific KinetAsyst SF-61 DX2 stopped-flow spectrophotometer at 4 °C. For experiments without actin, the instrument was used in its standard configuration, with a 1-cm optical path length and in dual-beam mode. For experiments that included actin, the instrument was reconfigured to a 1.5-mm optical path-length and single-beam detection. Enzyme solutions (~20 - 80 μM) were made anaerobic in a tonometer (*16*) in the presence or absence of 40 μM actin and mixed with anaerobic solutions of NADPH (up to 8 mM) or NADH (up to 16 mM) and *protio* (Research Products International), or *deutero* NADPH up to 4 mM. The oxidized flavin absorbance was recorded at 450 nm and charge-transfer absorbance was monitored at 550 nm. Kinetic traces were fit to sums of exponentials using Kaleidagraph (Synergy, Inc.). The observed rate constants for flavin reduction were plotted vs. NADH or NADPH concentration and fit to a square hyperbola to obtain $k_{red}$ and $K_d$.

### 2.2.8 Reduction Potentials

Reduction potentials were determined using enzyme (~20 μM) with or without actin (~ 40 μM) at 25 °C with 20 mM HEPES, pH 8.0 by the method of Massey (*17*) using 1-hydroxyphenazine as indicator dye ($E_m$ = -228 mV).

### 2.2.9 Extinction Coefficient

Absorbance spectra were recorded of enzyme (~20 μM) with and without 2-mercaptoethanol in 20 mM HEPES, pH 8.0 before and after the addition of 0.1 % SDS. The extinction coefficient of monoMICAL-2 was determined by calculating the amount of free FAD liberated using an extinction coefficient at 449 nm of 11.3 $mM^{-1}$ $cm^{-1}$.

## 2.3 Results

### 2.3.1 General Properties

As a starting point for studying the enzymology of the multi-domain MICAL-2, we expressed and purified the N-terminal monooxygenase domain (monoMICAL-2). A reasonable amount of enzyme – 0.30 μmol – could routinely be obtained from 18 L of *E. coli* culture. When the domain was purified, it was orange, not the yellow expected for most flavoenzymes. The spectrum of (Figure 2-1) monoMICAL-2 had absorbance at long wavelengths where oxidized flavins normally don't absorb, due to a charge-transfer interaction between Trp 405 and the *re*-face of the oxidized flavin (*5*). This interaction is only possible when the flavin is in the "out" conformation. An extinction coefficient at 455 nm of 9.8 $mM^{-1}$ $cm^{-1}$ was measured. We observed that high concentrations of enzyme precipitated when cold if the ionic strength of the solution was low. The precipitate could be redissolved by some combination of adding a reducing agent, NaCl, and warming.

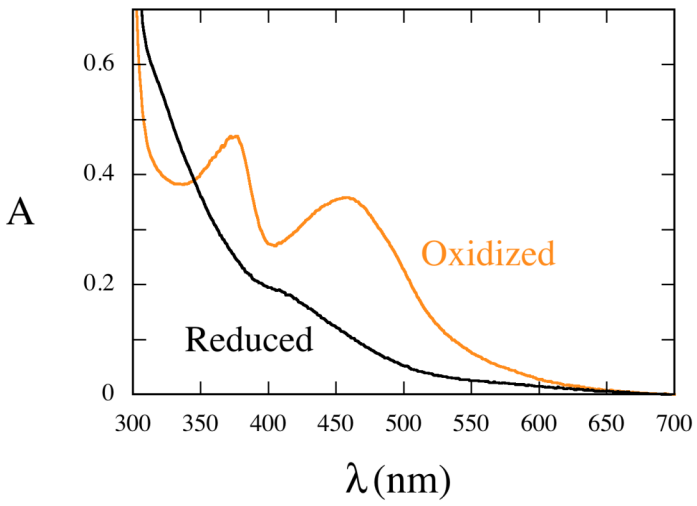


**Figure 2-2 The absorbance spectrum of monoMICAL-2**

The spectra of the oxidized and reduced form of monoMICAL-2 were recorded in 20 mM HEPES, pH 8.0 at 4 °C. Note the charge-transfer absorbance above 500 nm.

### 2.3.2 Reduction Potentials

The reduction potential of monoMICAL-2 was determined by using the method of Massey (*17*). Measurement of reduction potentials were first attempted using the standard 0.1 M $K_2HPO_4$, pH 7.0 buffer, however monoMICAL-2 would precipitate in this buffer. Thus experiments were performed in 20 mM HEPES buffer, pH 8.0. The indicator dye used was 1-hydroxyphenazine which has a reduction potential of -228 mV at pH 8.0 (*18*). The reduction potential of monoMICAL-2 without actin was found to be -240 mV (Figure 2-2). The potential is much higher than that of NADPH, therefore the hydride-transfer reaction is essentially irreversible. The reduction potential of the monoMICAL-2•actin complex was -212 mV. Actin raises the potential by ~30 mV, giving the monoMICAL-2•actin complex a higher affinity for electrons than enzyme alone.

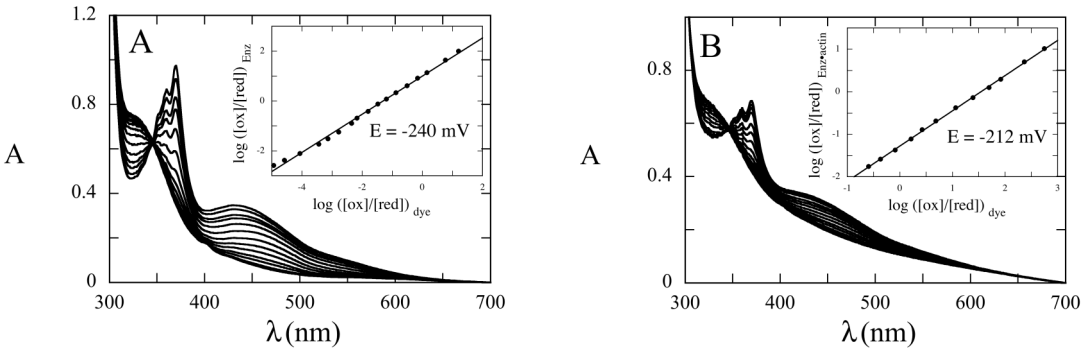


**Figure 2-3 Reduction potential of monoMICAL-2.**

Anaerobic mixtures of enzyme and 1-hydroxyphenazine dye were slowly reduced by xanthine and xanthine oxidase in 20 mM HEPES, pH 8.0 at 25 °C. Spectra were recorded to monitor the extent of reduction of the dye and enzyme. These were used to determine the potential (insets). **A.** monoMICAL-2 was reduced without actin giving a potential of -240 mV. **B.** monoMICAL-2 was reduced in the presence of 1 equivalent of f-actin, giving a potential of - 212 mV.

### 2.3.3 Substrate-Free Reductive Half-Reaction

Oxidized monoMICAL-2 monooxygenase was anaerobically mixed with varying concentrations of anaerobic NADPH in a stopped-flow instrument. Reactions were monitored by changes in absorbance of the flavin at 450 nm and fit to sums of exponentials (Figure 2-3). Flavin reduction occurred in one phase. The charge-transfer absorbance between FAD and Trp405, observed at 550 nm, disappeared simultaneously with flavin reduction. The $k_{obs}$ values were plotted vs concentration of NADPH, giving a square hyperbola with a $K_d$ of 944 ± 39 μM and a $k_{red}$ of 0.074 ± 0.0009 $s^{-1}$. The hyperbolic dependence of $k_{obs}$ on NADPH is most simply explained by the mechanism in Scheme 2-1, although the dissociation of NADP was not directly observed. The flavin conformation is shown in scheme 2-1. This is based on the crystal structure of monoMICAL-1 and the observation of charge-transfer absorbance in monoMICAL-2. The flavin is assigned to the “in” conformation in the reduced enzyme based on the crystal structure of monoMICAL-1. There are no data to assign a conformation to the flavin in the NADP complex. The value of $k_{red}$ is relatively low, consistent with the

behavior of an aromatic hydroxylase (Class A monooxygenase) in the absence of its substrate.

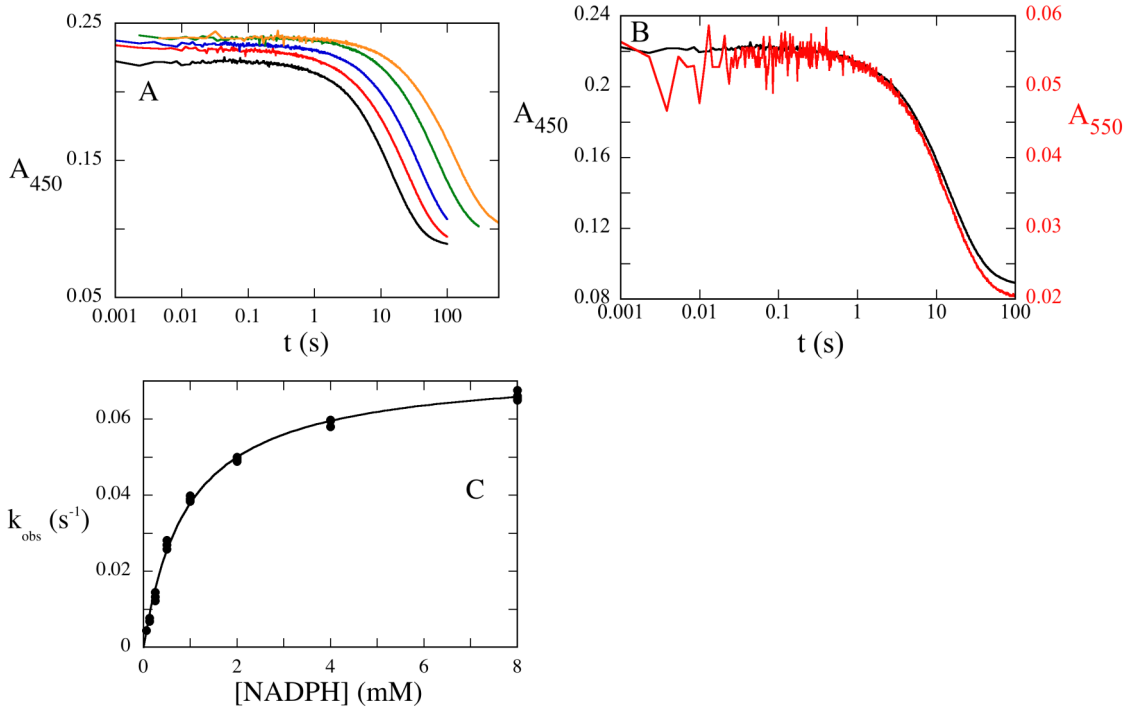


**Figure 2-4 The reduction of monoMICAL-2 with NADPH.**

Anaerobic enzyme (50 μM before mixing) was mixed with anaerobic NADPH solutions in a stopped-flow spectrophotometer. All reactions were in 20 mM HEPES, pH 8.0, at 4 °C. **A.** The reduction of the enzyme was monitored at 450 nm. Note the logarithmic time-scale. The concentrations of NADPH are 8 mM, 1 mM, 0.5 mM, 0.25 mM, and 0.125 mM. **B.** Traces for the reaction of 8 mM NADPH obtained at 450 nm and 550 nm are compared. Flavin reduction (black trace) and the disappearance of the charge-transfer complex (red) occur simultaneously. **C.** Observed rate constants as a function of NADPH concentration were obtained by fitting the traces in **A** to a single exponential. These values were fit to a square hyperbola, giving $k_{red}$ = 0.07 $s^{-1}$ and $K_d$ = 940 μM in this experiment.

$$E_{ox,\ out} + NADPH \overset{K_d}{\rightleftharpoons} E_{Ox}\bullet NADPH \xrightarrow{k_{red}} E_{red}\bullet NADP \longrightarrow E_{red,\ in} + NADP$$

**Scheme 2-1**

### 2.3.4 Reduction by NADH

To determine if MICAL-2 has a preference for NADPH or NADH, anaerobic monoMICAL-2 was mixed with different concentrations of anaerobic NADH in a stopped-flow instrument. Reduction of monoMICAL-2 was observed by monitoring the flavin absorbance at 450 nm (Figure 2-4). The traces were fit to a single exponential; the plot of $k_{obs}$ vs. NADH surprisingly looked linear. A linear increase of the observed rate constant for reduction indicates a direct bimolecular reaction of NADH with the oxidized enzyme without forming a complex. The slope of the dependence gives a bimolecular rate constant for the reaction of 1.1 ± 0.025 $M^{-1}$ $s^{-1}$. If a weak complex is assumed to proceed the reaction, then the observed rate constant should depend hyperbolically on NADH concentration. Fitting to a square hyperbola gave a half-saturating concentration estimated to be 53 ± 17 mM. If binding of NADPH is rapid equilibrium, then the half-saturating concentration is the $K_d$. In order for binding to be rapid equilibrium, the dissociation rate constant of NADPH should be significantly larger than 0.08 $s^{-1}$. This is almost always the case. The $k_{red}$ was essentially the same for NADH, 0.08 ± 0.02 $s^{-1}$, as for NADPH. Thus, if NADH actually does bind, MICAL-2 has a preference for NADPH over NADH due to a ~60-fold tighter binding. Regardless of the interpretation of these data, the 2'-phosphate of NADPH is extremely critical for binding. Interestingly, if the dependence really is hyperbolic, then the predicted $k_{red}$ for NADH and NADPH are the same suggesting that the same reactive complex forms.

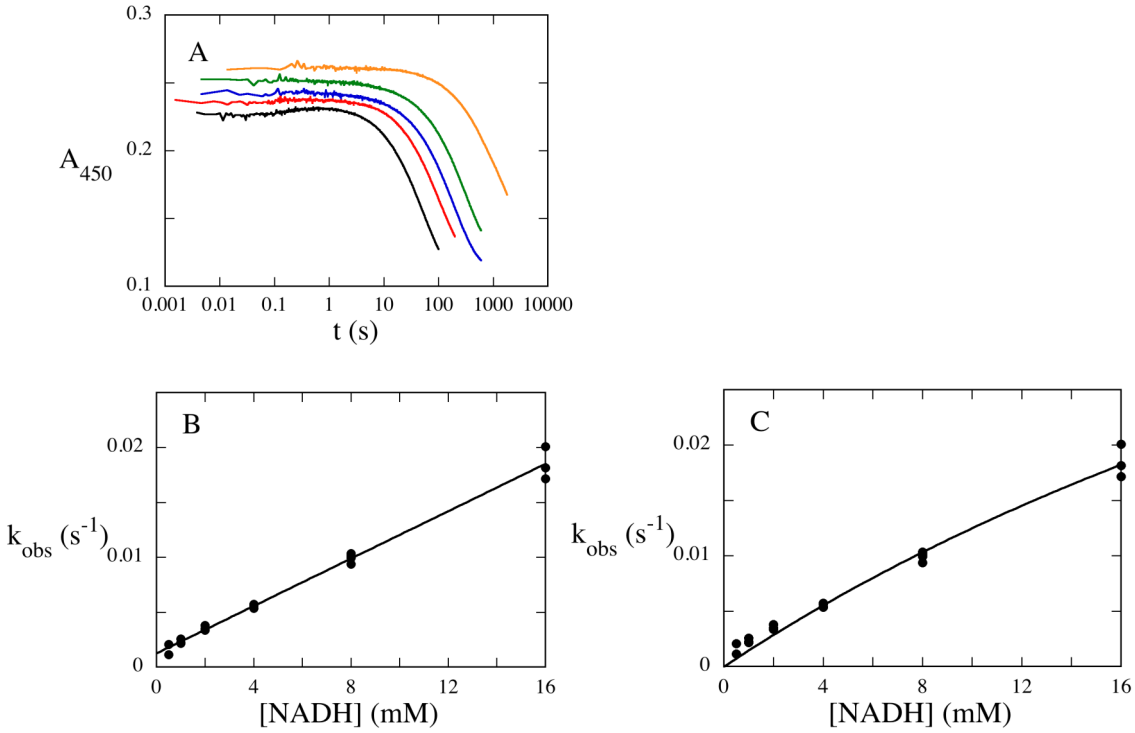


**Figure 2-5 The reduction of monoMICAL-2 with NADH.**

Anaerobic enzyme (50 μM before mixing) was mixed with anaerobic NADH solutions in a stopped-flow spectrophotometer. All reactions were in 20 mM HEPES, pH 8.0, at 4 °C. **A.** The reduction of the enzyme was monitored at 450 nm. Note the logarithmic time-scale. The concentrations of NADH are 16 mM, 8 mM, 4 mM, 2 mM, and 0.5 mM. **B.** Observed rate constants as a function of NADH concentration were obtained by fitting the traces in **A** to a single exponential. These values were fit to a line giving a bimolecular rate constant of 1.1 ± 0.025 $M^{-1}$ $s^{-1}$. **C.** These values of the observed rate constants were fit to a square hyperbola, giving $k_{red}$ = 0.078 $s^{-1}$ and $K_d$ = 53 mM in this experiment. Note the $K_d$ and $k_{red}$ values cannot be determined accurately.

### 2.3.5 KIE and Stereochemistry

Monooxygenases typically transfer the *proR* hydride of NADPH. A comparison of reduction kinetics using *protio* vs [4R-$^2$H]NADPH was performed to determine if the same stereochemistry would be observed with monoMICAL-2. monoMICAL-2 monooxygenase was mixed with varying concentrations of NADPH/D (Figure 2-5). The $k_{red}$ of *protio*-NADPH was 0.09 ± 0.004 $s^{-1}$. The $k_{red}$ for [4R-$^2$H]NADPH was 0.019 ± 0.0028 $s^{-1}$. Thus MICAL-2 transfers the *proR* hydride of NADPH, just

like aromatic hydroxylases and other monooxygenases. The substantial KIE of 4.8 ± 0.9 strongly suggests that hydride transfer, rather than a conformational change, controls the rate constant of reduction when actin is not bound. Therefore the charge-transfer absorbance disappears because of chemistry, rather than movement of the flavin away from Trp405.

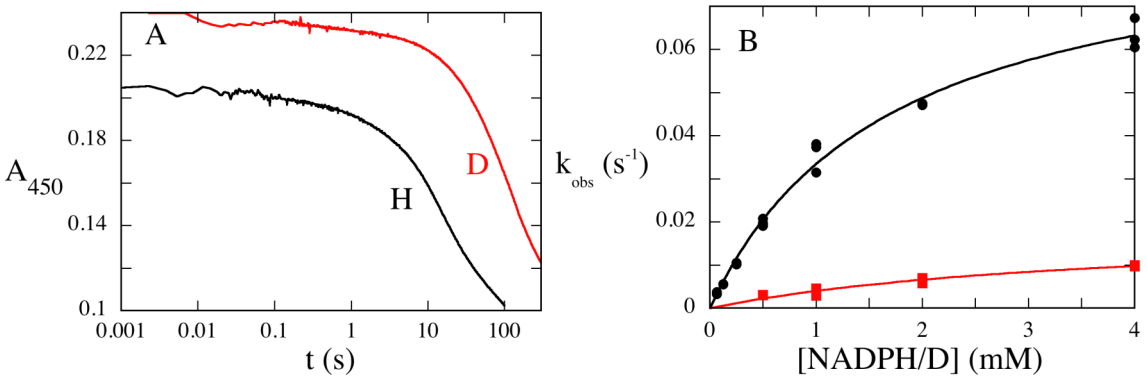


**Figure 2-6 KIE on the reduction of monoMICAL-2.**

Reactions using either *protio*-NADPH or [4R-$^2$H]NADPH were performed as described in Figure 2-3. **A.** Stopped-flow traces at 450 nm are shown comparing the reduction by 4 mM (after mixing) *deutero* NADPH in red and 4 mM (after mixing) *protio* NADPH in black. **B.** The observed rate constants varied with NADPH/D concentration. The values for $k_{red}$ were obtained by fitting to a square hyperbola, giving a KIE of 4.8 ± 0.9.

### 2.3.6 Reduction in the Presence of Actin

The substrate for monoMICAL is f-actin (*5, 10, 19*). Experiments were performed to study the reduction of monoMICAL-2 in the presence of f-actin. Our initial attempts at stopped-flow experiments were not successful; the binding of actin to monoMICAL-2 appears to be weak and increasing the concentration of actin obliterated the absorbance signal due to turbidity. To address this challenge the stopped-flow instrument was reconfigured to use a 1.5 mm path-length to allow us to increase our concentration of actin but still be within the detection limit of the instrument. This improved the quality of the data but there was still a high and inconsistent background of light scattering. Freshly polymerized actin (39 μM) was incubated with monoMICAL-2 (79 μM) anaerobically and mixed with different

concentrations of NADPH. Reduction was monitored by observing the change in the flavin absorbance at 450 nm (Figure 2-6). Three phases were observed. The first phase of reduction was difficult to characterize due to artifacts caused by actin. The first phase, 15% of total reduction, was most subject to interference by light scattering but we could still estimate a rate constant for reduction of 8 ± 3 $s^{-1}$. The second phase, 29% of total reduction, had a limiting rate constant of 1.7 ± 0.50 $s^{-1}$ and a rough apparent $K_d$ of 3.6 mM. The third phase, 57% of total reduction had essentially the same kinetics observed in experiments without actin ($k_{red}$ of 0.08 $s^{-1}$). This phase is ascribed to the reaction of actin-free monoMICAL-2. The reactions occurring in these experiments are explained by Scheme 2-2.

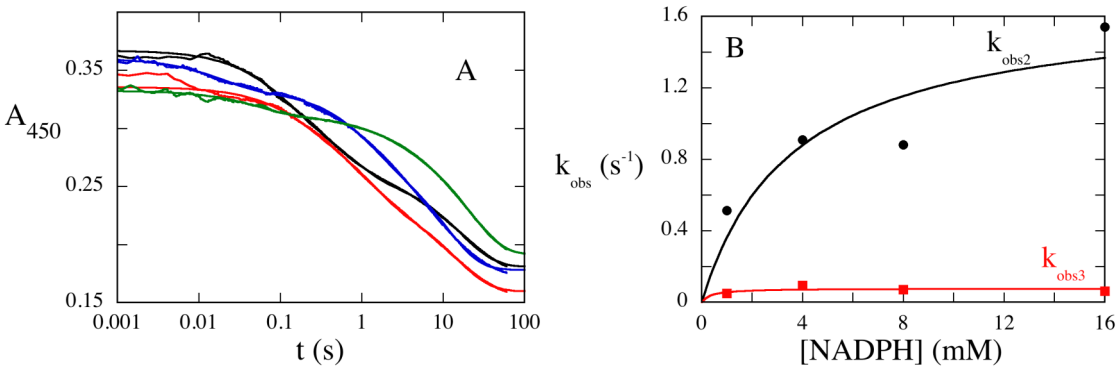


**Figure 2-7 The reduction of the monoMICAL-2•actin complex with NADPH.**

Anaerobic enzyme (79 μM before mixing) and 39 μM f-actin was mixed with anaerobic NADPH solutions in a stopped-flow spectrophotometer. All reactions were in 20 mM HEPES, pH 8.0, at 4 °C. **A.** The reduction of the enzyme•actin complex was monitored at 450 nm. Note the logarithmic time-scale. The concentrations of NADPH are 16 mM, 8 mM, 4 mM, and 1 mM. **B.** Observed rate constants as a function of NADPH concentration were obtained by fitting the traces in **A** to three exponentials. The values for the two slower phases are plotted as a function of NADPH concentration and were fit to a square hyperbola, giving $k_{obs,2}$ = 1.7 $s^{-1}$ and $k_{obs,3}$ = 0.08 $s^{-1}$ in this experiment.

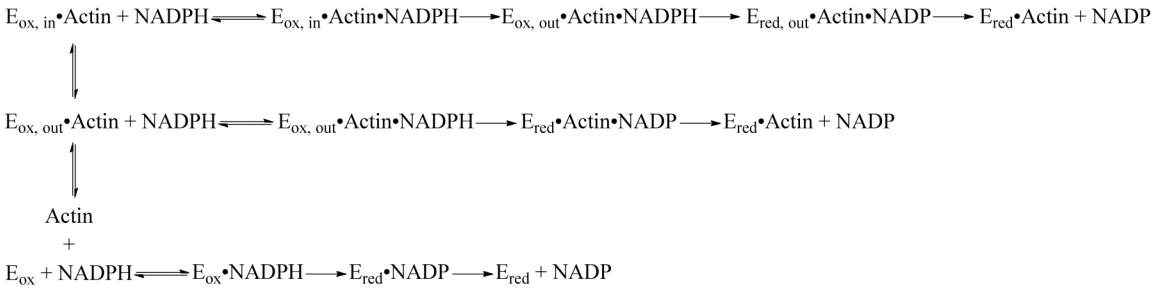


**Scheme 2-2**

## 2.4 Discussion

MICAL, a large protein of ~1000 residues, causes actin to depolymerize. Its N-terminus is a flavin monooxygenase domain, followed by several protein-protein interaction domains. The monooxygenase domain is vital for motor axons to be properly guided during embryonic development (*3, 20*). In order to understand how MICALs perform their biological roles, detailed enzymological studies are needed on the mechanism of the monooxygenase half-reactions.

There are many classes of monooxygenases, Class A-F (*7*); monoMICAL-2 has been classified, based on its sequence and the structure of monoMICAL-1, as an aromatic monooxygenase, Class A. monoMICAL-1 has one Rossman fold – for binding FAD – the same as Class A. In contrast, the structure and sequences of monoMICALs are very different from those of the Class B monooxygenases. Class B has two Rossman folds; one for binding FAD and another for pyridine nucleotides. The flavins of aromatic hydroxylases (Class A) change conformation from “in” to “out” while those in Class B do not. The oxidized flavin of monoMICAL-1 adopts an “out” conformation (*8, 9*), where it is more exposed to solvent, and when it is reduced moves to the “in” conformation, where it is partly buried in the protein. The high sequence identity between monoMICAL-2 and monoMICAL-1 (60 % using Lalign (*21*)) strongly suggests that the structure of monoMICAL-2 will be very similar to that of monoMICAL-1, allowing the structure of monoMICAL-1 to guide our interpretations. This idea is supported by the FAD-

Trp charge-transfer absorbance of monoMICAL-2, which was first reported for human monoMICAL-1 (*5*) and *Drosophila* MICAL (*3*). Thus, from a structural perspective, monoMICAL-2 seems to be an aromatic hydroxylase. However, MICAL oxygenates the sulfur of a methionine side-chain (*10*). The oxidation of thioethers is a classic reaction performed by Class B enzymes, not by aromatic hydroxylases (*6*). We performed experiments to determine how similar enzymatically monoMICAL-2 is to the aromatic hydroxylases.

There are two key differences between the reductive half-reactions of Class A and Class B enzymes (*6*): Class A enzymes are stimulated by their substrate, while Class B enzymes are always stimulated even in the absence of substrate; and the flavin in Class A enzymes moves to the "out" conformation in order to react with NAD(P)H, while the flavin of Class B enzymes is stationary. When f-actin (the reported substrate of MICAL (*10*)) was added to the reductive half-reaction in our experiments, monoMICAL-2 was stimulated. The presence of actin created two new phases that were faster than the reaction of free monoMICAL-2, showing that two different enzyme-actin complexes were present. The fastest phase was not defined well due to optical interference caused by actin, but is faster than free enzyme by about two orders of magnitude. The second phase is faster than free enzyme by about one order of magnitude. This population of enzyme seems to bind NADPH weaker than free enzyme. The two faster populations of enzyme might be attributed to actin bound to enzyme with the flavin in both the "in" and "out" conformations. The flavin of aromatic hydroxylases (Class A) reacts when in the "out" conformation. Therefore, we propose that the fastest phase is caused by reduction of oxidized enzyme in the "out" conformation with actin bound, and the second phase is due to the slower reaction of oxidized monoMICAL-2 in the "in" conformation with actin bound. A possible explanation for two actin complexes is that the missing C-terminal

protein-protein interacting domains might be needed to favor the actin complex with the flavin in the more reactive “out” conformation.

The flavins of Class A enzymes react with NAD(P)H in the “out” conformation and then their flavins move to the “in” conformation. The substantial KIE and synchronization of reduction with the disappearance of the charge-transfer shows that reduction happens in the “out” conformation, as with other aromatic hydroxylases. Subsequently, the reduced flavin moves to the “in” conformation seen in the crystal structure. Interestingly, reduction is slow for monoMICAL-2 even when the flavin is in the “out” conformation, which would allow full access by NADPH; something else besides access is responsible for slow reduction, and relieved by f-actin. Some PHBH mutants act this way too (*22*).

Our results contradict several published ideas about how MICAL controls its reactivity with NADPH. Nadella *et al.* reported (*9*) a high oxidase activity for monoMICAL-1 (77 $s^{-1}$) without control by substrate or protein-protein interaction domains, obtained by the Amplex Red assay for $H_2O_2$. This would require a $k_{red}$ greater than 77 $s^{-1}$, not slow as we report here, or as was reported for monoMICAL-1 (*5*). Zucchini *et al.* showed that the Amplex Red reaction is artifactually fast (*5*). We have found resorufin, the product of the Amplex Red reaction, reacts with the enzyme in a complex radical chain (unpublished). Schmidt *et al.* proposed that the C-terminal domains of MICAL-1 inhibit the reactivity of the monooxygenase domain (*23*) but the experimental data supporting these ideas seem inadequate to determine how this could happen. The steady-state assays of the oxidase activity used in that study were only semi-quantitative, not allowing a $k_{cat}$ (and, therefore, a lower limit on $k_{red}$) to be determined. Much of the work was done with crude preparations rather than with purified proteins, and some of the experiments used the artifactual Amplex Red assay or included high concentrations of $Cl^-$, an inhibitor of aromatic

hydroxylases. Therefore, although it is possible that C-terminal domains, or another protein such as collapsin response mediator proteins, could inhibit the reduction of the monooxygenase domain. Definitive enzymology has yet to be done.

## 2.5 Conclusion

Our data show that monoMICAL-2 has the classic regulatory behavior of flavin-dependent aromatic hydroxylases even without the protein-protein interaction domains. However, it is not like aromatic hydroxylases in its substrate preference (*10*), where it behaves like a Class B enzyme that oxygenates non-aromatics. monoMICAL-2 has behaviors of both families of enzymes. This would be the first time a Class A flavin monooxygenase oxygenates a thioether. mono-MICAL-2 is partly an aromatic hydroxylase, partly a Class B enzyme.

## 2.6 References


1. Pak, C. W., Flynn, K. C., and Bamburg, J. R. (2008) Actin-binding proteins take the reins in growth cones, *Nat. Rev. Neurosci. 9*, 136-147.
2. Zhou, Y., Gunput, R. A., Adolfs, Y., and Pasterkamp, R. J. (2011) MICALs in control of the cytoskeleton, exocytosis, and cell death, *Cell Mol. Life Sci. 68*, 4033-4044.
3. Terman, J. R., Mao, T., Pasterkamp, R. J., Yu, H. H., and Kolodkin, A. L. (2002) MICALs, a family of conserved flavoprotein oxidoreductases, function in plexin-mediated axonal repulsion, *Cell 109*, 887-900.
4. Ashida, S., Furihata, M., Katagiri, T., Tamura, K., Anazawa, Y., Yoshioka, H., Miki, T., Fujioka, T., Shuin, T., Nakamura, Y., and Nakagawa, H. (2006) Expression of novel molecules, MICAL2-PV (MICAL2 prostate cancer variants), increases with high Gleason score and prostate cancer progression, *Clin. Cancer Res. 12*, 2767-2773.
5. Zucchini, D., Caprini, G., Pasterkamp, R. J., Tedeschi, G., and Vanoni, M. A. (2011) Kinetic and spectroscopic characterization of the putative monooxygenase domain of human MICAL-1, *Arch. Biochem. Biophys. 515*, 1-13.
6. Palfey, B. A., and McDonald, C. A. (2010) Control of catalysis in flavin-dependent monooxygenases, *Arch. Biochem. Biophys. 493*, 26-36.
7. van Berkel, W. J., Kamerbeek, N. M., and Fraaije, M. W. (2006) Flavoprotein monooxygenases, a diverse class of oxidative biocatalysts, *J. Biotechnol. 124*, 670-689.
8. Siebold, C., Berrow, N., Walter, T. S., Harlos, K., Owens, R. J., Stuart, D. I., Terman, J. R., Kolodkin, A. L., Pasterkamp, R. J., and Jones, E. Y. (2005) High-resolution structure of the catalytic region of MICAL (molecule interacting with CasL), a multidomain flavoenzyme-signaling molecule, *Proc. Natl. Acad. Sci. U.S.A. 102*, 16836-16841.

9. Nadella, M., Bianchet, M. A., Gabelli, S. B., Barrila, J., and Amzel, L. M. (2005) Structure and activity of the axon guidance protein MICAL, *Proc. Natl. Acad. Sci. U.S.A. 102*, 16830-16835.
10. Hung, R. J., Pak, C. W., and Terman, J. R. (2011) Direct redox regulation of F-actin assembly and disassembly by Mical, *Science 334*, 1710-1713.
11. Stols, L., Gu, M., Dieckman, L., Raffen, R., Collart, F. R., and Donnelly, M. I. (2002) A new vector for high-throughput, ligation-independent cloning encoding a tobacco etch virus protease cleavage site, *Protein Expr. Purif. 25*, 8-15.
12. Pardee, J. D., and Spudich, J. A. (1982) Purification of muscle actin, *Methods Enzymol. 85 Pt B*, 164-181.
13. Ottolina, G., Riva, S., Carrea, G., Danieli, B., and Buckmann, A. F. (1989) Enzymatic synthesis of [4R-2H]NAD (P)H and [4S-2H]NAD(P)H and determination of the stereospecificity of 7 alpha- and 12 alpha hydroxysteroid dehydrogenase, *Biochim. Biophys. Acta. 998*, 173-178.
14. Rider, L. W., Ottosen, M. B., Gattis, S. G., and Palfey, B. A. (2009) Mechanism of dihydrouridine synthase 2 from yeast and the importance of modifications for efficient tRNA reduction, *J. Biol. Chem. 284*, 10324-10333.
15. Wu, J. T., Wu, L. H., and Knight, J. A. (1986) Stability of NADPH: effect of various factors on the kinetics of degradation, *Clin. Chem. 32*, 314-319.
16. Palfey, B. A. (2003) Kinetic Analysis of Macromolecules, In *Time Resolved Spectral Analysis* (Johnson, K. A., Ed.), pp 203-207, Oxford University Press, New York.
17. Massey, V. (1990) A simple method for the determination of redox potentials, In *Flavins and Flavoproteins* (Curti, B., Ronchi, S., and Zanetti, G., Ed.), pp 59-66, Walter de Gruyter, Berlin.
18. Clark, W. M. (1960) *Oxidation-Reduction Potentials of Organic Systems*, The Williams & Wilkins Company, Baltimore.

19. Hung, R. J., Yazdani, U., Yoon, J., Wu, H., Yang, T., Gupta, N., Huang, Z., van Berkel, W. J., and Terman, J. R. (2010) Mical links semaphorins to F-actin disassembly, *Nature 463*, 823-827.
20. Landgraf, M., Bossing, T., Technau, G. M., and Bate, M. (1997) The origin, location, and projections of the embryonic abdominal motorneurons of Drosophila, *J. Neurosci. 17*, 9642-9655.
21. Huang, X. Q., and Miller, W. (1991) A Time-Efficient, Linear-Space Local Similarity Algorithm, *Adv Appl Math 12*, 337-357.
22. Moran, G. R., Entsch, B., Palfey, B. A., and Ballou, D. P. (1996) Evidence for flavin movement in the function of p-hydroxybenzoate hydroxylase from studies of the mutant Arg220Lys, *Biochemistry 35*, 9278-9285.
23. Schmidt, E. F., Shim, S. O., and Strittmatter, S. M. (2008) Release of MICAL autoinhibition by semaphorin-plexin signaling promotes interaction with collapsin response mediator protein, *J. Neurosci. 28*, 2287-2297.

# Chapter 3
# Oxygen Intermediates in the Depolymerization of Actin by the Aromatic Hydroxylase Domain of MICAL-2

## 3.1 Introduction

Molecules interacting with CasL (MICALs) are multi-domain flavin-dependent monooxygenases that cause actin to depolymerize. MICALs are critical for motor axons to be guided to their destined muscles (*1*). When MICAL was deleted from *Drosophila* embryos, or when key residues that bind FAD were mutated, axons no longer found their path from the central nervous system to their target muscle groups. When MICAL was added back to such embryos, axons were able to navigate to their target muscles and proper development of the nervous system was restored (*1*).

There are three isoforms of MICALs: MICAL-1, MICAL-2, and MICAL-3 (*2, 3*). MICAL-2 is over-expressed in prostate cancer cells, while it is barely detectable in normal prostate epithelium (*4*). When MICAL-2 was knocked down by small interfering RNA, prostate cancer cells diminished significantly. MICALs are large proteins (~110 kDA) with many domains (up to five). The N-terminal domain is a monooxygenase domain, followed by protein-protein interacting domains. Our studies are focused on MICAL-2, the smallest of the MICALs, which has only two C-terminal domains; a calponin homology domain (CH) and a LIM domain.

The crystal structure of the monooxygenase domain of MICAL-1 (monoMICAL-1) was solved (*5, 6*) and is very similar to flavin-dependent aromatic hydroxylases. It has a single Rossmann fold that binds FAD. When the flavin is oxidized, it is

more exposed to solvent in the “out” conformation. When the flavin of MICAL is reduced, it is in a more buried position in the “in” conformation. Although the structure of the monooxygenase domain of MICAL-2 has not been determined, it shares a 60% sequence identity with the monooxygenase domain of MICAL-1, making the structure of monoMICAL-1 a useful model for guiding studies of monoMICAL-2.

Initially, it was thought that MICAL was an oxidase, making $H_2O_2$ to exert its physiological effect (*5-7*), but these experiments did not include a substrate that could be oxygenated. The sequence and structure of the N-terminus of MICAL suggest it is an aromatic hydroxylase (a Class A monooxygenase), not an oxidase (*8*). Aromatic hydroxylases have key features (*9*): they hydroxylate activated aromatics; flavin reduction is slow in the absence of substrate; they form a hydroperoxide intermediate that is unstable in the absence of substrate; and the flavin has different conformations (“in” and “out”). MICAL exhibits most of these characteristics. Reduction of monoMICAL-2 is stimulated by actin (Chapter 2), the sequence resembles those of Class A monooxygenases, and the structure has the “in”/ “out” conformation (*5, 6*). However recent studies showed that MICAL oxygenates actin on Met 44 making a methionine sulfoxide (*10*). This would be the first report of an aromatic hydroxylase oxygenating a sulfur nucleophile. Oxygenation of sulfur is performed by Class B monooxygenases which oxygenate non-aromatics (Scheme 3-1) (*8, 9*), as MICAL does. However Class B enzymes are very different from Class A enzymes, both structurally and mechanistically. They have two Rossmann folds and their reduction is fast even without substrate, unlike MICAL.

In this chapter, we examine the oxidative half-reaction of monoMICAL-2 in detail in order to discern whether the key reaction sequence behaves like that of a Class A monooxygenase, or that of a Class B enzyme. We found that the flavin

moves between the “in” and “out” conformation, and actin stimulates flavin oxidation. Flavin-oxygen intermediates were observed only in the presence of actin.

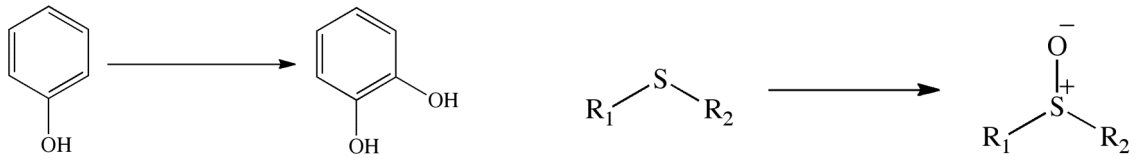


**Class A Reaction** **Class B Reaction**

**Scheme 3-1**

## 3.2 Experimental Procedures

### 3.2.1 Expression construct

To construct the pMICAL-2 plasmid, the segment of the MICAL-2 gene encoding the monooxygenase domain of MICAL-2 residues 1-494 from *Mus musculus* was cloned from Mammalian Gene Collection MICAL-2 cDNA Clone ID 40061128 (Thermo Scientific). The MICAL-2 monooxygenase gene was amplified using primers 5’-TACTTCCAATCCAATGCCATGGGAGAGAATGAAGATGAGAAG and 5’-TTATCCACTTCCAATGCTAGTCCATCTCCTTAGTGATGTACAAAT (Invitrogen). To generate an overhang for ligation-independent cloning (LIC), the PCR product was processed with DTT, dGTP (Roche) and T4 DNA polymerase (Novagen, LIC qualified) for 30 minutes at 22 °C and then 75 °C for 20 minutes. The pMCSG7 vector (*11*), which encodes a 6-His tag on its N-terminus, was digested with restriction enzyme SspI (New England Biolabs), processed with dCTP (Roche) and T4 DNA polymerase (Novagen, LIC qualified) for 30 minutes at 22 °C and then 75 °C for 20 minutes. To anneal the vector with the insert, they were mixed and incubated at 22 °C for 10 minutes, EDTA was added, and the reaction was incubated for an additional 5 minutes. The mixture was used to

transform *E. coli* XL-1 Blue cells (Agilent Technologies). The construct was verified by sequencing.

### 3.2.2 Enzyme expression

Rosetta2 DE3 pLysS (EMD Millipore) cells were transformed with pMICAL-2 and grown with shaking at 25 °C in Luria Bertani Broth with 100 µg/mL of ampicillin. Bacterial cultures were induced when $A_{600}$ = 1 with 1 mM IPTG and then harvested by centrifugation after 19-24 hours at 15 °C. Bacterial pellets were resuspended with MICAL buffer (50 mM $NaH_2PO_4$, 100 mM NaCl, 10% glycerol, pH 7.5) and stored at -20 °C until ready to purify.

### 3.2.3 Enzyme purification

After bacterial pellets were thawed, 1 mM PMSF and 5 mM 2-mercaptoethanol were added and sonicated for 10 minutes (30-second bursts followed by 1 min cooling) in an ice-salt bath. The lysate was centrifuged for 1 hour at 40,000 rpm (Beckman Ti45) at 4 °C. The supernatant was then loaded onto a nickel column (Clontec) pre-equilibrated in MICAL buffer with 5 mM 2-mercaptoethanol. To remove nonspecific binding proteins, the column was washed with MICAL buffer, 5 mM 2-mercaptoethanol, followed by MICAL Buffer, 10 mM imidazole, 5 mM 2-mercaptoethanol. To elute the enzyme, a gradient was applied starting with MICAL Buffer, 10 mM imidazole, 5 mM 2-mercaptoethanol, and running to MICAL Buffer, 300 mM imidazole, 5 mM 2-mercaptoethanol. Brownish-colored fractions were collected and pooled based on their absorbance spectra, which were recorded on a Shimadzu UV-2501PC scanning spectrophotometer. Purified enzyme was concentrated and exchanged into 20 mM HEPES, pH 8, 1 M NaCl, using Econo-Pac 10DG columns (Bio-Rad) and stored at 4 °C.

### 3.2.4 Actin Extraction and Purification

Actin was extracted from rabbit hind-leg skeletal muscle using a published method (*12*) to make an acetone powder. To isolate actin from the acetone powder, 3 grams of powder was dissolved into 45 mL of Buffer G (2 mM Tris-HCl, 0.1 mM $CaCl_2$, 0.2 mM ATP, 1 mM sodium azide, 0.5 mM 2-mercaptoethanol, pH 8) and stirred at 4 °C for 30 minutes. Sample was added to a new pair of woman's pantyhose (Leggs Everyday knee-highs, nude color) to strain the filtrate from the solid; this process was repeated twice. The filtrate was centrifuged at 5,000 or 10,000 rpm (Sorval SS34) for 20 minutes at 4 °C. The supernatant was polymerized by adding 50 mM KCl, 2 mM $MgCl_2$, and 1 mM $Na_2ATP$ or $K_2ATP$ (Fisher, MP Biomedicals) and stirred overnight at 4 °C. The next day more KCl was added to a final concentration of 0.8 M and stirred for 30 minutes at 4 °C. The sample was centrifuged for 45 minutes at 49,000 rpm (Beckman Ti70). Pellets were resuspended into 2 mM Tris-HCl, 0.1 mM $CaCl_2$, 0.6 M KCl, 2 mM $MgCl_2$, 1 mM ATP, 0.5 mM 2-mercaptoethanol, pH 8, homogenized using a pre-chilled dounce homogenizer, and centrifuged for 60 minutes at 49,000 rpm (Beckman Ti70) at 4 °C. The supernatant was dialyzed overnight in 4-6 L of 20 mM HEPES, 0.2 mM ATP, 0.1 mM $CaSO_4$, 0.5 mM 2-mercaptoethanol, pH 8 at 4 °C. The purity of actin was checked by SDS-PAGE (Lonza). If actin was not used immediately, it was centrifuged at 50,000 rpm (Beckman Ti70) for 90 minutes at 4 °C. Sucrose was added (10% (w/v)) to the supernatant (g-actin), and the solution was then lyophilized and stored in a desiccator for no more than 6 months.

### 3.2.5 Preparation of actin for stopped-flow experiments.

Lyophilized g-actin was resuspended in water and dialyzed overnight in 6 L of 20 mM HEPES, pH 8.0 at 4 °C. Actin was centrifuged at 50,000 rpm (Beckman Ti70) for 90 minutes at 4 °C. The concentration of g-actin in the supernatant was determined by diluting into 8 M guanidinium and recording the absorbance

spectrum (Shimadzu UV-2501PC scanning spectrophotometer). The extinction coefficient of unfolded actin (45,840 $M^{-1}cm^{-1}$) was calculated from the sequence using UniProtKB/Swiss-Prot database. Actin was polymerized by adding 10 mM $K_2SO_4$, 2 mM $MgSO_4$, and 0.5 mM 2-mercaptoethanol and incubating at room temperature for ~20 minutes. To remove aggregates actin was centrifuged for 10 minutes at room temperature at 14,500 rpm. To make polymers smaller, polymerized actin was passed twice through a 22½-gauge needle.

### 3.2.6 Oxidative Half-Reaction

Enzyme was exchanged into 20 mM HEPES with ~0.5 mM 2-mercaptoethanol, pH 8.0, using Econo-Pac 10DG columns (Bio-Rad). The reaction of the MICAL-2 monooxygenase (with or without actin) was studied in a Hi-Tech Scientific KinetAsyst SF-61 DX2 stopped-flow spectrophotometer at 4 °C. Enzyme solutions (~20 - 40 μM) with and without 1 equivalent of actin were made anaerobic in a tonometer (*13*) and then reduced either with 1 equivalent of NADPH or sodium dithionite. Reduction of enzyme or enzyme actin complex were verified by monitoring changes in the absorbance spectra with a Shimadzu UV-2501PC scanning spectrophotometer. Reduced enzyme or reduced enzyme actin complexes were mixed with 20 mM HEPES, pH 8.0 which had been bubbled at 25 °C with different percentages of oxygen, up to 100 %. Kinetic traces were fit to sums of exponentials using Kaleidagraph (Synergy, Inc.). Diodearray data were collected from 300-700 nm to obtain the absorbance spectra of the intermediates using a 1.5 ms integration time.

### 3.2.7 Enzyme-Monitored Turnover

Enzyme-monitored turnover of the MICAL-2 monooxygenase with NADPH and $O_2$ was studied in a Hi-Tech Scientific KinetAsyst SF-61 DX2 stopped-flow spectrophotometer at 4 °C. Oxidized enzyme was mixed with NADPH in 20 mM

HEPES, pH 8.0, which had been pre-bubbled in 100 % oxygen. Changes in the oxidized flavin absorbance were monitored at 450 nm and the charge-transfer was monitored at 550 nm.

### 3.2.8 Electron Microscopy Imaging

All samples were absorbed onto a carbon-coated grid and stained with 0.75% uranyl formate using conventional negative staining protocol (*14*). Specimens were imaged at room temperature with a Morgagni 268(D) transmission electron microscope operated at 100 kV. Images were recorded at a magnification of 12,193x on an Orius SC200W CCD camera.

## 3.3 Results

### 3.3.1 Oxidation Half-reaction

Oxidative Half-reaction – monoMICAL-2 was reduced with one equivalent of NADPH in 20 mM HEPES, pH 8.0 at 25 °C and loaded anaerobically into a stopped-flow instrument. Its oxidation was studied by mixing with buffer that had been equilibrated with different concentrations of $O_2$. The change of the flavin from reduced to oxidized was monitored at 450 nm and the reappearance of the charge-transfer absorbance was monitored at 550 nm. Two phases were observed at 450 nm. The first phase ended at ~200 milliseconds, and the second ended by 10 seconds. Two phases could be explained if the hydroperoxide intermediate was transiently stabilized, a definite possibility for a monooxygenase. Alternatively, there could be two populations of reduced enzyme that react independently with $O_2$ with different kinetics. In order to distinguish these two possibilities, reactions were monitored by diode-array detection, where spectra (350 nm – 700 nm) can be collected in 1.5 milliseconds. The spectrum at 200 milliseconds did not show the hydroperoxide intermediate, but instead showed a mixture of reduced and oxidized enzyme. The traces were

fit to sums of exponentials. The $k_{obs}$ values for the first phase were plotted versus concentration of $O_2$, giving a square hyperbola (Figure 3-1). A hyperbolic dependence on $O_2$-concentration is unusual for the reactions of flavoenzymes. It indicates an isomerization from a form of the reduced enzyme that is not capable of reacting with $O_2$ to one that is, so that at high $O_2$ the isomerization is rate-determining (Scheme 3-2). It had a $k_{iso}$ of 25.3 ± 1.8 $s^{-1}$ and a half-saturating $O_2^-$ concentration of 96 ± 26 μM. The second phase had a linear dependence on oxygen with a $k_{ox}$ of 270 ± 50 $M^{-1}$ $s^{-1}$, indicting a bimolecular reaction, and is best described by Scheme 3-3.

The charge-transfer absorbance is an indicator of the flavin position (*15*). It only occurs when the flavin is oxidized and in the “out” conformation. The population of enzyme that oxidizes in the first phase (as detected at 450 nm) forms the charge-transfer complex at the same time, suggesting that the isomerization places the reduced flavin in contact with Trp405, where it oxidizes. In contrast, the charge-transfer absorbance for the second population of enzyme returns much slower than flavin oxidation. This shows that in this population of reduced enzyme, the flavin does not react next to Trp405, i.e. the “out” conformation. This is shown in Scheme 3-3. Combining all these schemes gives Scheme 4, which describes the chemistry of the reaction of monoMICAL-2 with $O_2$.

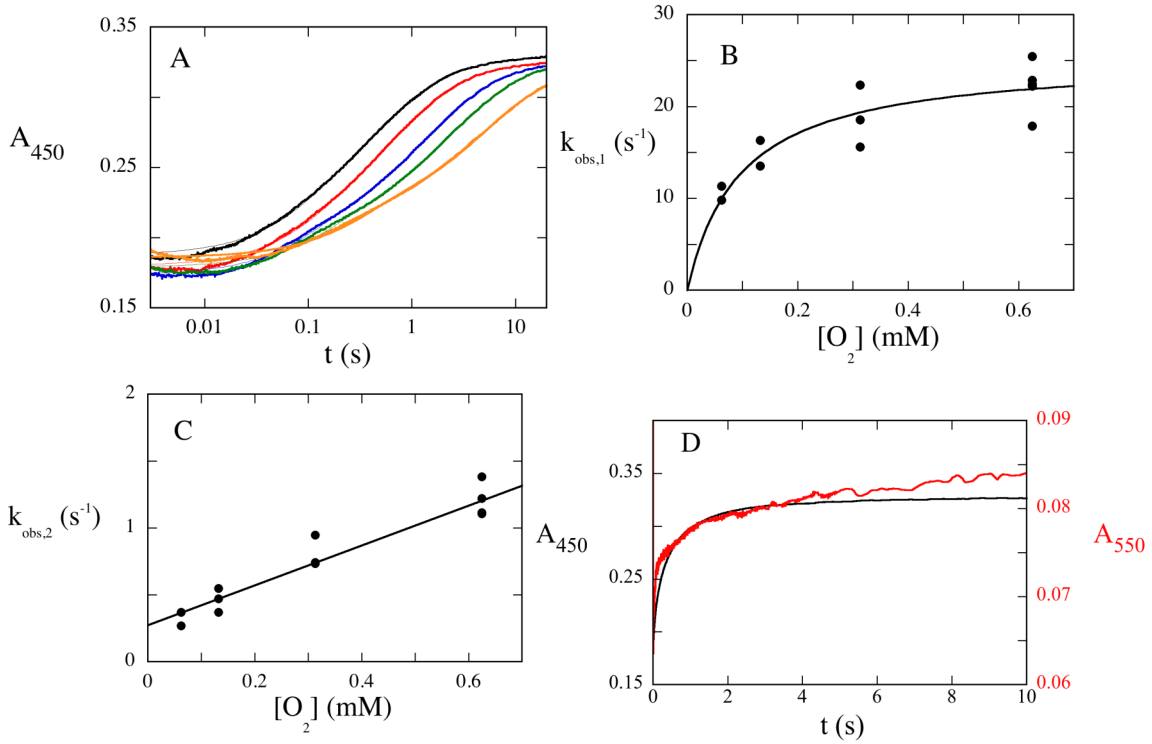


**Figure 3-1 The oxidation of monoMICAL-2 with $O_2$.**

Anaerobic enzyme (50 μM before mixing) was mixed with 20 mM HEPES, pH 8.0 equilibrated in $O_2$ (up to 1.25 mM before mixing) in a stopped-flow spectrophotometer. All reactions were performed at 4 °C. **A.** The oxidation of the enzyme was monitored at 450 nm. Note the logarithmic time-scale. The traces were fit starting at 2 milliseconds because of an early flow artifact. **B.** Observed rate constants as a function of $O_2$ concentration were obtained by fitting the data in **A** to two exponentials. The first exponential value was fit to a square hyperbola, giving $k_{iso}$ = 25.3 $s^{-1}$ and a half-saturating $O_2$ concentration of 96 μM in this experiment. **C.** The second exponential value was fit to a line, giving $k_{ox}$ = 270 $M^{-1}$ $s^{-1}$ in this experiment. **D.** Traces for the reaction of 0.975 mM $O_2$ obtained at 450 nm and 550 nm are compared. Flavin oxidation (black trace) and the reappearance of charge-transfer (red) occur simultaneously.

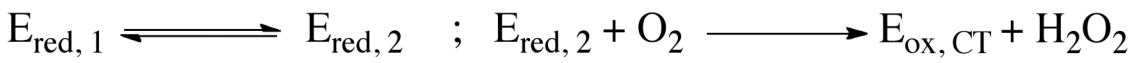


**Scheme 3-2**

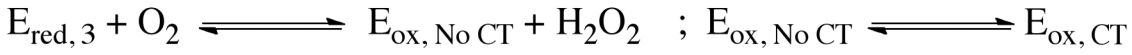


**Scheme 3-3**

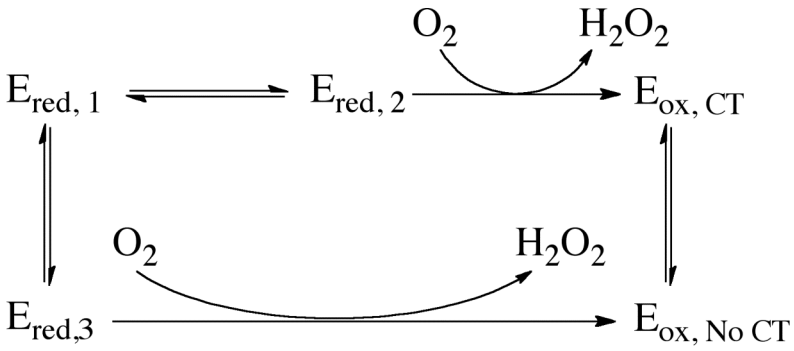


**Scheme 3-4**

### 3.3.2 Enzyme-Monitored Turnover

Enzyme-monitored turnover of oxidized monoMICAL-2 was studied by mixing enzyme with NADPH and $O_2$. The NADPH oxidase activity by enzyme-monitored turnover confirms the complexity of the monoMICAL-2 reaction. The reductive half-reaction of monoMICAL-2 is already known (Chapter 2); the $K_d$ of NADPH is ~1 mM and the $k_{red}$ is ~0.07 $s^{-1}$, much slower than the oxygen reactions; thus $K_M$ of NADPH must be approximately equal to $K_d$. The enzyme-monitored turnover traces shown in Figure 3-2A have a concentration of NADPH (8 mM) that is much greater than $K_M$, and very much greater than the starting concentration of $O_2$ (410 μM). There is an abrupt end to turnover when $O_2$ is completely consumed. The sudden end of the steady-state shows that the $K_M$ of oxygen is less than 5 μM. The $k_{cat}$ obtained from this experiment by integrating the trace (*16*) is about 0.07 $s^{-1}$, as predicted from the separate reductive and oxidative half-reactions. Interestingly, when the starting concentration of NADPH is about equal to its $K_M$, the steady-state level of the oxidized enzyme behaves differently from the steady-state level of the charge-transfer complex (Figure 3-2B). The charge-transfer absorbance disappears well before the absorbance of the oxidized flavin. The charge-transfer absorbance indicates that the flavin is “out” during about half of turnover, but then shifts to “in” as NADPH drops below its $K_M$. This change in steady-state that occurs at low NADPH, but not at high NADPH, indicates that saturation by NADPH prevents oxidized enzyme from converting from the $E_{ox,CT}$ form to the $E_{ox,noCT}$ form. However, if NADPH is low enough, enzyme can isomerize from $E_{ox,CT}$ to $E_{ox,noCT}$ and turnover in an alternate catalytic cycle. Our results from the oxidative half-reaction detected different enzyme forms. Combined with our data on the reductive half-reaction (Chapter 2), a scheme with two connected catalytic cycles can be written. At high NADPH, turnover is exclusively through the top cycle (Scheme 3-5); low NADPH allows the enzyme to turnover through the lower cycle.

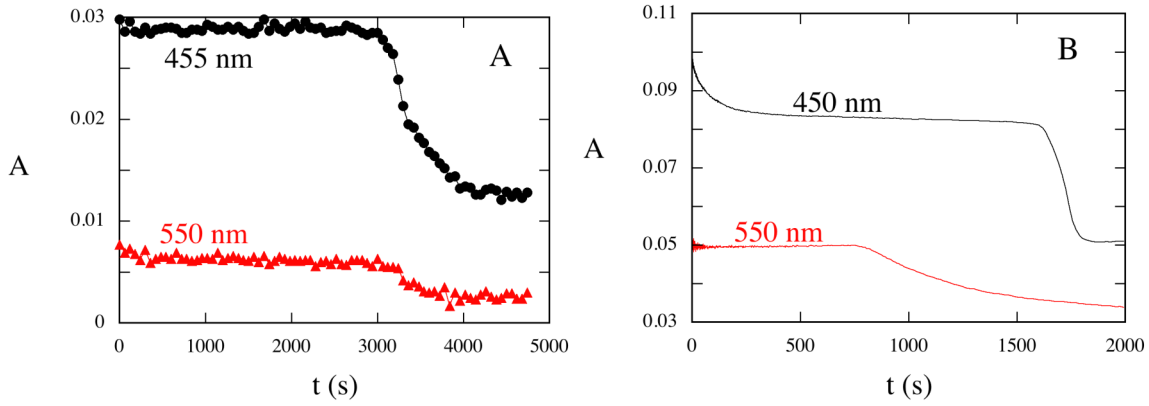


**Figure 3-2 Enzyme Monitor-Turnover NADPH oxidase activity.**

Oxidized enzyme was mixed with NADPH and $O_2$ at 4 °C in 20 mM HEPES, pH 8.0. **A.** The reaction mixture had 2 μM monoMICAL-2, 8 mM NADPH, and 410 μM $O_2$. This reaction was monitored in a spectrophotometer by scanning spectra over time. The absorbance at 455 nm and 550 nm from this experiment were plotted in **A** and show a steady-state followed by a sudden drop after the complete consumption of oxygen at ~3200 s. Traces at 455 nm and 550 nm have the same shape and the steady-state ends at the same time. **B.** The reaction mixture was 20 μM monoMICAL-2, 1 mM NADPH, and 740 μM $O_2$ in 20 mM HEPES, pH 8.0 at 4 °C. Enzyme was mixed with substrates in a stopped-flow spectrophotometer. Reactions were monitored at 450 nm or 550 nm. The 450 nm trace had a slow approach to the steady-state which abruptly ended at ~1700 s. The 550 nm trace was unusual because it reached the steady-state much quicker than the 450 nm trace but the steady-state ended much sooner (~700 s) and fell away gradually rather than abruptly.

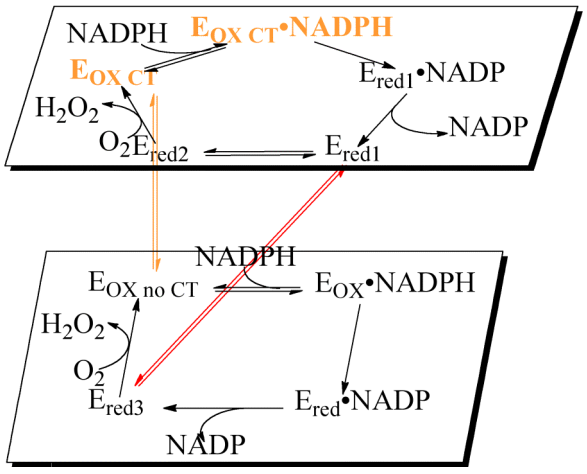


**Scheme 3-5**

### 3.3.3 Oxidative half-reaction with f-actin

*Oxidative half-reaction with f-actin* – monoMICAL-2 in complex with f-actin was reduced anaerobically with one equivalent of NADPH and mixed in a stopped-flow instrument with buffers bubbled with molecular oxygen. In single wavelength experiments, the absorbance at 390 nm, 400 nm, and 480 nm were monitored over time. Molecular oxygen (0.6 mM) reacts with the reduced enzyme-actin complex with a pseudo-first-order rate constant of ~240 $s^{-1}$. Assuming that the reaction with oxygen is bimolecular, as it is in all monooxygenases and almost all other reduced flavoenzymes, a bimolecular rate constant of ~4 x $10^5$ $M^{-1}s^{-1}$ was calculated. The absorbance at 480 nm decreased initially, while 390 nm and 400 nm increased, showing that the complex made the flavin hydroperoxide. There was a subsequent decrease in absorbance at 400 nm and an increase at 390 nm, due to the transfer of the terminal oxygen of the hydroperoxide, forming the flavin hydroxide-oxygenated-actin complex. The absorbance at 480 nm also increases during this phase. Thus about half of the enzyme eliminates hydrogen peroxide without oxygenating actin. In the next reaction phase, the flavin hydroxide eliminated water, causing the increases in absorbance at 390 nm, 400 nm, and the second increase at 480 nm. A final small slow change in absorbance occurred at 480 nm but not at 390 nm and 400 nm. Because the decay of the flavin intermediates is complete, other explanations are needed, such as the depolymerization of actin. The mechanism is depicted in Scheme 3-6.

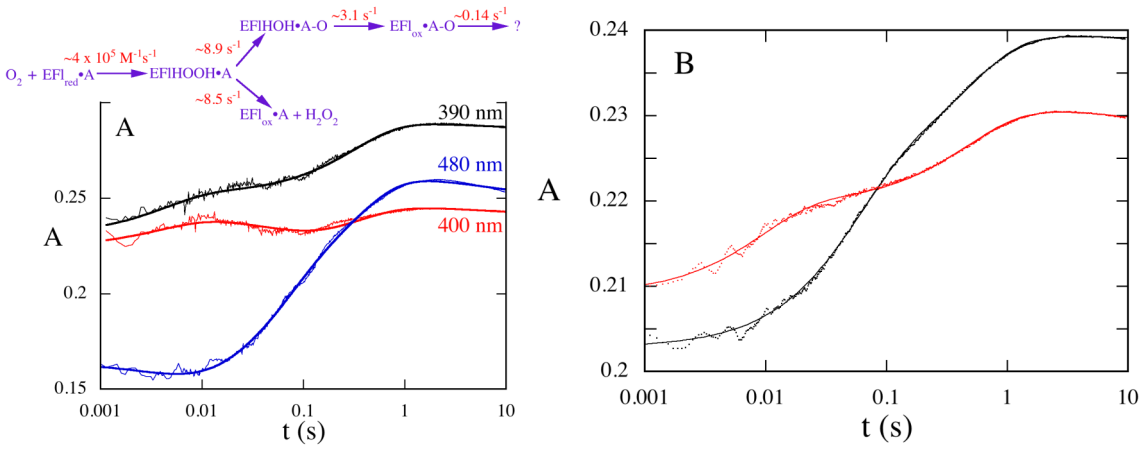


**Figure 3-3 The oxidation of monoMICAL-2 by $O_2$ in the presence of f-actin.**

An anaerobic mixture of monoMICAL-2 and actin was reduced and then mixed in a stopped-flow spectrophotometer with buffer saturated with $O_2$ at 4 °C. **A.** Traces are shown for the reaction at pH 7. The appearance of oxidized flavin, observed at 480 nm, occurs in two phases after an initial small decrease. The initial increases in absorbance at 390 nm and 400 nm are due to the formation of the flavin hydroperoxide. Oxygen transfer is evident from the subsequent decrease in absorbance at 400 nm. Note the logarithmic timescale. **B.** The same reaction was performed at pH 8.0. Note that more $H_2O_2$ is formed at the higher pH, as evidenced by the larger proportion of absorbance increasing in the first phase of appearance of oxidized enzyme.


**Scheme 3-6**

Electron microscopy was used to visualize the effects that monoMICAL-2 had on f-actin. Before treating with monoMICAL-2, there were many long fibers, which were polymers of f-actin. F-actin was then mixed with monoMICAL-2, reduced with one equivalent of NADPH, and mixed with 100% $O_2$. Images showed a loss of the f-actin polymers (Figure 3-4).

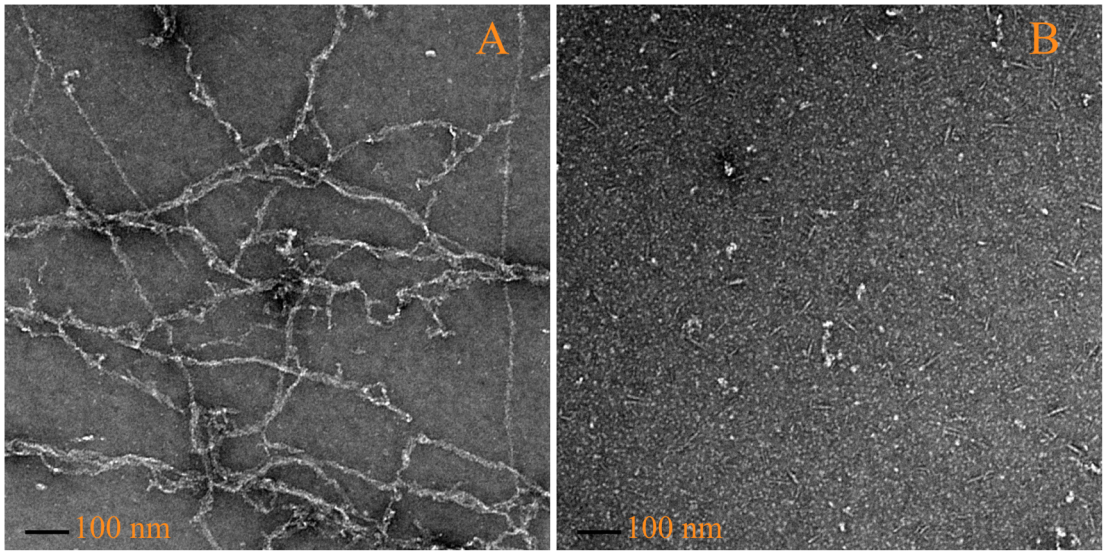


**Figure 3-4 EM images of actin**

**A.** A micrograph is shown of a sample of f-actin prepared by the method used in the oxidative half-reaction. Note the many long polymers. **B.** A sample is shown of f-actin from panel **A** after it was part of the oxidative half-reaction in a stopped-flow spectrophotometer. Note the loss of long polymers. Note that the line in the images is 100 nm long.

## 3.4 Discussion

MICALs are critical for the proper development of the nervous system (*1*). MICAL has an N-terminal monooxygenase domain and up to four protein-protein interacting domains (*2, 3*). It has been shown in *Drosophilia* that the activity of MICALs is controlled by its monooxygenase domain (*1*). The classification of MICAL as a flavoenzyme has been ill-defined. MICAL has been proposed to act as an oxidase, producing $H_2O_2$ to cause its biological effect (*5-7, 17*), but its similarity to Class A monooxygenases suggests that it would directly incorporate an oxygen atom into an activated aromatic substrate. Recently f-actin was found to be oxygenated by MICAL on Met44, forming a methionine sulfoxide (*10*). This would be similar to Class B monooxygenases which have non-aromatic substrates (*9*). Other data, such as our kinetic data, suggest monoMICAL-2 behaves most like the Class A enzymes. Schmidt *et al.* proposed a flavin hydroperoxide intermediate was stabilized by another putative substrate,

collapsin-response-mediator protein (CRMP) (*7*). If MICAL had many substrates this would suggest that MICAL was most similar to Class B enzymes, not Class A enzymes, which have a preference for only one substrate. Understanding the monoMICAL-2 oxidative half-reaction might help in the understanding of monoMICAL-2's classification.

To determine if monoMICAL-2 behaved as a Class A or Class B monooxygenase, the oxidative half-reaction of this enzyme was studied. The oxidative half-reaction of monoMICAL-2 without substrate had a low $k_{ox}$ as would be expected of a Class A enzyme, and no FlHOOH or FlHOH intermediates were detected, also similar to Class A enzymes. When actin was added to the oxidative half-reaction, oxidation of the enzyme was significantly faster and intermediates were detected. This behavior suggests that monoMICAL-2 behaves like a Class A monooxygenase not a Class B enzyme.

The reaction traces for the oxidative half-reaction of free monoMICAL-2 showed two phases due to two populations of monoMICAL-$2_{red}$. The crystal structure of the reduced hydroxylase domain of monoMICAL-1 shows two populations (*5*). Our data suggest that the two populations have faster and slower flavin movements without actin. In the fast population the flavin moves from the "in" to "out" conformations at ~20 $s^{-1}$, suggested by the simultaneous appearance of oxidized flavin and the charge-transfer absorbance. The reaction must occur next to Trp405 because the interaction between the Trp and the *re*-face of the flavin creates the charge-transfer absorbance (*15*). Some of the monoMICAL-2 in the "in" conformation reacts with oxygen, and then makes the charge-transfer interaction really slowly. We do not know why the reactions are slow with oxygen, nor do we know why the conformational changes of the flavin are also slow. This is especially puzzling since the active site of monoMICAL-1 is large and relatively open. The flavin is highly accessible in both the "in" and "out" conformations (*5,*

*6*). Thus access is not the reason why the enzyme reacts so slowly with oxygen. The structure of monoMICAL-$1_{red,in}$ shows that the flavin has a "butterfly-bend" (*5*) and therefore is the neutral hydroquinone, not $FADH^-$ (*18*-*20*). In order to react with $O_2$, N1 of the flavin must deprotonate. This could explain why we see two populations of enzyme. The deprotonation of the "fast" population could be causing the movement from "in" to "out". Another possible explanation could be that the flavin is already in the "out" conformation, but deprotonation occurs at ~20 $s^{-1}$. This seems very unlikely because deprotonation of non-carbon atoms exposed to solvent is generally extremely fast.

During enzyme monitored-turnover at a high concentration of NADPH, oxidase activity has a "normal" catalytic cycle. The $k_{cat}$ is as predicted by the reductive and oxidative half-reactions. Turnover happens with the flavin in the "out" position. When the concentration of NADPH is approximately the dissociation constant, which equals the $K_M$, enzyme-monitored turnover no longer follows the "normal" catalytic cycle. The oxidized enzyme has a longer steady-state than charge-transfer absorbance and the $k_{cat}$ obtained by integration no longer equals the value predicted by the two half-reactions. These data suggest that monoMICAL-2 has two catalytic cycles that are connected. This occasionally has been reported for flavoenzymes, for example, D-amino acid oxidase (*21*).

Adding actin changes the oxidative half-reaction significantly. The normal hydroxylase/monooxygenase pathway makes flavin hydroperoxide, flavin hydroxide, and oxidized enzyme. These flavin intermediates were detected in the presence of actin. Importantly, I saw the conversion of the flavin hydroperoxide to flavin hydroxide. This requires the breakage of the oxygen-oxygen bond and transfer of the distal oxygen to an acceptor. Because this only happens when actin is present, this shows that actin is oxygenated. Thus, our experiments show that a substrate for monoMICAL-2 is actin. It has been reported that actin is the

substrate for monoMICAL-1 (*15, 22*) and adds an oxygen to the sulfur on Met44 to make the sulfoxide (*10*). Other substrates for MICAL have been proposed, such as CRMP (*7*), vimentin (*23*), and rab1 (*24*). This remains untested by direct stopped-flow methods. This possible broad specificity would make MICAL more like Class B enzymes because Class A enzymes are generally substrate-specific. These intermediates were not detected in the oxidative half-reaction in the absence of f-actin. However, in the presence of actin, FlHOOH is formed, and half goes to FlHOH while the other 50 % makes $H_2O_2$. Many hydroxylases are essentially completely effective in transferring the oxygen of FlHOOH and do not make detectable $H_2O_2$ with their physiological substrates e.g., PHBH (*9*). On the other hand, some are inherently ineffective and make significant amounts of $H_2O_2$ even when acting on their physiological substrates, e.g. phenol hydroxylase. The uncoupling observed with monoMICAL-2 could be due to weak binding of actin. It is also plausible that the other C-terminal domains of MICAL-2 are needed to make actin bind tightly to the enzyme, making it more efficient.

monoMICAL-2 has many characteristics of the Class A monooxygenases (*8*). The flavin of monoMICAL-2 changes conformations between “in” and “out” and reduction and oxidation are stimulated with substrate. However unlike typical Class A monooxygenases, monoMICAL-2 oxygenates a non-aromatic substrate. Evolution has recruited a Class A enzyme to perform Class B chemistry of MICAL-2.

## 3.5 References


1. Terman, J. R., Mao, T., Pasterkamp, R. J., Yu, H. H., and Kolodkin, A. L. (2002) MICALs, a family of conserved flavoprotein oxidoreductases, function in plexin-mediated axonal repulsion, *Cell 109*, 887-900.
2. Hung, R. J., and Terman, J. R. (2011) Extracellular inhibitors, repellents, and semaphorin/plexin/MICAL-mediated actin filament disassembly, *Cytoskeleton (Hoboken) 68*, 415-433.
3. Zhou, Y., Gunput, R. A., Adolfs, Y., and Pasterkamp, R. J. (2011) MICALs in control of the cytoskeleton, exocytosis, and cell death, *Cell Mol. Life Sci. 68*, 4033-4044.
4. Ashida, S., Furihata, M., Katagiri, T., Tamura, K., Anazawa, Y., Yoshioka, H., Miki, T., Fujioka, T., Shuin, T., Nakamura, Y., and Nakagawa, H. (2006) Expression of novel molecules, MICAL2-PV (MICAL2 prostate cancer variants), increases with high Gleason score and prostate cancer progression, *Clin. Cancer Res. 12*, 2767-2773.
5. Siebold, C., Berrow, N., Walter, T. S., Harlos, K., Owens, R. J., Stuart, D. I., Terman, J. R., Kolodkin, A. L., Pasterkamp, R. J., and Jones, E. Y. (2005) High-resolution structure of the catalytic region of MICAL (molecule interacting with CasL), a multidomain flavoenzyme-signaling molecule, *Proc. Natl. Acad. Sci. U. S. A. 102*, 16836-16841.
6. Nadella, M., Bianchet, M. A., Gabelli, S. B., Barrila, J., and Amzel, L. M. (2005) Structure and activity of the axon guidance protein MICAL, *Proc. Natl. Acad. Sci. U. S. A. 102*, 16830-16835.
7. Schmidt, E. F., Shim, S. O., and Strittmatter, S. M. (2008) Release of MICAL autoinhibition by semaphorin-plexin signaling promotes interaction with collapsin response mediator protein, *J. Neurosci. 28*, 2287-2297.

8. van Berkel, W. J., Kamerbeek, N. M., and Fraaije, M. W. (2006) Flavoprotein monooxygenases, a diverse class of oxidative biocatalysts, *J. Biotechnol. 124*, 670-689.
9. Palfey, B. A., and McDonald, C. A. (2010) Control of catalysis in flavin-dependent monooxygenases, *Arch. Biochem. Biophys. 493*, 26-36.
10. Hung, R. J., Pak, C. W., and Terman, J. R. (2011) Direct redox regulation of F-actin assembly and disassembly by Mical, *Science 334*, 1710-1713.
11. Stols, L., Gu, M., Dieckman, L., Raffen, R., Collart, F. R., and Donnelly, M. I. (2002) A new vector for high-throughput, ligation-independent cloning encoding a tobacco etch virus protease cleavage site, *Protein Expr. Purif. 25*, 8-15.
12. Pardee, J. D., and Spudich, J. A. (1982) Purification of muscle actin, *Methods Enzymol. 85 Pt B*, 164-181.
13. Palfey, B. A. (2003) *Time Resolved Spectral Analysis*, Oxford Univerisity Press, New York.
14. Ohi, M., Li, Y., Cheng, Y., and Walz, T. (2004) Negative Staining and Image Classification - Powerful Tools in Modern Electron Microscopy, *Biol. Proced. Online 6*, 23-34.
15. Zucchini, D., Caprini, G., Pasterkamp, R. J., Tedeschi, G., and Vanoni, M. A. (2011) Kinetic and spectroscopic characterization of the putative monooxygenase domain of human MICAL-1, *Arch. Biochem. Biophys. 515*, 1-13.
16. Gibson, Q. H., Swoboda, B. E., and Massey, V. (1964) Kinetics and Mechanism of Action of Glucose Oxidase, *J. Biol. Chem. 239*, 3927-3934.
17. Morinaka, A., Yamada, M., Itofusa, R., Funato, Y., Yoshimura, Y., Nakamura, F., Yoshimura, T., Kaibuchi, K., Goshima, Y., Hoshino, M., Kamiguchi, H., and Miki, H. (2011) Thioredoxin mediates oxidation-dependent phosphorylation of CRMP2 and growth cone collapse, *Sci. Signal. 4*, ra26.

18. Lennon, B. W., Williams, C. H., Jr., and Ludwig, M. L. (1999) Crystal structure of reduced thioredoxin reductase from Escherichia coli: structural flexibility in the isoalloxazine ring of the flavin adenine dinucleotide cofactor, *Protein Sci. 8*, 2366-2379.
19. Rodriguez-Otero, J., Martinez-Nunez, E., Pena-Gallego, A., and Vazquez, S. A. (2002) The role of aromaticity in the planarity of lumiflavin, *J. Org. Chem. 67*, 6347-6352.
20. Zheng, Y.-J., and Ornstein, R. L. (1996) A Theoretical Study of the Structures of Flavin in Different Oxidation and Protonation States, *J. Am. Chem. Soc. 118*, 9402-9408.
21. Porter, D. J., Voet, J. G., and Bright, H. J. (1977) Mechanistic features of the D-amino acid oxidase reaction studied by double stopped flow spectrophotometry, *J. Biol. Chem. 252*, 4464-4473.
22. Hung, R. J., Yazdani, U., Yoon, J., Wu, H., Yang, T., Gupta, N., Huang, Z., van Berkel, W. J., and Terman, J. R. (2010) Mical links semaphorins to F-actin disassembly, *Nature 463*, 823-827.
23. Suzuki, T., Nakamoto, T., Ogawa, S., Seo, S., Matsumura, T., Tachibana, K., Morimoto, C., and Hirai, H. (2002) MICAL, a novel CasL interacting molecule, associates with vimentin, *J. Biol. Chem. 277*, 14933-14941.
24. Weide, T., Teuber, J., Bayer, M., and Barnekow, A. (2003) MICAL-1 isoforms, novel rab1 interacting proteins, *Biochem. Biophys. Res. Commun. 306*, 79-86.

# Chapter 4
# Conclusion and Future Directions

## 4.1 Summary

The results from this thesis have partly clarified the catalytic behavior and biological role of MICAL-2. Based on my kinetic results, the catalytic cycle can be drafted in detail (Scheme 4-1). Importantly, the reductive half-reaction and the oxidative half-reaction are both faster in the presence of f-actin, behavior typical of aromatic monooxygenases. Even more importantly, the detection of flavin oxygen intermediates shows that it is a monooxygenase – not an oxidase. A C4a-hydroperoxide has only been observed in one oxidase (*1*), and my observation of the C4a-hydroxide can only be explained by oxygen transfer – not a reaction done by oxidases.

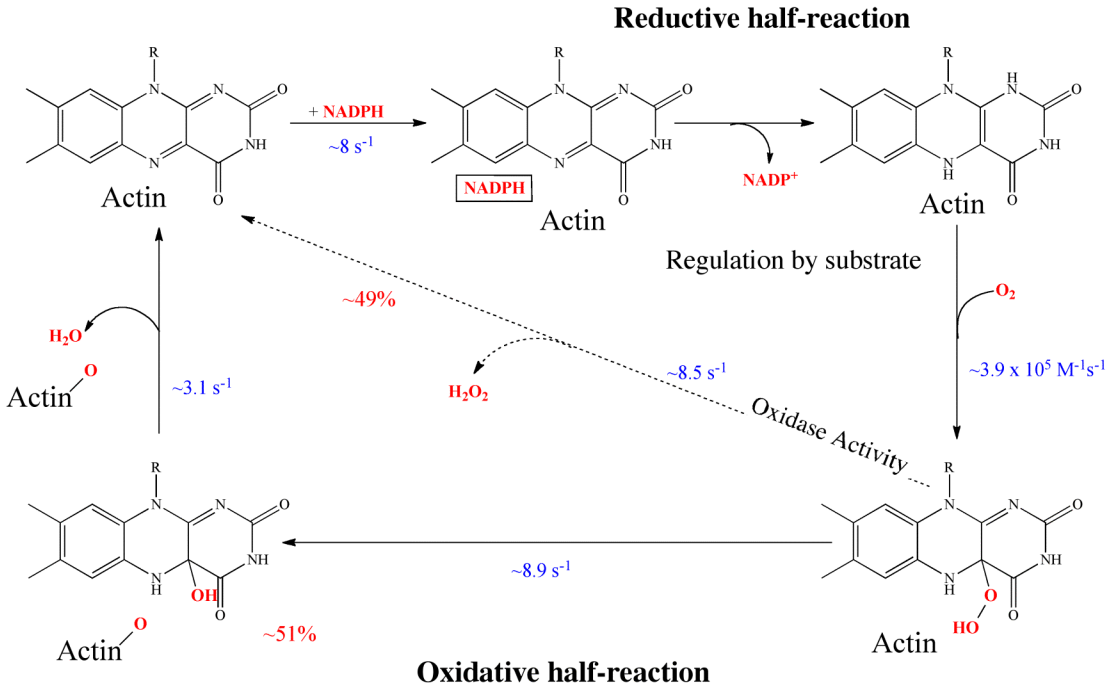


**Scheme 4-1**

Actin has important effects on both of the half-reactions. The rate constant for reduction of monoMICAL-2 with NADPH is 0.074 $s^{-1}$ without actin, and with f-actin, this rate constant increases to 8 $s^{-1}$, which is a 100-fold stimulation. In Class A monooxygenases such as *p*-hydroxybenzoate hydroxylase the rate constant for reduction increases by ~100,000-fold with its substrate *p*-hydroxybenzoate (*2*). Kynurenine-3-monooxygenase has a stimulation in reduction with kynureine of ~2500-fold (*2*). monoMICAL-2 shows stimulation but not as drastic as *p*-hydroxybenzoate hydroxylase or kynurenine-3-monooxygenase. This may be due to the absence of the other C-terminal domains in MICAL-2; thus their presence might stimulate reduction more. The oxidative half-reaction of monoMICAL-2 with f-actin gives a rate constant of 4 x $10^5$ $M^{-1}$ $s^{-1}$. *p*-Hydroxybenzoate hydroxylase has a similar rate constant with substrate bound, 3 x $10^5$ $M^{-1}$ $s^{-1}$ (*3*). Oxidation of monoMICAL-2 produced C4a intermediates – both the flavin hydroperoxide and flavin hydroxide. These would not have been seen if monoMICAL-2 were an oxidase. Electron microscopy

showed that actin depolymerizes when monoMICAL-2 was added. This combined data strongly argue that monoMICAL-2 is a monooxygenase that uses f-actin as its substrate. Although I still do not have the mass spectrometry product analysis, it is very likely that the methionine on the D-loop of actin has been modified with an oxygen atom to make it methionine sulfoxide.

Although the catalytic cycle of monoMICAL-2 is very similar in most ways to the cycles of Class A monooxygenases, it oxygenates a non-aromatic (actin). Class B monooxygenases such as flavin-containing monooxygenases and cyclohexanone monooxygenases oxygenate non-aromatic such as thioethers (*2*), while Class A enzymes have so far been found to oxygenate only aromatic substrates. There is no inherent chemical reason for Class A enzymes to only oxygenate aromatics, but it has never been seen before. It is interesting that evolution would adapt a Class A enzyme to modify a Class B substrate especially when there are few Class A enzymes in eukaryotes but there are plenty of Class B enzymes.

Regulation of monoMICAL-2 is like Class A monooxygenases. Actin regulates the reactions of the flavin monoMICAL-2 despite the fact that it is missing its C-terminal domains, thus the protein-protein interaction domains are not needed for stimulation of catalysis. The chemistry of MICAL-2 might be completely regulated by actin. However, it is possible that the C-terminal domains of MICAL-2 also play a role. They may bring actin to the right place for catalysis and not play an actual regulatory role in the reactions of the monooxygenase domain. Interestingly though, in the oxidative half-reaction of monoMICAL-2 with actin, 50% of the enzyme oxygenated the substrate, while the other half eliminated $H_2O_2$. This result could be a coincidence; perhaps I was only able to saturate 50% of monoMICAL-2 with actin. Perhaps the C-terminal domains help in binding actin. It is also possible that that is the best that monoMICAL-2 can hydroxylate;

some hydroxylases are less than 100% coupled (*2, 4*). Another possibility is that the C-terminal protein-protein interacting domains modulate $H_2O_2$ production. Thus, the real function of MICAL would be to switch between being an oxidase and being a monooxygenase.

### 4.2 Future experiments

The first task that is really important to help understand the chemistry of monoMICAL-2 would be to obtain the mass spectrometry results and perform product analysis. This is very important because it has been shown for monoMICAL-1 that it modifies actin on a Met44 (*5*). However it has not been shown yet which residue monoMICAL-2 modifies. It may be the same methionine, as I predict, or a different residue on actin. The structure of monoMICAL-1 has been solved (*6, 7*). However none exists for monoMICAL-2. The structure of monoMICAL-2 needs to be determined because it can provide insight on how the enzyme may function. For example, does monoMICAL-2 have a very exposed active site as was seen in monoMICAL-1? It would be interesting to see which residues are close to the flavin, and this would be crucial in helping to guide site-directed mutagenesis of residues that might be critical for catalysis.

Studies on the reactivity of monoMICAL-1 and monoMICAL-3 would be interesting. Their reactivities could be compared to monoMICAL-2. monoMICAL-2 reacted slowly without actin and was much faster with substrates. Also intermediates were observed in its oxidative half-reaction. monoMICAL-1 and monoMICAL-3 could be studied in the detail that monoMICAL-2 was studied. Important mechanistic information can be determined such as: a KIE on flavin reduction, the stimulation of reduction caused by actin, the kinetics of formation and reaction of the oxidative half-reaction intermediates. All these questions would be very interesting to answer and might help us understand why evolution

has created three MICALs and help us further understand the distinct ions or similarities in their mechanisms of catalysis.

I used f-actin in my studies of monoMICAL-2. However this was problematic. Actin in its filamentous form is a large polymer and scatters a tremendous amount of light, thus causing high turbidity. Because of this problem, I wasn't able to use very high concentrations of f-actin. I was only able to saturate my enzyme with substrate to a maximum of 50%. Also analyzing the data was very difficult because of the high turbidity caused by actin. Alternative substrates might allow higher quantities of substrate to be used; this would allow unstable intermediates to be observed and aid in obtaining a concentration dependence. Alternative substrates might be free methionine, peptides, or proteins that are easy to express and manipulate with a substrate loop that could be engineered to serve as a substrate. Stopped-flow experiments of monoMICAL-2 could be performed with free methionine or methionine derivatives that neutralize the charge such as N-acetyl methionine, O-methyl methionine, and N-acetyl-O-methyl methionine. However a single amino acid might not be enough for the enzyme to react so peptides should also be tested. Peptides could be generated with a sequence surrounding the Met44 on actin. It is unknown how long of an actin sequence is needed for monoMICAL-2 to react. It is possible that a small peptide sequence would be suffice for reactivity, or monoMICAL-2 might need a long sequence for reactivity; thus peptides of varying length would need to be made and then tested for their reactivity with monoMICAL-2. Obtaining synthesized peptides might become expensive if very high concentrations are needed. A more economic alternative would be to engineer a loop on an "ideal" protein of our choice. This ideal protein would contain a sequence from actin that would contain Met44 and its surrounding amino acids. The ideal protein would also need to be easy to express and purify. It would also need to be soluble at high concentrations, in case my experiments require high concentrations of

substrate. The ideal protein would need to have its surface surrounding Met44 have the same charge as the surface of actin. Some possible ideal proteins could be one of the Rab proteins (Rab1, 8a, 10, 13, 15, 35, 36) or maybe CasL since these proteins have already been shown to interact with MICALs (*8*).

Although it is now known that actin is the substrate that MICAL modifies, it is unknown what controls the binding of actin. I have made a docking model (Figure 4-2) of how actin might bind to monoMICAL-1 with actin's Met44 residue positioned in monoMICAL-1's active site. From this model, it is possible to predict residues on actin that might be involved in its binding to the enzyme. It would be interesting to mutate some of these residues and test to see if the binding of actin is affected. These experiments would provide structural information on how monoMICAL-2 interacts with actin during catalysis. Met44 is the residue that monoMICAL-1 modifies. It would be interesting to mutate this residue to alanine, leucine, tyrosine etc. and determine if changes are observed in the binding and reactivity of monoMICAL-2. Alanine – because it removes most contact from the side chain. Leucine – because it is a bulky hydrophobic residue but does not have a sulfur to be oxygenated. Tyrosine – because it is an activated aromatic which is typically oxygenated by Class A enzymes. Since Met44 is the residue that monoMICAL oxygenates, mutating it would not allow this process to happen. I would expect to see more of the intermediate C4a-hydroperoxide and then the elimination of $H_2O_2$. I wouldn't expect any changes in the reductive half-reaction of monoMICAL-2 with mutated actin but maybe mutating on Met44 would decrease reactivity. If reactivity was decreased in the reductive half-reaction, it would suggest that the methionine on actin interacts somehow with NADPH or monoMICAL assisting its interaction with pyridines nucleotide. An interesting actin mutant to test would be Met44Tyr. Tyrosine is an activated aromatic – the type of substrate all other Class A enzymes oxygenate – and it is very likely that monoMICAL-2 would modify it and the flavin intermediates; C4a-flavin hydroxide

and C4a-flavin hydroperoxide would be observed. If that occurred, monoMICAL-2 would be acting like a typical Class A monooxygenase performing a Class A reaction. However, if monoMICAL-2 didn't modify Met44Tyr actin, that would also be interesting.

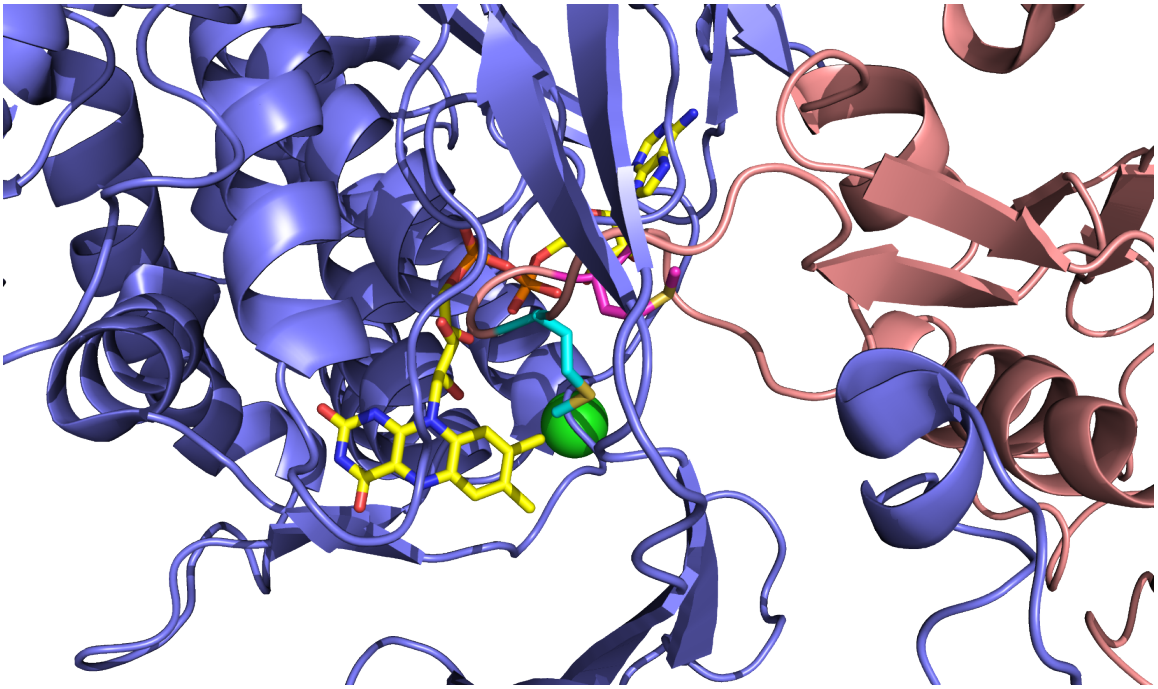

**Figure 4-1 Docking model of monoMICAL-1 with actin.**

The monoMICAL-1 active site is shown in purple. The green ball is a chloride ion. Met44 (shown in pink) was manually positioned near the flavin while attempting to avoid steric clashes. No attempt was made to optimize the energy of the complex.

CRMP, vimentin, and NDR kinases interact with MICALs (*8*). Sometimes these proteins have even been called substrates of MICALs. My methods can be applied to test these different interactors with monoMICAL-2, and determine if their presence changes catalysis. It would be very interesting to see what affect they may have on the reductive and oxidative half-reactions of monoMICAL-2. These proteins might stimulate reduction or oxidation. If they did, it would imply that monoMICAL-2 is not substrate-specific, a behavior more typically seen in Class B monooxygenases. Schmidt *et al.* proposed that CRMP preserves the

flavin hydroperoxide (*9*). Performing stopped-flow and diodearray experiments with reduced monoMICAL-2 with CRMP and oxygen would allow us to determine if that was true. If monoMICAL-2 with CRMP preserves the flavin hydroperoxide then the enzyme would be showing Class B behavior. These experiments with interactors and enzyme could also be done with the addition of actin. It is possible that CRMP, vimentin or NDR kinase could interfere with actin.

All of my studies have focused on the monooxygenase domain of MICAL-2. However MICAL-2 has CH and LIM domains. Constructs could be made with different domains tethered to the monooxygenase domain such as monoMICAL-2-CH or the full-length MICAL-2 protein. Also, these other domains could be expressed separately. It has been proposed that the C-terminal domains of MICAL-1 are auto-inhibitory towards the reactivity of the monooxygenase domain. The stopped-flow methods I used can determine which domains might inhibit the reductive and oxidative half-reactions. This would provide information on the roles these different domains have on catalysis. There are three MICALs in mammals. Do monoMICAL-1 and monoMICAL-3 react similarly to monoMICAL-2? The reductive and oxidative half-reactions of monoMICAL-1 and monoMICAL-3 could be studied using my methods to determine if their half-reactions are stimulated by actin. The oxidative half-reactions of monoMICAL-1 and monoMICAL-3 would be performed to determine if any of the flavin intermediates (FlHOOH or FlHOH) were detected. It is possible that these three monooxygenase domains behave similarly, thus their catalytic cycles would be the same. If intermediates were detected, mass spectrometery would need to be used to analyze the products of these reactions to determine what residue(s) were modified on actin. All three MICALs might modify actin on the same residue or they might not.

The active site of monoMICAL-1 shows some residues that may play a role in catalysis and are conserved in monoMICAL-2. The roles of active site residues could be explored in the reductive and oxidative half-reactions of monoMICAL-2 by mutating some residues of interest. My results show that monoMICAL-2 has flavin movement, a classic hydroxylase characteristic. I believe that this movement is caused by a tryptophan near the *re* face of the flavin. Trp405 is conserved in all MICALs, not just the ones in mammals. This suggests that this residue is important. I have already mutated Trp405 to an alanine residue. The Trp405Ala mutation changed my enzyme's color from orange (wild-type) to yellow (mutant). The tryptophan near the flavin causes a charge-transfer interaction that is no longer present in the mutant enzyme. I have not yet tested the reactivity of the Trp405Ala mutant. It will be interesting to see how this mutation has affected the reductive and oxidative half-reactions, as well as the ways that the enzyme reacts with actin. MICALs have tyrosines in their active site which is also similar to several Class A monooxygenase enzymes. Mutating active site tyrosines in Class A monooxygenases caused drastic changes in reactivity. Some of these tyrosines are conserved in MICALs. It is very likely that these tyrosines are playing a role in catalysis. I would mutate the tyrosines and perform stopped-flow experiments, checking for any changes in the reductive and oxidative half-reactions. Tyrosines in Class A monooxygenases have been shown to be directly involved in the transfer from the flavin of oxygen to their substrate (*10*). This has never been tested in MICAL. If tyrosines were mutated and intermediates were not detected in the oxidative half-reaction, this would imply that these tyrosines were involved in the transfer of the oxygen atom to actin, like Class A enzymes. However, if intermediates were detected and it was determined that the tyrosines in the active site of monoMICAL-2 did not play a role in catalysis, this would be more like Class B enzymes.

## 4.3 References


1. Sucharitakul, J., Prongjit, M., Haltrich, D., and Chaiyen, P. (2008) Detection of a C4a-hydroperoxyflavin intermediate in the reaction of a flavoprotein oxidase, *Biochemistry 47*, 8485-8490.
2. Palfey, B. A., and McDonald, C. A. (2010) Control of catalysis in flavin-dependent monooxygenases, *Arch. Biochem. Biophys. 493*, 26-36.
3. Entsch, B., and Ballou, D. P. (1989) Purification, properties, and oxygen reactivity of p-hydroxybenzoate hydroxylase from Pseudomonas aeruginosa, *Biochim Biophys Acta 999*, 313-322.
4. Maeda-Yorita, K., and Massey, V. (1993) On the reaction mechanism of phenol hydroxylase. New information obtained by correlation of fluorescence and absorbance stopped flow studies, *J Biol Chem 268*, 4134-4144.
5. Hung, R. J., Pak, C. W., and Terman, J. R. (2011) Direct redox regulation of F-actin assembly and disassembly by Mical, *Science 334*, 1710-1713.
6. Nadella, M., Bianchet, M. A., Gabelli, S. B., Barrila, J., and Amzel, L. M. (2005) Structure and activity of the axon guidance protein MICAL, *Proc. Natl. Acad. Sci. U. S. A. 102*, 16830-16835.
7. Siebold, C., Berrow, N., Walter, T. S., Harlos, K., Owens, R. J., Stuart, D. I., Terman, J. R., Kolodkin, A. L., Pasterkamp, R. J., and Jones, E. Y. (2005) High-resolution structure of the catalytic region of MICAL (molecule interacting with CasL), a multidomain flavoenzyme-signaling molecule, *Proc. Natl. Acad. Sci. U. S. A. 102*, 16836-16841.
8. Zhou, Y., Gunput, R. A., Adolfs, Y., and Pasterkamp, R. J. (2011) MICALs in control of the cytoskeleton, exocytosis, and cell death, *Cell Mol. Life Sci. 68*, 4033-4044.

9. Schmidt, E. F., Shim, S. O., and Strittmatter, S. M. (2008) Release of MICAL autoinhibition by semaphorin-plexin signaling promotes interaction with collapsin response mediator protein, *J. Neurosci. 28*, 2287-2297.

10. Entsch, B., Palfey, B. A., Ballou, D. P., and Massey, V. (1991) Catalytic function of tyrosine residues in para-hydroxybenzoate hydroxylase as determined by the study of site-directed mutants, *J Biol Chem 266*, 17341-17349.

# Appendix A
# Substrate Binding and Reactivity are Not Linked: Grafting a Proton-Transfer Network into a Class 1A Dihydroorotate Dehydrogenase

The content of this chapter was previously published by the author as a Rapid Report in Biochemistry [15].

Dihydroorotate dehydrogenases (DHODs) catalyze the only redox reaction in the biosynthesis of pyrimidines. DHODs convert dihydroorotate (DHO) to orotate (OA). An active site base from DHOD removes a proton at C5 of DHO, and a hydride is transferred from DHO at the C6 position to FMN, reducing the flavin (Figure A-1). The DHODs are phylogentically classified into Class 1 and Class 2 (*1*). The Class 1 DHODs are further grouped into 1A and 1B. The oxidizing substrate used by DHOD is different for each phylogenetic class; Class 2 DHODs use ubiquinone (*2*), Class 1A DHODs use fumarate (*3*), and Class 1B DHODs use NAD (*4*). The location of the DHODs in the cell is also different; Class 2 DHODs are membrane-bound (*2*) while Class 1 DHODs reside in the cytosol (*3*). The oligomerization state is also different, Class 2 DHODs are monomers (*2*), Class 1A DHODs are dimers (*3*) and Class 1B DHODs are $\alpha_2\beta_2$ heterotetramers (*4*).

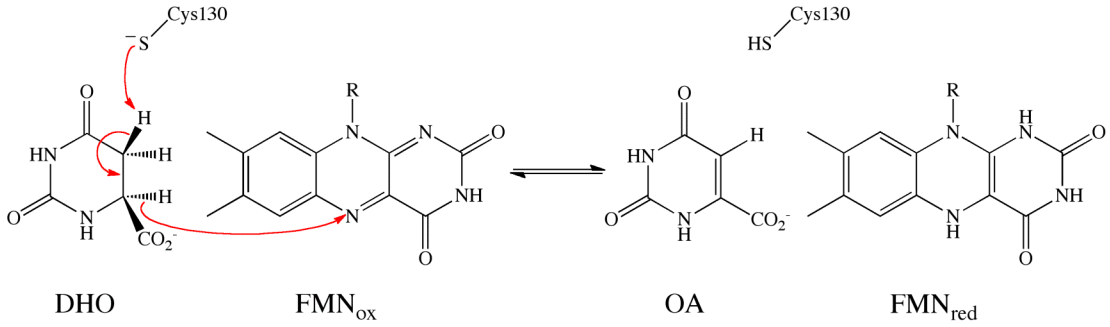


**Figure A-1 The reaction of a Class 1A DHOD with DHO.**

A hydride from C6 of DHO is transferred to N5 of FMN, while the proton from C5 of DHO is removed by the active site base, Cys130. In Class 2 DHODs, the active site base is serine.

The structure of the pyrimidine binding site appears to be nearly the same in all DHODs (Figure A-2), except that the active site bases which deprotonate DHO are different for the DHOD classes (*5, 6*). The Class 2 DHODs use a serine as their active site base while the Class 1 DHODs use a cysteine. Despite the nearly identical active sites, the two bases are not interchangeable. The *L. lactis* Class 1A Cys130Ser mutant enzyme oxidizes DHO ~5 orders of magnitude slower than wild-type enzyme (*7*). This suggests that residues not immediately in contact with DHO or FMN are critical for reactivity. The serine of the Class 2 enzyme passes a proton from DHO to solvent via a proton-transfer network. A threonine and a water molecule form the network, and a phenylalanine helps orient the hydrogen bonds (*8*). The Class 1A enzyme does not have a proton-transfer network (*9*). Its active site base is more exposed to solvent than the Class 2 enzyme.

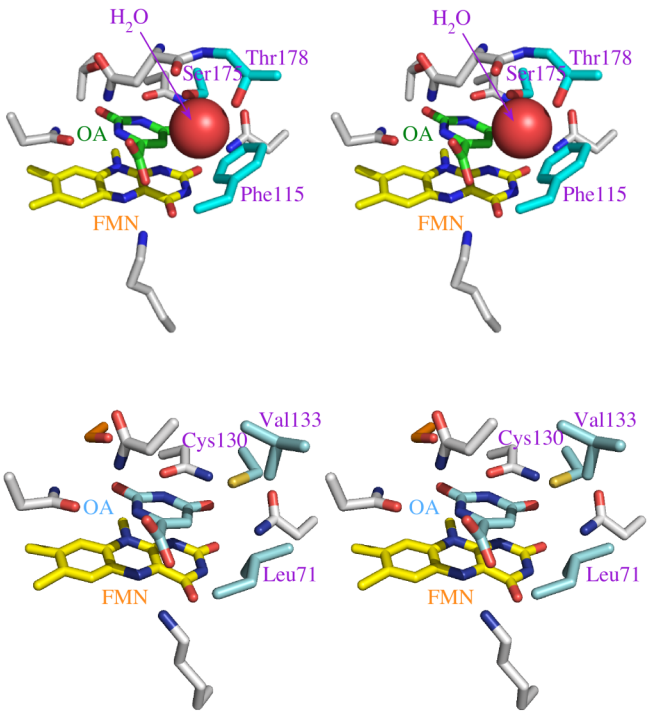


**Figure A-2 Stereoview of Class 2 and Class 1A DHODs.**

Class 2 DHODs (Top) have a proton-transfer network that is made up of Thr178, Ser175, a water molecule, and Phe115 (shown in lavender). Class 1A DHODs (Bottom) do not have a proton-transfer network, however mutations were made to residues Val133, Cys130, and Leu71 (shown in lavender) to incorporate a Class 2 proton-transfer network into the Class 1A enzyme.

The absence of the proton-transfer network in the Class 1A enzyme (*9*) may be the critical factor for the lack of reactivity of serine as base. This was tested by making the Class 1A triple-mutant Leu71Phe/Cys130Ser/Val133Thr. The usual red-shift (*10*) was seen upon addition of DHO. Therefore DHO binds. The triple-mutant reacted excruciatingly slowly, with a $k_{red}$ of 9.7 x $10^{-6}$ ± 3 x $10^{-7}$ $s^{-1}$ at 25 °C.

| Enzyme | $k_{red}$ (DHO) ($s^{-1}$) | $K_d$ (DHO) (μM) | $K_d$ (OA) (μM) | $K_d$ (3,4-diOHB) (μM) | $K_d$ (3,5-diOHB) (μM) |
|---|---|---|---|---|---|
| *E.coli* wild-type Class 2 | 46 ± 0.3[a] | 20 ± 1[a] | 3.4 ± 0.8[b] | No binding[c] | No binding[c] |
| *L.lactis* wild-type Class 1A | 170 ± 12 | 145 ± 54[d] | 13.1 ± 0.7[e] | 19 ± 2[c] | 18 ± 0.2[c] |
| Leu71Phe | 0.015 ± 0.002 | << 125[f] | 13.5 ± 0.8[g] | No binding[g] | 417 ± 17[g] |
| Val133Thr | 41 ± 0.8 | 84 ± 9[d] | 25 ± 0.7[g] | 640 ± 40[g] | 156 ± 4[g] |
| Leu71Phe/Val133Thr | 0.0010 ± 0.0001 | 22 ± 0.9[g] | 12 ± 0.6[g] | No binding[g] | 453 ± 27[g] |
| Leu71Phe/Cys130Ser/Val133Thr | Too slow TBD | 57 ± 2[g] | 16 ± 1.1[g] | No binding[g] | 392 ± 38[g] |

[a]Data taken from ref (14). [b]Data taken from ref (9). [c]Data taken from ref (13). [d]Data taken from stopped-flow experiments. [e]Data taken from ref (1). [f]Binding value too low to be determined. [g]Data taken from aerobic titrations.

**Table A-1 Reduction rate constants at 4 °C and dissociation constants 25 °C**

The reduction of the triple-mutant with DHO at 4 °C took so long (~one month) that its $k_{red}$ is not reported. Thus, installation of a proton-transfer network next to serine 130 did not restore rapid reduction. The very slow reactivity of DHO allowed aerobic titrations. Interestingly titrations of the triple-mutant with DHO at 25 °C showed that it had a $K_d$ of 57 ± 2 μM which is about three times tighter than the wild-type Class 1A enzyme. The reduction potential of the triple-mutant was determined by the method of Massey (*11*) using phenosafranine as the indicator dye and found to be -264 mV, very similar to that of the wild-type Class 1A enzyme (-245 mV) (*10*), thus confirming that the active site had not been severely disrupted despite mutating three residues.

The *E. coli* wild-type Class 2 enzyme does not bind the ligands 3,4-dihydroxybenzoate (3,4-diOHB) or 3,5-dihydroxybenzoate (3,5-diOHB), while the *L. lactis* wild-type enzyme does (*12, 13*). The binding affinity of the *L. lactis* Class 1A triple-mutant with these ligands was tested by aerobic titrations at 25 °C. Surprisingly, the triple-mutant did not bind 3,4-diOHB and had weak binding for 3,5-diOHB ($K_d$ = 392 ± 38 μM). The installation of the proton-transfer network

changed the ligand selectivity and in this regard made the triple-mutant more like the Class 2 enzyme. However, installing a proton-transfer network into a Class 1A DHOD does not convert it completely into a Class 2 DHOD because its rate of reduction is slow.

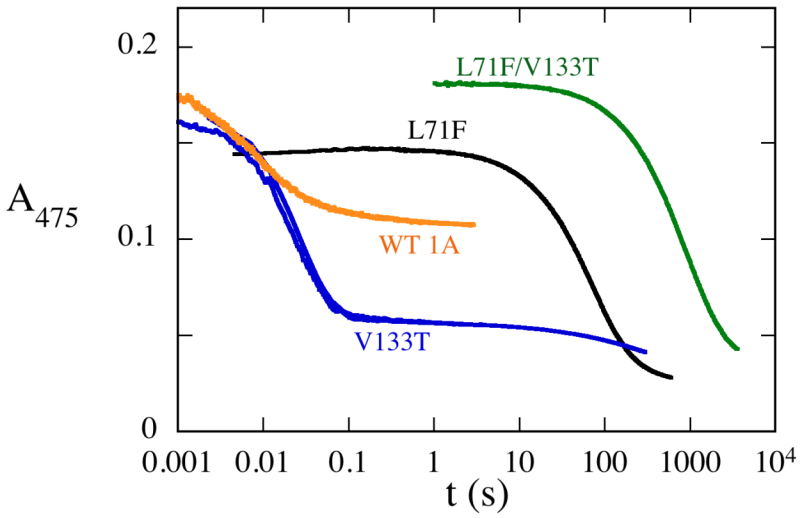


**Figure A-3 Reduction of Class 1A variants.**

The reduction of the wild-type Class 1A enzyme and the Leu71Phe, Val133Thr, Leu71Phe/Val133Thr variants was studied by mixing anaerobic solutions of the oxidized enzyme with anaerobic solutions of DHO in a stopped-flow spectrophotometer. The wild-type did not reduce fully because the preparation had significant amounts of damaged enzyme but the kinetics were the same as reported in reference (*7*). All reactions were in 27.8 mM Taps 22 mM KCl, pH 8.5 at 4 °C. Note the logarithmic timescale.

It was surprising that the leucine to phenylalanine and valine to threonine substitutions did not make the serine a functional base. The possibility was investigated that these residues actually inhibit the function of the residue at position 130 of the Class 1A enzyme. Therefore the double-mutant Leu71Phe/Val133Thr was created. Based on the reduction potential of the double mutant (-262 mV) the integrity of the active site seems to be preserved despite the two mutated residues. Installation of the proton-transfer network inhibited reduction. The reaction of the double-mutant with DHO had a $k_{red}$ of

0.0010 ± 0.0001 $s^{-1}$ at 4 °C (Figure A-3) which was faster than the triple-mutant but still drastically slower than the wild-type Class 1A and Class 2 enzymes. Despite the large decrease in the speed of reduction with DHO, the $K_d$ was 22 ± 0.9 μM, about eight-fold tighter than the wild-type Class 1A enzyme and nearly the same as wild-type Class 2 enzyme. The double-mutant, like the triple-mutant, also does not bind 3,4-diOHB and weakly binds 3,5-diOHB ($K_d$ = 453 ± 27 μM). Adding the two residues of the proton-transfer network when the base is cysteine resulted in a mutant that had more Class 2-like properties, like the triple-mutant, except for reactivity.

To determine whether one residue or both residues in the proton-transfer network were responsible for the behavior of the triple and double-mutants described above, the two residues were mutated individually. The reduction potential of the Val133Thr mutant enzyme (-266 mV) was also almost the same as wild-type Class 1A enzyme. The Val133Thr mutant enzyme was just a little slower ($k_{red}$ = 41 ± 0.8 $s^{-1}$ at 4 °C; Figure A-3 and 100 ± 1.9 $s^{-1}$ at 25 °C) than the wild-type Class 2 enzyme ($k_{red}$ = 46 ± 0.3 $s^{-1}$ at 4 °C). Binding of DHO to the Val133Thr mutant enzyme was much weaker ($K_d$ = 84 ± 0.9 μM) than the Class 2 wild-type enzyme but tighter than the wild-type Class 1A enzyme ($K_d$ = 145 ± 50 μM). The Val133Thr mutation did not inhibit binding of 3,4-diOHB as had been observed in both the double and triple Class 1A mutants. Therefore the Val133Thr mutation did not change the ligand binding behavior to that of the Class 2 enzyme. The Val133Thr mutant had weak binding for 3,4-diOHB and 3,5-diOHB with $K_d$ values of 640 ± 40 and 156 ± 4 μM, respectively. The Val133Thr mutant enzyme-3,4-diOHB complex had charge-transfer absorbance, as seen by large spectral increases from 550-800 nm, as does the wild-type Class 1A-3,4-diOHB complex, and none was observed in the presence of 3,5-diOHB, similar to the wild-type Class 1A enzyme (*13*).

The Leu71Phe mutant enzyme had a slower rate of reduction with DHO ($k_{red}$ = 0.015 ± 0.002 $s^{-1}$ at 4 °C; Figure A-3 and 0.07 ± 0.001 $s^{-1}$ at 25 °C) compared to both the wild-type Class 1A and Class 2 enzymes. The $k_{obs}$ did not vary with DHO concentration, indicating that the $K_d$ of DHO was much less than 125 μM - tighter than the wild-type Class 1A enzyme but not the wild-type Class 2 enzyme. The Leu71Phe enzyme did not bind 3,4-diOHB and had weak binding for 3,5-diOHB with a $K_d$ of 417 ± 17 μM. The reduction potential of Leu71Phe was -259 mV. These data show that residue 71 is partly responsible for ligand-binding specificity, in particular that of 3,4-diOHB.

Mutating the residues at positions 71 and 133 had different effects on the enzyme. The changes in free energies of activation for the double and both single mutants were calculated from transition state theory in order to decide whether position 71 interacts with position 133. In order to compare changes in free energies of activation the rate constants from 4 °C were used because the Class 1A wild-type enzyme reduces too quickly to measure at higher temperatures. The change in Gibbs free energy caused by mutating wild-type Class 1A enzyme to Leu71Phe ($\Delta\Delta G^{\ddagger}$ = 5.1 ± 0.4 kcal $mol^{-1}$) and then from Leu71Phe to Leu71Phe/Val133Thr ($\Delta\Delta G^{\ddagger}$ = 1.49 ± 0.07 kcal $mol^{-1}$) was no different than that obtained when taking the Class 1A wild-type enzyme and mutating it to Val133Thr ($\Delta\Delta G^{\ddagger}$ = 0.80 ± 0.4 kcal $mol^{-1}$) and then creating the double-mutant ($\Delta\Delta G^{\ddagger}$ = 5.83 ± 0.01 kcal $mol^{-1}$). The free energy analysis shows additive effects on the two mutations – a total of 6.6 ± 0.4 kcal $mol^{-1}$ for the double-mutant, obtained directly or by either sequence of mutations. The two residues are non-interacting.

Overall, installing a proton-transfer network into a Class 1A DHOD does not cleanly convert it into a Class 2 DHOD. The mutations had a range of effects on the binding of different ligands. Installing the proton-transfer network caused

DHO to bind tighter, mimicking Class 2 enzymes. However, the binding of only one of a pair of benzoate ligands became more like Class 2. Curiously the binding of OA was never perturbed by these mutations (Table A-1). The difference between OA and DHO is that OA is planar, but DHO is not. Apparently a Phe at position 71 is better suited to accommodate the non-planar ligand, although it is not yet possible to say why. Leu71, a key conserved residue in Class 1A enzymes, is critical for the binding of 3,4-diOHB but not as important for the binding of 3,5-diOHB and its mutation had large effects on reactivity. The proton-transfer network that enhances reactivity in the Class 2 enzymes inhibits reactivity when grafted into the Class 1A enzyme yet seems to be responsible for the tight DHO binding of Class 2 DHODs. Thus substrate binding is not linked to reactivity; the residues of the proton-transfer network are important for transition-state stabilization rather than reactant stabilization.

ACKNOWLEDGMENT: †This work was supported by National Institutes of Health Grant GM61087 to B.A.P. C.A.M. was supported by University of Michigan Rackham Merit Fellowship and National Institute of Health Grant GM061087-08-S1.

## References


1. Björnberg, O., Rowland, P., Larsen, S., and Jensen, K. F. (1997) Active site of dihydroorotate dehydrogenase A from Lactococcus lactis investigated by chemical modification and mutagenesis, *Biochemistry 36*, 16197-16205.
2. Jones, M. E. (1980) Pyrimidine nucleotide biosynthesis in animals: genes, enzymes, and regulation of UMP biosynthesis, *Annu. Rev. Biochem. 49*, 253-279.
3. Nagy, M., Lacroute, F., and Thomas, D. (1992) Divergent evolution of pyrimidine biosynthesis between anaerobic and aerobic yeasts, *Proc. Natl. Acad. Sci. U. S. A. 89*, 8966-8970.
4. Nielsen, F. S., Andersen, P. S., and Jensen, K. F. (1996) The B form of dihydroorotate dehydrogenase from Lactococcus lactis consists of two different subunits, encoded by the pyrDb and pyrK genes, and contains FMN, FAD, and [FeS] redox centers, *J. Biol. Chem. 271*, 29359-29365.
5. Rowland, P., Nielsen, F. S., Jensen, K. F., and Larsen, S. (1997) The crystal structure of the flavin containing enzyme dihydroorotate dehydrogenase A from Lactococcus lactis, *Structure 5*, 239-252.
6. Norager, S., Jensen, K. F., Björnberg, O., and Larsen, S. (2002) E. coli dihydroorotate dehydrogenase reveals structural and functional distinctions between different classes of dihydroorotate dehydrogenases, *Structure 10*, 1211-1223.
7. Fagan, R. L., Jensen, K. F., Björnberg, O., and Palfey, B. A. (2007) Mechanism of flavin reduction in the class 1A dihydroorotate dehydrogenase from Lactococcus lactis, *Biochemistry 46*, 4028-4036.
8. Small, Y. A., Guallar, V., Soudackov, A. V., and Hammes-Schiffer, S. (2006) Hydrogen bonding pathways in human dihydroorotate dehydrogenase, *J. Phys. Chem. B. 110*, 19704-19710.

9. Kow, R. L., Whicher, J. R., McDonald, C. A., Palfey, B. A., and Fagan, R. L. (2009) Disruption of the proton relay network in the class 2 dihydroorotate dehydrogenase from Escherichia coli, *Biochemistry 48*, 9801-9809.
10. Norager, S., Arent, S., Björnberg, O., Ottosen, M., Lo Leggio, L., Jensen, K. F., and Larsen, S. (2003) Lactococcus lactis dihydroorotate dehydrogenase A mutants reveal important facets of the enzymatic function, *J. Biol. Chem. 278*, 28812-28822.
11. Massey, V. (1990) A simple method for the determination of redox potentials, In *Flavins and Flavoproteins* (Curti, B., Ronchi, S., and Zanetti, G.,, Ed.), pp 59-66, Walter de Gruyter, Berlin.
12. Wolfe, A. E., Thymark, M., Gattis, S. G., Fagan, R. L., Hu, Y. C., Johansson, E., Arent, S., Larsen, S., and Palfey, B. A. (2007) Interaction of benzoate pyrimidine analogues with class 1A dihydroorotate dehydrogenase from Lactococcus lactis, *Biochemistry 46*, 5741-5753.
13. Palfey, B. A., Björnberg, O., and Jensen, K. F. (2001) Specific inhibition of a family 1A dihydroorotate dehydrogenase by benzoate pyrimidine analogues, *J. Med. Chem. 44*, 2861-2864.
14. Palfey, B. A., Björnberg, O., and Jensen, K. F. (2001) Insight into the chemistry of flavin reduction and oxidation in Escherichia coli dihydroorotate dehydrogenase obtained by rapid reaction studies, *Biochemistry 40*, 4381-4390.
15. McDonald, C.A., and Palfey, B.A. (2011) Substrate binding and reactivity are not linked: grafting a proton-transfer network into a Class 1A Dihydroorotoate dehydrogenase, *Biochemistry* 50, 2714-2716.

# Appendix B
# Oxygen Reactivity in Flavoenzymes: Context Matters

The content of this chapter was previously published by the author as a Communication in the Journal of the American Chemical Society [29].

Flavins in solution, when reduced, react with molecular oxygen. However this reaction is not very fast. The reaction is slow because spin inversion is required for the reaction of a singlet (reduced flavin) with a triplet ($O_2$) to form singlet products, oxidized flavin and $H_2O_2$ [1, 2]. This reaction occurs by electron transfer from reduced flavin to $O_2$ yielding a caged radical pair – superoxide anion and semiquinone - which collapses to the C4a-hydroperoxide, which decomposes into $H_2O_2$ and oxidized flavin (Figure B-1).

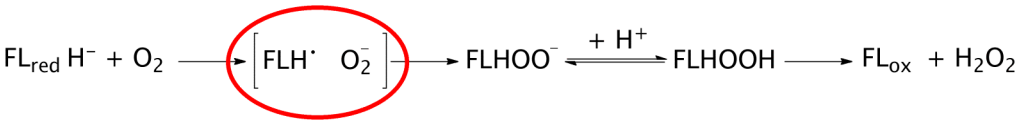


**Figure B-1 Mechanism of reaction of reduced flavin with oxygen.**

It has been proposed that stabilizing the superoxide-semiquinone pair (circled in red) allows rapid reaction with O2.

Flavoproteins can be categorized based on their reactivity with $O_2$ and the products that are formed from their reactions [3]. Reduced oxidases react rapidly with $O_2$ to give oxidized enzyme and $H_2O_2$ [3]. Reduced monooxygenases react rapidly to form the flavin hydroperoxide, which either oxygenates a substrate or eliminates $H_2O_2$ [4]. Although the radical pair in Figure B-1 is thought to be an intermediate in oxidases and monooxygenases, it has not been observed, with the possible exception of one enzyme [5], suggesting that forming the radical pair

is rate-determining. Dehydrogenases usually react slowly with $O_2$, sometimes more slowly than free flavins, to give a mixture of $H_2O_2$ and superoxide anion [6]. There is considerable interest in understanding how reduced flavoenzymes control oxygen reactivity [6]. Structures of flavoproteins have been studied in an attempt to uncover clues for the basis of the acceleration of the reaction. At this time there is no clear understanding of how structures may explain oxygen reactivity.

There are many ideas on how enzymes can speed the reaction of reduced flavins with $O_2$. These either focus on controlling the access of $O_2$ to the flavin, or on stabilizing $O_2^-$ in the caged radical intermediate. Access has been proposed to be controlled by channels through which $O_2$ would approach the flavin, facilitating their encounter [7, 8]. Recent molecular dynamics studies suggested that the protein matrix guides oxygen to a spot over C4a of the flavin for the reaction in some enzymes [9, 10]. Crystal structures of L-galactono-γ-lactone dehydrogenase (GALDH), which belong to the vanillyl-alcohol oxidase family, reveal that an alanine is near the C4a position of the flavin; it reacts poorly with $O_2$ [11]. Replacing the alanine residue of GALDH with a glycine increased oxygen activation by 400-fold, suggesting that the bulk of the alanine side-chain inhibits the flavoprotein dehydrogenase from reacting with molecular oxygen.

Ideas that consider increasing reactivity emphasize ways in which the protein could stabilize the obligate semiquinone–superoxide intermediate, especially by considering the polarity of the local environment in which $O_2^-$ would form [12]. Lewis acid catalysis could promote superoxide formation [13, 14]. For example, glucose oxidase has two histidines near the flavin that appear to be important for oxygen activation. The positive charge of one of the histidines stabilizes the developing negative charge of $O_2^-$. The positive charge that activates oxygen is

thought to be located on the product bound to the active site in choline oxidase [15].

Recent studies have shown that a lysine near N5 is important for reactivity of several enzymes with $O_2$. Monomeric sarcosine oxidase, an enzyme which contains covalently bound flavin, catalyzes the oxidation of sarcosine [16, 17]. Monomeric sarcosine oxidase has a lysine that hydrogen-bonds to a water which hydrogen-bonds to N5 of the flavin [18]. Mutating Lys265 to the neutral methionine decreased the rate constant for the reaction of $O_2$ by 8,000-fold [19]. Crystallography showed that $Cl^-$ can bind in a pocket, near N5 of the flavin, lysine, and the water, suggesting that this is a pre-organized site for the reaction of $O_2$ [20]. Another oxidase, N-methyltryptophan oxidase, also has a lysine near N5 of the flavin. Mutating this residue to glutamine decreased the rate constant for the oxygen reaction by ~2,500 fold [21]. These are among the largest decreases in oxygen reactivity seen as an effect of site directed mutagenesis.

These observations show that a lysine near N5 is a key player in oxygen activation in these oxidases and thus sparked our interest in exploring the generality of lysine's ability to accelerate the reaction of $O_2$. The model-enzymes fructosamine oxidase and dihydroorotate dehydrogenases (DHODs) were studied because they all have lysines near N5 (Figure B-2).

Fructosamine oxidase from the fungus *Aspergillus fumigatus* is a flavoprotein oxidase that catalyzes the oxidation of the carbon-nitrogen bond of fructosamines. The amine substrate of the enzyme, formed physiologically by the spontaneous reaction of glucose and amino groups of amino acids, is oxidized to an imine and hydrolyzed non-enzymatically [22].

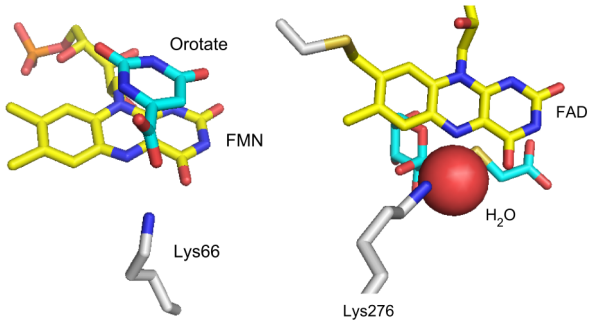


**Figure B-2 Fructosamine oxidase and *E. coli* DHOD active site structures.**

Fructosamine oxidase (left, from 3dje.pdb) and *E. coli* DHOD (right, from 1f76.pdb) active site structures.The DHOD complex with orotate is shown, but the structure remains the same in its absence. Note that each enzyme has a lysine near N5 of the flavin. The structure of a Class 1A DHOD is not shown, but is essentially identical.

The reaction of the reduced wild-type fructosamine oxidase with $O_2$ was studied in stopped-flow experiments. Flavin oxidation was observed by an increase in absorbance at 450 nm without any indication of an intermediate. Observed rate constants varied linearly with $O_2$ concentrations, giving a bimolecular rate constant of 1.6 x $10^5$ $M^{-1}s^{-1}$ [23]. Fructosamine oxidase has a lysine orthologous to that of monomeric sarcosine oxidase, the residue identified to be important in $O_2$ reactivity. Lys276 was mutated to methionine. The reduced Lys276Met mutant reacts with $O_2$ with a rate constant of 291 $M^{-1}s^{-1}$, a 550-fold decrease (Table B-1). Again, there was no indication of an intermediate and the reaction produced $H_2O_2$ [a]. As with monomeric sarcosine oxidase, a large decrease in reactivity occurred, showing that lysine plays an important role in oxygen-activation in these two oxidases. The location of this positive charge is important. The Lys53Met mutant enzyme, where the lysine is nearly centered over the aromatic ring of the flavin on the *si*-face, reacted with $O_2$ only 30-fold slower than wild-type [23].

Unrelated enzymes, DHODs, catalyze the oxidation of dihydroorotate to orotate during the only redox reaction in the pyrimidine biosynthetic pathway. DHODs

can be categorized into two different classes based on their sequences: Class 1 and Class 2 [24]. The Class 1 and 2 enzymes have different selectivity for oxidizing substrates and are also located in different compartments of the cell. The Class 2 enzymes are mitochondrial membrane proteins while Class 1 enzymes are cytosolic. Class 2 DHODs *in vivo* are oxidized by ubiquinone while Class 1A enzymes are oxidized by fumarate [3].

**Table B-1 Oxidative half-reaction rate constants.**

| Enzyme | $k_{ox}$ ($M^{-1}s^{-1}$) | $k_{ox}$ (wild-type) / $k_{ox}$ (mutant) |
|---|---|---|
| Wild-type FAOX[a] | $1.6 \times 10^{5}$ [b] | |
| Lys276Met FAOX[a] | 291 | 550 |
| Lys53Met FAOX[a] | $5.6 \times 10^{3}$ [b] | 29 |
| Wild-type *L. lactis* DHOD | $3.0 \times 10^{3}$ | |
| Lys43Met *L. lactis* DHOD | $2.6 \times 10^{3}$ | 1.2 |
| Wild-type *E. coli* DHOD | $6.2 \times 10^{4}$ [c] | |
| Wild-type *E. coli* DHOD•Orotate | $5.0 \times 10^{3}$ [c] | 12.4 [d] |
| *E. coli* Lys66Met | $6.2 \times 10^{4}$ | 1.0 |
| *E. coli* His19Asn | $3.7 \times 10^{4}$ | 1.7 |
| *E. coli* Arg102Met | $5.9 \times 10^{4}$ | 1.1 |

[a]FAOX, fructosamine oxidase. [b]Ref [23]. [c]Ref [25]. [d]This is $k_{ox}$ (free wild-type) / $k_{ox}$ (orotate complex).

Class 2 *E. coli* DHOD has a lysine (Lys 66) near N5 of the isoalloxazine of the flavin [26]. The rate constant for the reaction of $O_2$ with the reduced wild-type enzyme is $6.2 \times 10^{4}$ $M^{-1}s^{-1}$ [25], a value that is similar to that seen in some oxidases [27]. The oxidative half-reaction of the Lys66Met mutant enzyme was studied by mixing the reduced enzyme with buffer containing various concentrations of $O_2$. The Lys66Met mutant enzyme reacted with a rate constant of $6.2 \times 10^{4}$ $M^{-1}s^{-1}$, no

change. Neither the wild-type nor the mutant enzyme formed an observable intermediate during their reactions and each produced $H_2O_2$ [a].

The Class 1A DHOD from *Lactococcus lactis* also has a lysine (Lys43) near N5 of the isoalloxazine of the flavin [28]. The rate constant for the reaction of $O_2$ with the reduced wild-type enzyme is 3.0 x $10^3$ $M^{-1}s^{-1}$. The Lys43Met mutant enzyme reacted with a rate constant of 2.6 x $10^3$ $M^{-1}s^{-1}$, only 1.2-fold slower – virtually no change. Again, the removal of the lysine residue near N5 of the flavin had no significant impact. Neither the mutant nor the wild-type enzyme formed an intermediate during their reactions and each produced $H_2O_2$ [a].

The reactivity of the mutant DHODs shows that lysine near N5 is not guaranteed to be important for oxygen reactivity. If $O_2$ reacts elsewhere in DHOD, then the Lys66Met substitution should have little affect in the Class 2 enzyme, as observed. The physiological oxidizing substrate of Class 2 DHODs is ubiquinone, which binds near the methyls of the isoalloxazine of the flavin; the reaction occurs by two single-electron transfers [25]. Therefore, Class 2 DHODs have evolved to transiently stabilize the flavin semiquinone. There are two conserved positively charged residues in the ubiquinone binding site, His19 and Arg102 in the *E. coli* enzyme. Conceivably, either of these positive charges could stabilize a developing negative charge if $O_2$ reacted at this site. Therefore the reactivity of the His19Asn and Arg102Met mutant enzymes was determined. Neither change significantly altered the bimolecular rate constant for the reaction of $O_2$ (Table B-1), eliminating this site as the site where $O_2$ reacts.

A unifying mechanism for oxygen activation by flavoproteins is being sought by many researchers. Our results show that a single mechanism cannot explain oxygen activation. The lysine near N5, a critical ingredient in oxygen activation for some oxidases, does not exert an effect without an appropriate context –

some feature (or features) of the active site allows it to activate oxygen. Aligning the isoalloxazines of the structures of fructosamine oxidase and Class 1A and 2 DHODs shows that there is enough space near N5 and the lysine in each to accommodate $O_2$. DHOD (not an oxidase) reacts with $O_2$ at virtually the same rate regardless of the presence of a lysine near N5 – it plays no role in oxygen activation. Other structural features must be responsible. Mutagenesis eliminated the quinone binding bucket as the site of the reaction of $O_2$. The hydrophilic pyrimidine binding site over the *si*-face of the flavin, ringed by hydrogen-bonding side-chains, does not appear to be the site of the reaction of $O_2$ because the reduced enzyme-orotate complex reacts only about ten-fold slower than the free enzyme (Table B-1) [25]. The site of the reaction of $O_2$ in DHODs remains a mystery. Our results suggest that many mechanisms are possible for oxygen activation by flavoproteins. This is consistent with the variety of structures of flavoproteins that react with oxygen [3]. A small, reactive molecule like $O_2$, which appeared after the origin of life and flavoenzymes, would be expected to find many sites to react.

## References


1. Bruice, T. C., Isr. J. Chem. **1984,** 24, 54-61.
2. Massey, V., *J. Biol. Chem.* **1994,** *269*, 22459-62.
3. Fagan, R. L.; Palfey, B. A., *Flavin-Dependent Enzymes*. Elsevier: Oxford, UK, 2010; Vol. 7.
4. Palfey, B. A.; McDonald, C. A., *Arch. Biochem. Biophys.* **2010,** *493*, 26-36.
5. Pennati, A.; Gadda, G., *Biochemistry* **2010**.
6. Mattevi, A., *Trends Biochem. Sci.* **2006,** *31*, 276-83.
7. Coulombe, R.; Yue, K. Q.; Ghisla, S.; Vrielink, A., *J. Biol. Chem.* **2001,** *276*, 30435-41.
8. Chen, L.; Lyubimov, A. Y.; Brammer, L.; Vrielink, A.; Sampson, N. S., *Biochemistry* **2008,** *47*, 5368-77.
9. Baron, R.; Riley, C.; Chenprakhon, P.; Thotsaporn, K.; Winter, R. T.; Alfieri, A.; Forneris, F.; van Berkel, W. J.; Chaiyen, P.; Fraaije, M. W.; Mattevi, A.; McCammon, J. A., *Proc. Natl. Acad. Sci. U. S. A.* **2009,** *106*, 10603-8.
10. Saam, J.; Rosini, E.; Molla, G.; Schulten, K.; Pollegioni, L.; Ghisla, S., *J Biol Chem* **2010,** *285*, 24439-46.
11. Leferink, N. G.; Fraaije, M. W.; Joosten, H. J.; Schaap, P. J.; Mattevi, A.; van Berkel, W. J., *J. Biol. Chem.* **2009,** *284*, 4392-7.
12. Wang, R.; Thorpe, C., *Biochemistry* **1991,** *30*, 7895-901.
13. Roth, J. P.; Klinman, J. P., *Proc. Natl. Acad. Sci. U. S. A.* **2003,** *100*, 62-7.
14. Roth, J. P.; Wincek, R.; Nodet, G.; Edmondson, D. E.; McIntire, W. S.; Klinman, J. P., *J. Am. Chem. Soc.* **2004,** *126*, 15120-31.
15. Ghanem, M.; Gadda, G., *Biochemistry* **2005,** *44*, 893-904.
16. Wagner, M. A.; Trickey, P.; Chen, Z. W.; Mathews, F. S.; Jorns, M. S., *Biochemistry* **2000,** *39*, 8813-24.
17. Wagner, M. A.; Jorns, M. S., *Biochemistry* **2000,** *39*, 8825-9.

18. Trickey, P.; Wagner, M. A.; Jorns, M. S.; Mathews, F. S., *Structure* **1999,** *7* (3), 331-45.
19. Zhao, G.; Bruckner, R. C.; Jorns, M. S., *Biochemistry* **2008,** *47*, 9124-35.
20. Kommoju, P. R.; Chen, Z. W.; Bruckner, R. C.; Mathews, F. S.; Jorns, M. S., *Biochemistry* **2011,** *50*, 5521-34.
21. Bruckner, R. C.; Winans, J.; Jorns, M. S., *Biochemistry* **2011,** *50*, 4949-62.
22. Gerhardinger, C.; Taneda, S.; Marion, M. S.; Monnier, V. M., *J Biol Chem* **1994,** *269*, 27297-302.
23. Collard, F.; Fagan, R. L.; Zhang, J.; Palfey, B. A.; Monnier, V. M., *Biochemistry* **2011**.
24. Björnberg, O.; Rowland, P.; Larsen, S.; Jensen, K. F., *Biochemistry* **1997,** *36*, 16197-205.
25. Palfey, B. A.; Björnberg, O.; Jensen, K. F., *Biochemistry* **2001,** *40*, 4381-90.
26. Nørager, S.; Jensen, K. F.; Björnberg, O.; Larsen, S., *Structure* **2002,** *10*, 1211-23.
27. Macheroux, P.; Massey, V.; Thiele, D. J.; Volokita, M., *Biochemistry* **1991,** *30*, 4612-9.
28. Rowland, P.; Nielsen, F. S.; Jensen, K. F.; Larsen, S., *Structure* **1997,** *5*, 239-52.
29. Mc Donald, C. A., Fagan, R. L., Collard, F., Monnier, V. M., and Palfey, B. A. (2011) *J. Am. Chem. Soc.* **133**, 16809-16811.